UNDERSTANDING THE ROLE OF *MAT2* IN THE SEXUAL DEVELOPMENT OF *CRYPTOCOCCUS NEOFORMANS*

A Dissertation

by

RACHANA GYAWALI

Submitted to the Office of Graduate and Professional Studies of
Texas A&M University
in partial fulfillment of the requirements for the degree of

DOCTOR OF PHILOSOPHY

Chair of Committee,	Xiaorong Lin
Committee Members,	Arne Lekven
	Brian D. Shaw
	Joseph Sorg
Head of Department,	Thomas D. McKnight

December 2016

Major Subject: Biology

ABSTRACT

Sexual reproduction is conserved and maintained in all major eukaryotic lineages. The fungus *Cryptococcus neoformans* is known to undergo **a**-α bisexual mating and also unisexual mating, with bisexual mating being far more efficient under laboratory conditions. During bisexual mating, the mating types of the progeny are segregated in the Mendelian fashion, with half of the progeny inheriting the mating type **a** and the other half inheriting the mating type α. However, *MAT*α dominates in the environment as well as in the clinical settings. Given that similar factors such as pheromone and environmental conditions are known to stimulate both unisexual and bisexual mating, it is unknown how and when *C. neoformans* chooses one mode of reproduction over the other. One important event that takes place during sexual development is the transmission of parental mitochondrial DNA. During bisexual reproduction between isogamic **a** and α cells, most of the progeny inherit the mitochondrial DNA from only the **a** parent. How this eukaryotic microbe selects and preserves only one parental mitochondrial DNA is unclear. Here, we have identified a key transcription factor Mat2 as the prezygotic decision maker for the transmission of mitochondrial DNA to the progeny. Mat2 also cooperates with postzygotic control to ensure tight uniparental mitochondrial DNA inheritance during bisexual mating. Although Mat2 is absolutely critical for bisexual mating, our studies indicate that the absence of Mat2 (or under conditions when Mat2 is repressed) promotes *C. neoformans* cells to undergo unisexual development. Thus, the findings of this study advanced our

understanding of the regulation of different developmental trajectories by genetic and environmental factors.

ACKNOWLEDGEMENTS

I would like to express my most sincere gratitude towards my advisor Dr. Xiaorong Lin. This journey would not have been possible without your guidance, patience and constant support. You inspire me not just to be a better scientist but a better person as well.

I am grateful to my committee members Dr. Arne Lekven, Dr. Brain D. Shaw and Dr. Joseph Sorg for all their support and guidance. You have encouraged me to become a better scientist.

Special thanks to all the previous and current members of Linlab whom I had the joy and privilege of spending time with. I would like to thank Linqi Wang for his guidance and advice during my early years of Ph.D which I value to this day. Thanks to Xiuyun Tian, Bing Zhai, Yunfang Meng and Nadia Chacko for all the fun times we shared together. I would like to thank Youbao Zhaoy for his numerous help and suggestions both inside the lab as well as outside. Thanks to Xinping Xu for his support in one way or the other. Thanks to Yumeng Fan for her willingness to help even at the last minute. In addition to all his help, I would like to Jianfeng Lin for making the lab so much fun either with his awkward or untactful social conversations or the updates on the departmental news feed. And lastly, I would like to thank Srijana Upadhyay for everything she has done for me. I thank her for being a mentor, a friend and a family to me.

And finally, I would like to thank my dad and mom for their support, their unconditional faith in me, and my choices. My sisters for keeping me grounded. And all my family members and friends for their support during this period. And lastly, special thanks to my husband for having my back on through every ups and downs which has made this journey much smoother.

NOMENCLATURE

AIDS	Acquired Immune Deficiency Syndrome
CFU	Colony Forming Unit
CNS	Central Nervous System
DMEM	Dulbecco's Modified Eagle Medium
HIV	Human Immunodeficiency Virus
MAT	Mating Type
YPD	Yeast Peptone Dextrose
YNB	Yeast Nitrogen Base
mtDNA	Mitochondrial DNA
BCS	Bathocuproinedisulfonic acid

TABLE OF CONTENTS

Page

Page

Page

LIST OF FIGURES

Page

LIST OF TABLES

1 INTRODUCTION AND LITERATURE REVIEW

1.1 Cryptococcus neoformans Infection

There are around 1.5 million fungal species on earth. Fungi most likely first appeared on earth about 1.5 billion years ago. Most of them are not harmful and to date only 300 of them are known to cause human infection (Lin 2009). Historically, fungal infections are thought to be associated with only superficial infections (such as skin, hair, and nail). However, sharp rise in systemic fungal infections seen in past three decades due to organ transplant, cancer therapy, or HIV infections have raised the awareness of fungal infections among clinicians and mycologists. Increased use of immunosuppressive drugs and chemotherapy have increased the number of infections caused by opportunistic fungal pathogens. Fungal infections can be life-threatening and are particularly devastating in resource limited regions in Africa and Southeast Asia. Lack of early diagnosis, limited options and potency of the treatment, and lack of vaccines further compounds the battle against these pathogens [10].

The fungus *Cryptococcus neoformans* of the phylum Basidiomycota is an opportunistic human fungal pathogen. It is an environmental fungus, and people are exposed to it since early childhood. Inhaled *C. neoformans* can get cleared by the host immune system, or remain in a dormant state without causing any symptoms. When the host immune system is suppressed or compromised (due to AIDS, organ transplant, or chemotherapy), they disseminate from lungs to different parts of the body to cause systemic infection. *C. neoformans* can cross blood brain barrier and reach central

nervous system causing meningoencephalitis, which is fatal without treatment. According to a report from CDC (Centers for Disease Control and Prevention), *C. neoformans* alone causes 1 million infections and 600, 000 deaths per year. Globally, almost 30% of the AIDS patients die each year due to cryptococcal meningitis. Annual deaths caused by *C. neoformans* is more than that claimed by breast cancer [11]. Death tolls in Sub-Saharan Africa region due to cryptococcosis is more than that caused by tuberculosis [11].

There is a dire need for understanding the mechanism of its pathogenesis. One way to tackle this problem is through understanding its life cycle and its development that can be selectively targeted by antifungal drugs or immunotherapy. Sexual development is an important part of its life cycle. This research focuses on understanding its sexual cycle. This research is focused on understanding the changes in morphology and gene expression concomitant with sexual development.

1.1.1 Cryptococcal infection route and virulence factors

C. neoformans was first isolated from a patient in 1894 [12]. *C. neoformans* enters the host through the inhalation of spores or desiccated yeast cells. It can colonize the respiratory tract of the host for months or even years without causing any symptoms. Often *C. neoformans* is cleared by the host immune system, but this fungus can remain in a dormant state for years without causing any symptoms. When the host immune system is suppressed or compromised, they can reactivate and disseminate from lungs to different parts of the body. *C. neoformans* has a predilection for the brain and can cause

cryptococcal meningitis [13]. And it is the most common clinical form of cryptococcocis.

Once inhaled, *C. neoformans* cells are small enough to reach the alveoli of the lungs. They can either get phagocytosed by alveolar macrophage cells or remain extracellular [14]. Thus *C. neoformans* is a facultative intracellular pathogen. It can survive and replicate within the acidic environment of the phagolysosome of macrophages [14-16]. This fungus can also escape from the macrophage either through host cell lysis or expulsion. Some of *C. neoformans* cells can also become big and polypoid known as titan cells. Titan cells can resist phagocytosis [17]. During dissemination, the fungus transverses from the lungs into bloodstream [14]. There are several hypothesis regarding how *C. neoformans* gets access to brain. The first one is "Trojan horse" mechanism where *C. neofomans* gets access to the brain through transport within phagocytic cells. Second mechanism is through direct transcytosis of the endothelial cells of the blood brain barrier. The third is through paracellular traversal where the *Cryptcoccus* cell is thought to cross the BBB endothelial barrier cells with or without disruption of the tight junctions [14, 18].

Why *Cryptococcos neoformans* has a predilection for the brain is still unknown. There are several hypotheses that can explain some aspects of neurotropism. First is that CNS can provide a refuge for *Cryptococcus neoformans* and hence protect it from host immune response [19]. Host immune response within the CNS might be different and weaker from that of other parts of the body. A second is that the substances within the CNS might be suitable for the growth of *Cryptococcus neoformans* [19]. For example,

inositol is highly enriched in brain [20]. Interestingly, neurotransmitters such as dopamine and epinephrine which are present in CNS can be used by *Cryptococcus neoformans* to produce melanin, a polymer that can protect fungi against phagocytosis, oxidative stress and antifungal drugs. Melanin also helps *Cryptococcus neoformans* for survival within the lung macrophage by providing resistance against reactive oxygen and nitrogen species [21].

Classical virulence factors of *Cryptococcus neoformans* include the formation of capsule, melanin and the ability to grow at high temperatures [22]. *Cryptococcus neoformans* capsule is attached to its cell wall and is composed of glucose, xylose, glucuronic acid and galactose. Capsule is very hydrophilic consisting of 99% of water [23, 24]. The size of capsule can vary depending on the environmental conditions. CO_2, iron limitation, mammalian serum, alkaline conditions are some of the factors that are known to induce the synthesis of capsule of *Cryptococcus neoformans*. It is said to be the first line of contact between host and the *C. neoformans*. Capsule helps *Cryptococcus neoformans* during it interaction with host. Cells with larger capsule are less likely to be phagocytosed by macrophage. Capsule is also said to protect *Cryptococcus* during its encounter with environmental predators such as amoeba [24]. Formation of melanin is another virulence trait of *Cryptococcus*. Melanin is a dark brown pigment synthesized by *C. neoformans* when grown on medium containing diphenolic substrates [12, 25]. It is one of the distinctive features of *C. neoformans*. Melanin deficient mutants are less virulent in a murine model of Cryptococcosis [12]. Though melanin contributes to

virulence, not all *C. neoformans* strains isolated from patients form melanin. This suggest there are other virulence factors in *C. neoformans* in addition to melanin.

1.1.2 *Cryptococcus neoformans* varieties and their habitats

C. neoformans is an environmental fungal pathogen. It is a species complex that include A, D and AD varieties. *Cryptococcus* is divided into five serotypes (A, B, C, and A/D) based on the agglutination reaction against the major capsular material glucuronoxylomannan (GXM) [26]. Alternative methods for serotyping include the use of selective media, differential staining, restriction fragment length polymorphism (RFLP) and amplification of polymorphic DNA fragment [26, 27]. *Cryptococcus neoformans* was originally divided into two varieties: *C. neoformans var neoformans* (Serotype A and D) and *C. neoformans var gattii* (Serotype B and C). Currently, serotype A and D are divided into separate varieties *C. neoformans var neoformans* (serotype D) and *C. neoformans var grubii* (serotype A). And *C. neoformans var gattii* is classified as a distinct species [28-30]. Serotype A, D and AD varieties are generally found to be associated with pigeon droppings [31, 32]. Pigeon guano can support the vegetative growth as well as the mating of this organism [13]. *Cryptococcus neoformans* has also been isolated from decaying woods, vegetation, and soil, suggesting that it has a wide variety of niches in the environment [33-35]. Pigeons most likely serve as a carrier of *C. neoformans* that might have caused its worldwide distribution. *C. gattii* isolates (serotype B and C) have been commonly isolated from trees such as eucalyptus [36, 37].

The majority (> 99%) of the cryptococcal infections are caused by serotypes A and D isolates. These isolates are distributed worldwide and mostly cause infection in immunocompromised individuals. Serotype B and C isolates which include *C. gattii* are found in tropical and subtropical regions such as Papua New Guinea, Australia and South America. However, its recent outbreak in Vancouver Island in British Columbia and Northern California indicate that *C. gattii* has expanded to temperate climate as well [38, 39]. It can cause infection mostly in immunocompetent individual. About 70-80% of the infection caused by *C. gattii* is in immunocompetent individuals. However, it can cause infection in immunocompromised individuals as well but at a much lower frequency [23, 40, 41]. Of all the varieties, serotype A is the most prevalent and is responsible for causing more than 95% of cryptococcosis cases worldwide [23, 42, 43].

1.1.3 Treatment options for cryptococcosis

To date, treating fungal infections has been challenging. There are no clinically available vaccines against fungal pathogens. One challenge in developing vaccines against fungal infection is that most systemic fungal infections take place in individuals whose immune systems are compromised. The risk of vaccinating these individuals is that their immune system might be too weak to respond to the vaccines [44].

Generally, three classes of compound are used in the treatment of fungal infections: polyenes, azoles and echinocandins. The current treatment plan for AIDS related cryptococcal meningitis include 2 week induction treatment with amphotericin B (polyenes) with or without flucytosine followed by maintenance therapy with azole

(fluconazole, Itraconazole) drugs [45]. The latter can last a lifetime. Though amphotericin has been used for the last 60 years (since 1950's) for fungal treatment, it has its limitations due to infusion related side effects and its toxicity [46]. Fluconazole (azoles) was introduced in 1980s. Fluconazole has good distribution in a wide variety of tissues and can penetrate the blood brain barrier. It is well tolerated in patients as well. However, it is fungistatic rather than fungicidal. Moreover, it is not effective against some fungal species such as *Aspergillus*, *Mucorales* and *Fusarium* [46]. Also, some environmental and clinical isolates of *Cryptococcus* have been found to be resistant to fluconazole [47]. The most recent antifungal drugs introduced to the market are echinocandins. They target synthesis of β-1,3-d-glucan in fungi, leading to fungal cell wall damage [47]. They are effective against *Candida* and *Aspergillus* species. However, they lack activity against *C. neoformans* and some molds, such as *Fusarium* [47, 48]. Hence, the currently available antifungal drugs are limited in their use due to efficacy, toxicity and feasibility. Thus, we are in need of better treatment options and therapeutics.

1.2 Morphogenesis and Sexual Development

Fungal cells in the environment are exposed to unprecedented environmental insults and fluctuations. Since they are not motile, fungi adapt by making physiological or morphological changes which are necessary for their dispersal, survive and reproduction. Like many fungal species, *Cryptococcus* adapts to certain stress and nutrient limitation by undergoing sexual reproduction. Morphological transition is prominently seen during sexual development in *Cryptococcus neoformans*.

1.2.1 Evolution of sex

The majority of the eukaryotic organisms undergo sexual reproduction. Given the cost associated with sexual reproduction, it has managed to evolve and maintain in the organisms. There is a twofold cost associated with sexual reproduction [49-53]. A sexually reproducing parent transmits only 50% of its genes to its progeny whereas the parent reproducing asexually transmits 100% of its genes to its progeny [51, 54]. Sexual reproduction is risky. Mixing of the genome with other individual can result in the transmission of harmful genetic or sexually transmitted diseases [54, 55]. In terms of time, sexual reproduction is costly. Finding the compatible mating partner is often time challenging [56]. It takes 5-100 times longer than mitosis for the completion of sexual reproduction. For a unicellular eukaryote, mitosis can take place in 15 minutes whereas for meiosis it can take more than 10 hours. In *Saccharomyces cerevisiae* mitosis can take place in 90 minutes, but meiosis can take days [54]. Despite all the cost, the benefits associated with sexual reproduction is much greater. Sexual reproduction is one of the major driving force for evolution. It purges the genome of deleterious mutations and generates genetic diversity on which selection acts upon [51, 57]. Thus, the genotypic variation created by sexual reproduction allows for the long term survival of the offspring or the species [56, 58]. Studies on experimental yeast population indicate that sexual reproduction can provide selective advantage when exposed to a new environment [59].

Hallmark of sexual reproduction include increase in ploidy and then reduction to haploid gametes through meiosis [60, 61]. All major eukaryotic lineages have a set of

meiotic machinery, suggesting that it is an ancestral trait that was present in the last common ancestor of eukaryotes [50, 52, 62]. However, there is no one common theory that can explain the evolution and maintenance of sexual development in eukaryotes. The function of meiosis seems to be more than just creating genetic diversity. According to Cleveland and Niklas, meiosis has evolved and maintained in various organisms for different reasons [60, 63, 64]. Increase in ploidy can occur as a result of environmental stress or to provide extra copy of the genome during DNA repair [63, 64]. And reduction division of meiosis might have evolved for a number of different functions such as to deal with autopolyploidy, to repair double stranded DNA damage, or to purge deleterious mutations from genome. Natural selection acted on each of its functions in different organisms for different purpose [60, 63, 64].

1.2.2 Modes of sexual reproduction in fungi

Sexual reproduction in fungi can also occur through unisexual/homothallism (fusion between genetically identical haploid cells or endoduplication) or bisexual/ heterothallism (fusion between haploid cells which differ at the mating type locus) [65]. Some are strictly bisexual or unisexual whereas some can undergo both [66, 67]. Each has its own cost and benefits. Bisexual mating can create more genetic diversity in offspring. However, it requires finding the compatible mating partner which is often time consuming. Unisexual mating in fungi has evolved a number of mechanism to avoid this cost associated with finding the mating partners. One way to achieve self-fertility is to have both the mating type genes within the same individual. Such is the case in *Aspergillus nidulans*. Another way of achieving self-fertility is through mating

type switching. In this case, an individual has the genome that encodes both mating types but only expresses one at a time. A cell can switch the active expression of the mating type genes and thus their mating types. Hence, a colony derived from a single cell will have individuals expressing one mating type and some the other. Such is the case in *Saccharomyces cerevisiae* [67]. The third type of sexual development also known as unisexual mating involves an individual containing genes of only one mating type but is able to complete its sexual development without the need for opposite mating partner or the expression of genes of the other mating type locus [67]. Such is the case in species like *Neurospora africana*, and *Cryptococcus neoformans* [68-71]. For instance, *N. africiana* contains genes from mat A locus, only one *MAT* idiomorphs [67, 70]. *Cryptococcus* α isolates have been shown to complete sexual development without the need for opposite **a** mating partner [68]. Initially this process was thought to be mitotic and asexual. However, later studies showed that spores produced through this process were recombinant spores and key meiotic regulators like Dmc1 are required for the completion of unisexual development [52, 68, 72]. In the rest of the thesis, we will be using the term unisexual reproduction in *Cryptococcus neoformans* to mean such form of sexual reproduction.

What drives an organism to a particular mode of sexual reproduction is unknown. In fungi, the same species can undergo homothallic or heterothallic sexual development depending on the condition [69]. For instance, in the homothallic fungus *A. nidulans*, mating has been suggested to preferentially occur between genetically different individuals [65]. The plant *Arabdiopsis thaliana*, is self-pollinating the majority of the

times and engages in cross pollination only 1% of the time [52]. This strategy ensures that the organism can undergo sexual reproduction and it does not have to waste time in finding the compatible mating partner. So, it seems based on the environmental conditions or their niches, organisms are capable of choosing their mode of sexual reproduction. The ability of the organism to undergo reproduction either sexual, asexual or parasexual is a tactic adopted by the organisms to adjust in the environment [49]. And studies have shown that unisex can also generate genetic diversity de novo [52, 73]. So, it seems the ability to undergo unisexual development by these non-motile fungi might be a strategy for them to propagate and maintain sex at conditions which is not favorable for finding mating partners.

1.2.2.1 Bisexual and unisexual development

Cryptococcus neoformans has two different mating types, *MAT***a** and *MAT*α which is similar to the sexualities in higher organisms. Mating between *MAT***a** and *MAT*α cells take place in mating inducing conditions [74, 75]. Initially, **a** and α cells fuse together after which the formation of heterokaryotic dikaryon takes place. Two nuclei from **a** and α cells remain unfused after cell fusion. This dikaryon continues to grow to form a hypha with septa separating each hyphal compartment and clamp connections between adjacent hyphal compartment to ensure the proper migration of **a** and α nuclei in each hyphal cell [76, 77]. Some hyphae continue to grow to form invasive hyphae into substrate whereas others grow to form aerial hyphae. Some of the aerial hyphae form a swollen structure at the hyphal tip called a basidium where the **a** and α nuclei fuse, after which meiosis and sporulation take place. A single meiosis event takes place which

produces 4 haploid gametes. Repeated rounds of mitosis lead to the formation of four long chains of spores [78]. Spores are produced basipetally with new spores towards the base and old ones in the apex [74, 76]. Transmission of organelles also take place during sexual development. Bisexual mating of *Cryptococcus* involves two isogamous cells **a** and α, yet the mitochondrial DNA inheritance in majority of the progeny is from *MAT***a** parent. Bisexual mating is very efficient in laboratory conditions and generates an equal number of **a** and α progeny. However, majority of the isolates (about 99%) found in the clinics and environment are of mating type α [79, 80].

Cryptococcus α cells can also undergo self filamentaiton through a process known as unisexual reproduction. Before 2005, this process of self-filamentation was considered asexual [81]. In 2005, Lin et. al showed that this self filamentation was actually a sexual process which culminates with the formation of basidium and sexual basidiospores similar to that of bisexual reproduction [68]. Enhanced ability of *C. neoformans* α cells to undergo unisexual reproduction can partly explain the skewed distribution of α population. However, unlike bisexual reproduction, unisexual reproduction of *Cryptococcus* is not efficient under laboratory conditions used. One explanation for this is that the cues that promote unisexual reproduction might be different from that of bisexual reproduction. The laboratory conditions currently used might not mimic the natural habitat of *Cryptococcus* that promotes unisexual reproduction. There might be some cues present in the environment that we do not recapitulate under laboratory conditions. We will discuss more about unisexual development in more detail in Chapter IV.

1.2.3 Factors affecting sexual development

Currently known factors that promote sexual development are similar in both bisexual and unisexual mating. Sexual reproduction preferentially occurs in dark at 22 °C [82]. Nitrogen starvation, dehydrated substrate, pheromone have been shown to enhance mating, and inositol also stimulates filamentation [13, 83-86]. Similarly, copper also enhances mating under certain concentrations [87, 88]. On the other hand, other factors such as temperature and CO_2 have been shown to inhibit mating.

The *MAT* locus is important for certain processes during the sexual development of *Cryptococcus,* including cell fusion, dikaryotic hypha formation, and nuclear fusion, and sporulation. *Cryptococcus MAT* locus is ~100 kb and contains greater than 20 genes. The *MAT* locus mostly contains a common set of genes of divergent alleles and only a few genes that are unique to each mating type [89]. The genes of the pheromone sensing pathway such as *MF*α (pheromone), *STE3*α (pheromone receptor), *STE20*, *STE12*, *STE11* and homeodomain proteins (*SXI1*α, *SXI2***a**) lie within this region. The *MAT* locus of *Cryptococcus* also contains cell type specific Sex Inducer genes *SXI1*α and *SXI2***a** which function after cell fusion and are required for the completion of sexual development. The *MAT* locus was found to be one of the factors that affected hyphal growth in *Cryptococcus*. The presence of *MAT*α locus enhanced hyphal growth in *Cryptococcus neoformans* [87].

1.2.3.1 Signaling pathways regulating sexual development in *Cryptococcus neoformans*

Various signaling pathways are known to regulate growth, virulence, and sexual development in fungi [90]. Many G-protein coupled receptors together with heterotrimeric G-proteins are known to be involved in the growth and development of an organism. G-protein coupled receptors (GPCR) are transmembrane receptors, and together with G-proteins, they are involved in mediating a wide range of signals such as proteins, peptide, hormones, amino acids, light, calcium etc [91]. Heterotrimeric G-proteins consist of three main subunits, G alpha (α), G beta (β) and G gamma (γ). Binding of the signals to the receptor GPCR stimulates exchange of GDP-GTP on Gα subunit. As result, there is a conformation change in Gα subunit which promotes the dissociation of Gαβγ complex. Dissociated Gα and Gβγ subunits in turn interact with downstream components to transduce the signal. In *Cryptococcus neoformans*, a total of 31 putative G-protein coupled receptors have been identified [92, 93]. Three Galpha subunits (Gpa1, Gpa2 and Gpa3), one Gβ subunit (Gpb1) and two Gγ subunits (Gpg1 and Gpg2) have been identified in *Cryptococcus* [92, 93].

Some of the signaling pathways known to regulate sexual development in *Cryptococcus* include pheromone sensing MAPK pathway, the nutrient sensing cAMP pathway and the calcineurin pathway. Gα subunit and Gβ subunits seem to function in different pathway to regulate mating in *Cryptococcus neoformans*. The *gpb1* mutant is completely sterile even in bisexual mating, however, the *gpa1* mutant is leaky and can still produce spores after longer incubation with a mating partner. cAMP can overcome

the mating defect of *gpa1* mutant but not that of *gpb1* mutant. Similarly, further evidence such as confrontation assays suggest that *gpa1* is not required for pheromone sensing. Moreover, *gpa1* deletion only reduces the frequency of cell fusion whereas the deletion of *GPB1* completely blocks cell fusion. Gpb1 was found to be required for pheromone sensing and mating. Hence these two pathways, one sensing nutrients via Gpa1-cAMP and another sensing pheromone through *GPB1* regulates mating in *Cryptococcus* [94, 95]. The pheromone pathway is essential for bisexual reproduction and functional cAMP pathway help mating.

1.2.3.1.1 Pheromone sensing MAPK pathway in *C. neoformans*

One of the well-studied signaling pathways that is crucial for sexual development in *Cryptococcus* is the pheromone sensing MAPK pathway. *Cryptococcus neoformans* genome encodes 3 pheromone genes which are located the *MAT* locus. *MFα1* and *MFα2* are located 18.5kb apart whereas *MFα3* is located 613 bp upstream of *MFα2* [84]. *MFα* pheromone functions in an autocrine manner to regulate filamentation and sporulation in *MAT*α cells. It also acts on cells of opposite mating type in a paracrine manner to regulate sexual development similar to what has been found in other fungi [84]. Pheromone is exported out of the cell through the pheromone transporter *STE6*. Binding of the pheromone to the pheromone receptor Ste3 causes Galpha subunit to exchange GDP to GTP which in turn leads to conformational change causing dissociation of Gβγ subunits. Gα and Gβγ subunit in turn activate the downstream cascade. Gpa1 is known to sense and respond to nutrients whereas Gβ subunit is required for sensing pheromone [93, 96]. The pheromone pathway MAPK cascade downstream of Gpb1 consists of

STE20, *STE11*, *STE7,* and *CPK1*. In *Saccharomyces cerevisiae*, Ste12 is the downstream transcription factor of pheromone pathway. However, Ste12 shows different function in *Cryptococcus*. Transcription factor Mat2 functions downstream of the MAPK cascade of the pheromone pathway to induce transcription of the genes in pheromone sensing pathway [97]. Mat2 is a 660 amino acid long HMG (high mobility group) domain protein. It was identified as one of the candidate genes required for yeast to hyphae transition during insertional mutagenesis [4]. Mat2 is required for cell fusion and activation of the pheromone pathway [4]. Deletion of Mat2 locks the cells in yeast for and no further cellular differentiation takes place in both unilateral and bilateral mating [4].

Studies have shown that components of the pheromone sensing pathway severely impair bisexual mating in *Cryptococcus*. Deletion of pheromone genes reduces the cell fusion products obtained from bisexual mating and also affects unisexual mating. A similar defect in bisexual mating is found for the deletion of pheromone receptor *STE3* and pheromone transporter *STE6* [98, 99]. Other components of pheromone sensing pathway such as Ste11, Ste7 and Cpk1 display unilateral mating defect due to block in pheromone sensing [95, 100]. However, for unisexual mating some of the components of pheromone sensing pathway have been shown to have minimal effect (Wang et al. 2000, Davidson et al. 2003, Hsueh et al. 2007, Chung et al. 2002, Hsueh et al. 2005). The effect and implication of the pheromone pathway on unisex will be discussed again in Chapter IV.

1.3 Relationship between Morphology and Virulence

Hyphal cells are better in expansion and penetrating physical barriers. However, yeast cells better tolerate osmotic stress and are more efficient in dispersal in liquid [101-107]. Morphotype transition is a common strategy adopted by many fungal pathogens. *Ustilago maydis* is a biotrophic plant pathogen which needs a dikaryotic hypha state for this fungus to infect plant [108]. This relationship between morphology and virulence has been observed in dimorphic fungi such as *Penecillium marnefiii*, *Blastomyces dermatitidis* and *Histoplasma capsulatum* [109-112]. Dimorphism refers to the ability of these fungi to generate two different morphotypes of cells mainly yeast and hyphae. These dimorphic fungi are in filamentous form under ambient temperature in soil, which is the non-pathogenic form. They switch to a pathogenic yeast form in mammalian host at high temperature.

The morphological switch is associated with changes in the composition of components within the cell wall as well as induced expression of phase-specific proteins. For *Blastomyces dermatitidis*, one of the yeast phase specific genes that is required for its virulence is *BAD1* [113]. In *Blastomyces dermatitidis*, the change to the yeast morphotype is associated with increased α-(1,3)-glucan and decreased β-(1,3) glucan. The level of α-(1,3)-glucan is correlated with virulence in this fungus as well as in other dimorphic fungi [111, 114, 115]. For *C. albicans*, however, yeast is the commensal form and its transition to hypha form is required to cause invasive infection. It also provides a means for the fungus to escape from the phagocytic cells [116]. Hence, understanding the relationship between morphology and virulence can provide insight regarding the

pathogenesis of these fungi. *Cryptococcus neoformans* can undergo morphological transition during sexual development.

1.3.1 *C. neoformans* morphotypes and morphotype transition

C. neoformans can exist in different morphotypes such as yeast, giant cells (titan cells), hyphae and pseudohyphae. Yeast is the most common form found in human and animal tissues during infection. Yeast cells usually range in diameter from 5-10 μm. Pseudohyphae are short chains of yeast like cells and they are intermediate between yeast and true hyphae. Cells of pseudohyphae are separated by constriction rather than septa as in hyphae. Hyphal forms are the multicellular forms in which the cells are marked by septa. Pseudopyphal and hyphal form are rarely found during infections [117]. Giant /titan cells on average have a diameter between 20-60 μm. However, cells with diameter up to 100 μm have been observed. Giant cells not only have larger capsule but also larger body size with upto 900-fold increase in cell volume [118, 119]. And these were mostly polyploid cells with 4C or 8C DNA content [119]. These cells were more resistant to oxidative stress such as H_2O_2 [119, 120]. The hyphal form of *Cryptococcus* was first discovered when a *Cryptococcus* strain, named as Coward strain (NIH-12α) of Serotype D was isolated from a patient. The strain formed hyphae when grown on solid media [121]. The sexual state of *Cryptococcus* was later reported by June Kwon-Chung in 1975 [74, 76].

The switch between different morphotypes occurs in *Cryptococcus* either during sexual development or during interaction other organisms. For example, the

pseudohyphal form of *Cryptococcus* was observed during co-incubation with soil amoeba, *Acanthamoeba polyphaga* for a period of 2-3 weeks [122]. During co-incubation, yeast cells were phagocytosed and killed by amoeba whereas the few surviving cells were found to assume the pseudohyphal form. *Cryptococcus* can efficiently mutate to pseudohyphal form and revert back to yeast form [123]. Because both *Cryptococcus* and amoeba are free living organism in the soil, amoeba represents the natural predator of *Cryptococcus*. Hence, assuming a pseudohyphal form might be a strategy to escape the killing by amoeba.

In *C. neoformans*, subtle clues between morphology and virulence have been observed from early times. In the majority of cryptococcal infections, yeast cells are found within tissues. First hyphal forming strain of *Cryptococcus* Coward strain, was isolate from a patient with cryptococcal osteomyelitis and cellulitis. It was a nonmeningitic form of cryptococcosis. Hyphal fragments of this Coward strain, when injected into mice, developed cryptococcosis at lower rate compared to the yeast cells [124, 125]. Similarly, animal experiments have been done on the pseudohyphae of *Cryptococcus* as well. Animals infected with yeast cells died, whereas the majority of the animals infected with pseudohyphae did not die [122, 126]. No viable cells were recovered from the brain of the mice infected with pseudohyphae. However, the presence of mixed population of yeast cells and pseudohyphal cells could be observed in the brain homogenized tissue after 28 days of infection [126]. When pseudohyphal cells revert back to yeast, the cells regain its virulence potential [123].

1.3.2 Molecular link between morphology and virulence

The genetic link for the morphotype transition from yeast to hyphae was identified in 2010 [4]. Znf2, the master regulator of filamentation in *Cryptococcus*, was identified through transcriptome analysis of the microarray data in which the genes that were highly expressed in the hyperfilamentous strain XL280α was compared to a non-filamentous strain XL34α [4]. *ZNF2* is located on chromosome 8, which is different from that of the *MAT* locus on chromosome 4. It is a C2H2 zinc finger transcription factor with four zinc fingers at the N-terminus and encodes for a 738 amino acid protein.

Deletion of *ZNF2* abolishes filamentation during both unisex as well as bisexual reproduction. More details about the phenotype of Znf2 can be found Chapter II and Chapter IV. Even though filamentation is abolished in the *znf2*Δ deletion mutant, the ability to produce or respond to pheromone is not affected in this mutant. Cell fusion is not impaired during bisexual mating of *znf2*Δ mutants [4]. These data clearly suggest that inability of *znf2*Δ mutant to filament in not a result of any defect in early mating process. Rather its inability to grow hyphae prevent this fungus from completing its sexual development. Overexpression of *ZNF2* drives filamentation under all conditions tested [9].

Until the identification of Znf2, it has been challenging to conduct in vivo study to investigate the relationship between morphology and virulence in *Cryptococcus*. Host relevant conditions (such as high temperature, high levels of CO_2 and aqueous environment) are all inhibitory to mating or the formation of filaments. Hence, the

filamentous state is hard to maintain under host relevant conditions. Identification of Znf2 as the master regulator of filamentation makes it feasible to induce filamentation under host conditions to study the relationship between morphology and virulence. Animal experiments done with WT and *ZNF2*^{oe} showed that mice inoculated with WT died within 3 weeks [9]. However, mice inoculated with *ZNF2*^{oe} continued to live till 60 days when the experiment was terminated [9]. Thus, Znf2 bridges morphotype with *Cryptococcus* virulence potential.

1.4 Summary and Thesis Research

C. neoformans can exist in yeast or filamentous forms, with the yeast form being the pathogenic form. This yeast to hyphae transition occurs in this fungus during sexual reproduction. This study focuses on trying to understand the key events that take place during sexual development of this fungus.

The study in chapter II of this thesis was designed to understand one of the events that takes place during sexual development, transmission of parental mitochondrial DNA in the progeny. During sexual reproduction, in addition to the faithful transmission of nuclear genome, organelles also get transmitted to the progeny. The nuclear genome of meiotic progeny comes from the recombination of both parental genomes, whereas the meiotic progeny could inherit mitochondria from one, the other, or both parents. In fact, one fascinating phenomenon is that mitochondrial DNA in majority of eukaryotes is inherited from only one particular parent. Typically, such unidirectional and uniparental inheritance of mitochondrial DNA can be explained by

the size of the gametes involved in mating, with the larger gamete contributing towards mitochondrial DNA inheritance. However, in *C. neoformans*, bisexual mating involves the fusion of two isogamous cells of mating type (*MAT*) a and *MAT*α, yet the mitochondrial DNA is inherited predominantly from the *MAT***a** parent. Studies done on higher eukaryotes have shown that the transmission of paternal mitochondrial DNA is controlled at both prefertilization and postfertilization stages to produce such precise uniparental inheritance. Here, we show that even in a simple microbe there is prezygotic control in addition to the postzygotic control for the mitochondrial inheritance underscoring the importance of this ubiquitous phenomenon.

Chapter III of this study is designed to understand the changes in the expression of some important genes in the development of *C. neoformans*. *Cryptococcus* mating colony is heterogeneous. Heterogeneity is an important bet-hedging strategy for non-mobile microbes like fungi to adapt to the unpredictable environmental changes. Only a subset of yeast cells switch to hyphae, and only a fraction of the hyphal subpopulation will develop into fruiting bodies where meiosis and sporulation occurs. Through the investigation of a basidiomycetes-specific secretory protein family, we found that some of these proteins are cell-type specific, thus contributing to the heterogeneity of a mating colony. Our study also demonstrates the importance of examining the protein expression pattern at individual cell level in addition to the population gene expression profiling in the investigation of a heterogeneous community. Furthermore, our findings also suggest that secretory proteins with no known enzymatic functions might serve as sensors for the non-mobile microbe of its immediate environment.

Chapter IV of this study tries to understand the sexual reproduction conundrum present within the population of *Cryptococcus*. *Cryptococcus neoformans* can undergo **a**-α bisexual and unisexual reproduction. Although similar factors such as pheromone and environmental conditions are known to stimulate both unisexual and bisexexual reproduction, bisexual reproduction is far more efficient under laboratory conditions. Bisexual reproduction generates equal number of **a** and α progeny, but α dominates in nature. Population genetic studies suggest that unisex might have contributed to the sharply skewed distribution of the mating types. However, the predominance of the α mating type and the seemingly inefficient unisexual reproduction presents a conundrum. Through this study we discovered that unisexual reproduction is more efficient than bisexual reproduction under a previously unrecognized condition. These findings of this study indicate that *Cryptococcus neoformans* can propagate sexually under conditions that might have been considered non-conducive for mating. Importantly, these findings also demonstrate that pheromone, although crucial for non-self-recognition, is not critical for the completion of sexual development.

Hence, the studies in this thesis provide new insight regarding the events that take place during sexual development in this fungus with regards to the transmission of mitochondrial DNA and the changes in the expression of cell surface proteins with different morphotypes. Furthermore, the findings of this study that there are conditions, previously unknown, that can promote very efficient unisexual sexual development can provide insight regarding the plasticity of sexual development rewired by this fungus for adaptation in different environment.

2 PREZYGOTIC AND POSTZYGOTIC CONTROL OF UNIPARENTAL MITOCHONDRIAL DNA INHERITANCE IN *CRYPTOCOCCUS NEOFORMANS*[1]

2.1 Introduction

Organelle genomes are unique from nuclear genomes in their ability to replicate multiple times per cell cycle, to segregate during both mitosis and meiosis, and to be inherited uniparentally [127, 128]. Uniparental inheritance of organelle genomes is pervasive in sexual eukaryotes and is observed across a wide variety of organisms, including fungi, protists, plants, and animals [127-131]. Uniparental inheritance of organelle genomes is shown to help prevent the spread of deleterious mutations present in organelle genomes as well as harmful parasites present in the cytoplasm [127]. In particular, defects in mitochondrial inheritance can cause senescence in fungi [132], and male sterility in plants [133]. Thus, uniparental mitochondrial inheritance has been a subject of intense interest. However, despite the widely accepted view regarding the importance of uniparental mitochondrial inheritance, the timing and the underlying mechanisms of such inheritance pattern during sexual reproduction are highly debated.

In the fungus *Cryptococcus neoformans*, bisexual reproduction commences when yeast cells of opposite mating types (**a** and α) are in close proximity under appropriate

[1] Content of this section has been published in this or similar form in mBio and has been used here with the permission of American Society for Microbiology. Copyright retained by the authors.
Gyawali R, Lin X. 2013. Prezygotic and Postzygotic Control of Uniparental Mitochondrial DNA Inheritance in *Cryptococcus neoformans*. mBio **4**:e0012-13.

conditions. Mating in this fungus involves the formation of conjugation tubes by α cells in response to the pheromone produced by nearby **a** cells [134]. Cytological studies showed that there is unidirectional nuclear migration from the α cell to the **a** cell during conjugation [134]. The cell fusion product contains the nuclear genomes of both parents and is equivalent to the zygote of plants and animals [135]. The parental nuclei congress but do not fuse after the α-**a** cell fusion event. A dikaryotic mating hypha emerges from the zygote by the side of the original **a** parental cell, followed by septation between the zygote and the growing dikaryotic hyphae [134]. The dikaryon can be maintained in the hyphal form indefinitely until the formation of basidia, where nuclear fusion and meiosis occur. Recombinant spores are generated subsequently from the basidia, forming four spore chains (Figure 2.1). If the environmental temperature is high, nuclear fusion takes place in dikaryon to form a stable diploid, which can differentiate to form monokaryotic hyphae and give rise to spores when the temperature lowers [136]. It has been well-established that progeny of α-**a** sexual reproduction inherit mitochondrial DNA (mtDNA) predominantly from the **a** parent [137, 138]. The uniparental mtDNA inheritance pattern appears to be established early during sexual reproduction as intermediate cell types examined predominantly inherit the **a** parental mtDNA [137, 138], but the timing of such event has not been defined. The protein complex Sxi1α/Sxi2**a** formed after cell fusion event was shown to control the uniparental mtDNA inheritance postzytotically [3, 139]. This protein complex is required for the production of dikaryotic hyphae and the completion of sexual development [140, 141]. Sxi1α/Sxi2**a** have no apparent role in the early mating events such as pheromone sensing and cell

fusion. How the Sxi1α/Sxi2**a** complex formed in the zygote helps achieve the uniparental mtDNA inheritance is currently unknown.

Based on these previous observations, several non-exclusive hypotheses can be envisioned to explain the uniparental mtDNA inheritance from the **a** parent in *C. neoformans*: 1) blockage of the α mitochondria from entering the zygote (prezygotic control); 1) incomplete cytoplasmic mixing and preferential mating hyphal formation from the **a** parental side (postzygotic control due to position effect); or 3) selective degradation of α mitochondria or selectively preservation of the **a** mitochondria in the zygote due to prezygotic marking (a cooperation between the between both control).

In this study, we employed genetic approaches to examine the timing and the factors that control the mtDNA inheritance in *C. neoformans*. We specifically focused on the key components that function during sexual development as uniparental mtDNA inheritance is only observed during **a**-α matings [2]. Our findings argue against the hypothesis that postzygotic control due to position effect is important for the determination of the uniparental mtDNA inheritance pattern. The data indicate that mtDNA inheritance pattern is determined in the original mature zygote and α mitochondria can efficiently enter the zygote but are subsequently degraded during zygote maturation. Our observations support the role of prezygotic factor Mat2 in the control of uniparental mtDNA inheritance. We propose that the **a** mtDNA inheritance in *C. neoformans* is determined through selective preservation of **a** mitochondria and elimination of α mitochondria in the zygote, assisted by differential marking by Mat2 prior to the cell fusion event and degradation mediated by Sxi1α/Sxi2**a** in the zygote.

Thus, uniparental mtDNA inheritance in *C. neoformans* is controlled both at the postzytotic level as well as the prezytotic level.

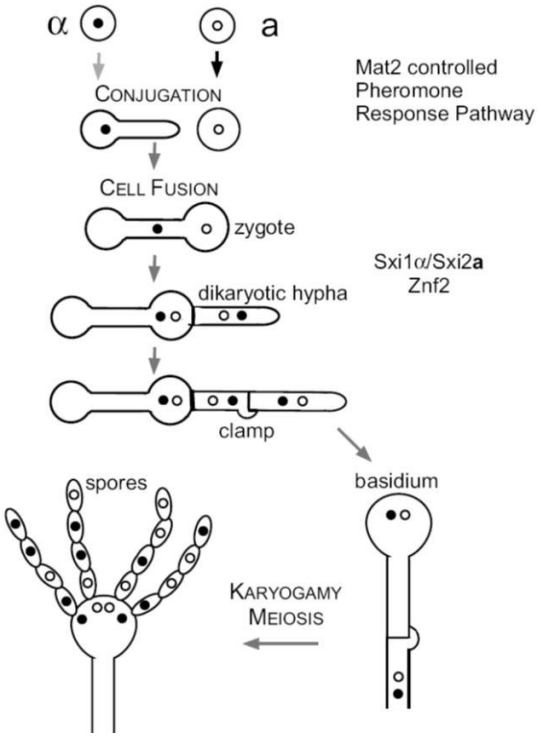

Figure 2.1 Bisexual mating of *Cryptococcus neoformans*.
Under mating-inducing conditions, **a** and α cells undergo cell fusion. The early events during mating are controlled by the pheromone sensing and response pathway. Following cell fusion, the original zygote sends out the dikaryotic hypha, which grows filamentously as heterokaryotic dikaryons. Nuclear fusion and meiosis occur in the basidium formed at the tip of the aerial hypha. Four chains of spores are then generated from the basidium. Transcription factor Mat2 is essential for cell fusion [4, 5], the mating-type-specific homeodomain complex Sxi1α/Sxi2**a** is specifically required for dikaryotic hypha formation and the completion of sexual development [6, 7] , and the transcription factor Znf2 is essential for hyphal formation under all conditions [9].

2.2 Materials and Methods

2.2.1 Strains

Strains used in this study are listed in Table 2.1 along with their genotypes. Mating was carried out on V8 medium at 22˚C in dark as described previously [4].

Table 2.1 Strains used in this study.

Strain name	Genotype	Source and comments	Background
XL280α	*MAT*α (WT)	[87]	XL280
XL280**a**	*MAT***a** (WT)	[142]	XL280
LW192α	P_{CFL1}-*CFL1::mCherry:: NEO*^{r}	Wang, Zhai [9]	XL280
JEC21α	*MAT*α (WT)	[143, 144]	JEC21
JEC20**a**	*MAT***a** (WT)	Congenic with JEC21 [143, 144]	
KN99α	wild type	Isogenic with H99 [145]	H99
KN99**a**	wild type	Congenic with H99/KN99α [145]	H99
XL574α	*znf2*::*NAT*^{r}	[146]	XL280
XL942α	*mat2::NAT*^{r}	[4]	XL280
RG354α	*cnb1::NEO*^{r}	This study	XL280
RG359α	*cnb1::NEO*^{r}*mat2::NAT*^{r}	This study	XL280
RG426α	*cna1::NAT*^{r}	This study	XL280
RG437α	*cna1::NAT*^{r} *mat2::HYG*^{r}	This study	XL280
RG438α	P_{CTR4}-*mCherry-ZNF2-NEO*^{r}*cna1::NAT*	This study	XL280
RG427α	*cna1::NAT*^{r}*CNA1::NEO*	This study	XL280
RG428α	*cna1::NAT*^{r}*CNA1::NEO*	This study	XL280
XL926α	*mat2::NAT*^{r}	[4]	JEC21
LW329	*mat2::NAT*^{r} P_{CFL1}-*CFL1::mCherry:: NEO*^{r}	This study	XL280
RG446	*mat2::NAT*^{r} P_{GPD1}-*DHA1::mCherry:: NEO*^{r}	This study	XL280
RG421	P_{GPD1}-*DHA1::mCherry:: NEO*^{r}	This study	XL280

Table 2.1 Continued

Strain name	Genotype	Source and comments	Background
RG410	*cnb1::NEO*^{r}*mat2::NAT*^{r}P_{GPD1}-*ZNF2::HYG*^{r}	This study	XL280
RG341	*mat2::NAT*^{r}*MAT2::NEO*^{r}	This study	XL280
RG450	*mat2::NAT*^{r}P_{GPD1}-*ZNF2::HYG*^{r}	This study	XL280
RG349	*crz1*::*NEO*	This study	XL280
RG379	*crz1*::*NEO*, *mat2*::*NAT*	This study	XL280
RG318	*znf2*::*NAT mat2*::*NEO*	This study	XL280
LW538	P_{CTR4}-*mCherry-ZNF2-NEO*^{r}	This study	XL280
WSC18	*mfα1::ADE2 mfα2,3::URA5 ade2 ura5*	[147]	JEC21
YPH134	*ste6::URA5*	[99]	JEC21
	*MAT*α, *dha1*::*NAT*	Madhani HD, FGSC 2015, Plate 11, well F7	H99
	*MAT*α, *dha2*::*NAT*	Madhani HD, FGSC 2015, Plate 8, well G4	H99
	*MAT*α, *cpl1*::*NAT*	Madhani HD, FGSC 2015, Plate 3, well C9	H99
	*MAT*α, *cfl105*::*ss*	Madhani HD, FGSC 2015, Plate 10, well C8	H99
BZ30α	*cfl1*::*HYG*	This study	H99
LW303α	P_{CTR4}-*CFL1::mCherry*(sigPΔ)*:: NEO*^{r}	[9]	H99
RG249α	P_{CTR4}-*DHA1::mCherry:: NEO*^{r}	This study	H99
RG264α	P_{CTR4}-*CPL1::mCherry:: NEO*^{r}	This study	H99
RG251α	P_{CTR4}-*CFL105::mCherry:: NEO*^{r}	This study	H99
RG425α	P_{CTR4}-*DHA2::mCherry:: NEO*^{r}	This study	H99
LW204α	P_{CTR4}-*CFL1::mCherry:: NEO*^{r}	[9]	H99
RG48α	*dha1*::*NEO*	This study	XL280
RG117α	*dha2*::*NAT*	This study	XL280
RG212α	*cpl1*::*NEO*	This study	XL280
RG192α	*cfl105*::*NEO*	This study	XL280
XL1359α	*cfl1*::*NEO*	[9]	XL280
RG107α	*dha1*::*NAT*	This study	H99
RG83α	P_{DHA1}-*DHA1::mCherry:: NEO*^{r}	This study	XL280
RG153α	P_{DHA2}-*DHA2::mCherry:: NEO*^{r}	This study	XL280

Table 2.1 Continued

Strain name	Genotype	Source and comments	Background
RG182**a**	*dha2*::*NAT*	This study	XL280
JW7**a**	*cpl1*::*NEO*	This study	XL280
JW1**a**	*cfl105*::*NEO*	This study	XL280
BZXL2**a**	*cfl1*::*NEO*	This study	XL280
XL342	Dα, *ade2*	[148]	JEC21
XL368	D**a**, *ade2*	This study	JEC21
F99	Aα, *ura5*	[149]	H99
JF99	A**a**, *ura5*	[150]	H99
XL875	Dα, *znf2*::NAT, *ade2*	[4]	JEC21
XL873	Dα, *znf2*::*NAT*^{r} *ura5*	[4]	JEC21
XL1601	Aα, *znf2*::NEO, *ura5*	[4]	H99
XL1723	A**a**, *znf2*::NEO, *ura5*	Isolated from a cross between XL1601 and JF99. Selected on 5-FOA medium	H99
XL870	D**a**, *znf2.2*::NAT, *ura5*	[4]	JEC21
XL1559	A**a**, *ade2*	Isolated from a cross between M049 and KN99**a**	H99
XL1721	Aα, *znf2*:: NEO, *ade2*	Isolated from a cross between XL1601 and XL1559	H99
YSB119	Aα *aca1*::NAT ^{r} *ura5 ACA1-URA5*	[151]	H99
YSB121	A**a** *aca1*::NEO ^{r} *ura5 ACA1-URA5*	[151]	H99
CHY618	Dα, *ura5*, *sxi1*α::NAT	[140]	JEC21
CHY766	D**a**, *ura5*, *sxi2***a**::*URA5*	[152]	JE21
RG40	A**a,** P$_{GPD1}$-*MAT2*-NEO	Isolated from a cross between LW80α and JF99**a**	H99
RG43	Aα, P$_{GPD1}$-*MAT2*-NEO	5-FOA selection of the LW80α strain	H99
LW80	Aα, P$_{GPD1}$-*MAT2*-NEO	[9]	H99
JF271	A**a,** *sxi2***a**::NAT *ura5*	[153]	H99
RG44	A**a,** *sxi2***a**::NAT *ura5* P$_{GPD1}$-*MAT2*-NEO	Introduction of P$_{GPD1}$-*MAT2*-NEO into JF271	H99

Table 2.1 Continued

Strain name	Genotype	Source and comments	Background
RG37	A**a**, P_{GPD1}-*MAT2*-NEO, ura5	Isolated from a cross between LW80α and JF99**a**	H99
RG48	D**a**, *ura5*, *sxi2***a**::*URA5,*G418	Introduction of NEO marker in CHY766	JEC21
CPS3	Aα *aif1::NAT*	[154]	H99
CPS15	A**a** *aif1::NAT*	[154]	H99
XL491	D**a**, NEO	Introduction of NEO marker in JEC20	JEC21
XL1413	Dα, NEO	Introduction of NEO marker in JEC21	JEC21

2.2.2 Generation of *MAT2* overexpression strains

The *MAT2* overexpression in mating type **a** strain was obtained by crossing LW80 (*MAT*α, P_{GPD1}-*MAT2*-NEO) [9] and JF99 (*MAT***a**, *ura5*). Mating was carried out for 14 days on V8 pH5. The mating type of the spores generated was confirmed by mating with reference strains JEC20**a** or JEC21α on V8 juice agar media. Colonies that mated with JEC21α but not with JEC20**a** and are resistant to G418 were selected. Auxotrophic strains were confirmed by the absence of growth on the selective SD-URA media.

The *MAT2* overexpression in the *sxi2***a**Δ strain was obtained by transforming the construct P_{GPD1}-*MAT2*-NEO [9] into the *sxi2***a**Δ mutant through electroporation as described previously [155]. Stable transformants were selected and the ability of these

strains to produce filamentation on its own and enhanced mating filaments were confirmed on V8 juice agar media as described previously [9].

2.2.3 Generation of *ura5* auxotrophic strains

For generating *ura5* auxotrophic strains, freshly grown strains on YPD were collected and washed twice with water. Strains were then plated on 5-FOA plates (6.7 g/L or 0.67% Yeast Nitrogen Base without amino acids, 50 mg/L Uracil, 2% Bacto Agar, 2% Dextrose, 1g/L 5FOA, SC media without uracil). Strains that grew on 5-FOA plates but failed to grow on SD-URA5 plates were selected as *ura5* auxotrophic strains as described previously [156]. Only strains showed stable auxotrophic phenotype after several passages were used in this study.

2.2.4 Mating assays

Parental strains of serotype D and serotype A of different mating types were grown on YPD agar (2% Bacto Peptone, 1% Yeast Extract, 2% Dextrose, 2% Bacto Agar) at 30°C. Mating was performed on V8 juice agar plates (5% V8 juice, 0.5 g/L KH_2PO_4 , 4% Bacto Agar, pH 7) by mixing equal number of cells of opposite mating types. The coculture was incubated at 22°C in dark for 2-3 days. Mating mixtures were then scrapped off the V8 agar plates, washed with water, and plated on selective media. To select products of the cell fusion events between two auxotrophic strains, cells were plated on minimal YNB media (6.7 g/L or 0.67% Yeast Nitrogen Base with no amino acids, 2% Bacto Agar, 2% Dextrose) and grown for additional 3 days at 37°C. To select products of the cell fusion events between two dominant marked strains, cells were

plated on YPD agar media supplemented with G418 and NAT and incubated for additional 3 days at 37°C. To select products of the cell fusion events between a *ura5* auxotrophic strain and a dominant marked strain (NAT or NEO), cells were plated on Proline+NAT or Proline+G418 agar media and incubated for additional 3 days at 37°C as described previously [140].

2.2.5 Determining the mitochondrial genotype

The natural size polymorphism present in the cytochrome B subunit 1 gene (*COB1*) between Serotype D and Serotype A strains was used to determine mitochondrial DNA genotype of the fusion product as described previously [1]. In Serotype A, *COB1* contains 1 intron whereas in case of Serotype D, it carries 2 introns. Thus, PCR amplification of *COB1* gene using the forward primer (5'-CCACAACCTATTAACATTAGCTACGC-3) and the reverse primer (5-CGTCTCCATCTACAAAGCCAGCAAAC-3') yielded products of 610 bp in serotype A and 1585 bp in serotype D [1]. PCR reaction condition used was as follows: 2 mins at 96°C, then a cycle of 35 times with 15 seconds at 96°C, 15 seconds at 55°C and 1 minute 30 seconds at 72°C and a final extension of 7 minutes at 72°C. PCR products were run on agarose gels and stained with ethidium bromide for visualization under ultraviolet light.

2.2.6 Statistical test

Statistical tests were performed using GraphPad Prism version 5.04. Fisher's exact test was used to analyze if the inheritance pattern of mitochondrial DNA from the

a and the α parent is statistically different across various crosses compared to the control crosses. A p-value lower than 0.05 is considered statistically significant.

2.2.7 Phenotypic assays

Phenotypic assays were performed as previously described [148]. Briefly, yeast cells of strains to be tested were grown on YPD liquid medium overnight and washed three times with water. The optical density of the cultures was measured at 600 nm and all cultures were adjusted to the same cell density. Cells were then serially diluted by 10 fold. To examine melanin production, cells were spotted on melanin-inducing media containing L-dihydroxyphenylalanine (L-DOPA) (100 mg/liter) and incubated at 22°C and 37°C in the dark for 2 to 6 days. Melanization was visualized as the colonies developed a brown color. To analyze growth at different temperatures, cells were spotted on YPD medium and incubated at the indicated temperatures for 2 days. To characterize capsule production, cells were transferred to Dulbecco's modified Eagle's medium (Invitrogen, California) and grown for 3 days at 37°C. Cells were then suspended in India ink, and the capsule was visualized as a white halo surrounding the yeast cell due to the exclusion of ink particles.

2.2.8 Measurement of gene expression levels using real time PCR

Cells of overnight culture of JEC20 and JEC21 in liquid YPD medium were washed twice with water. For **a** and α alone cultures, equal number of JEC20 and JEC21 cells were plated on V8 pH7 plate separately. The cell number was determined via measurement of optical density at OD600. For **a**-α mating cultures, equal number of

JEC20 and JEC21 cells were mixed and then plated on V8 pH7 plates. Cells were collected at 0.5 hr, 1 hr, 2 hr, 3 hr, 4 hr, 6hr, 8 hr, and 10 hr of incubation. Collected cells were lyophilized before RNA extraction. The total RNA was extracted using the Ambion RNA extraction kit according to the manufacturer's instructions. The RNA samples were treated with DNase I and potential DNA contamination was examined using the treated RNA as template for PCR using the *TEF1* gene (Lin lab 327/328; 5'-CTCTGGTTGGCACGGTG-3' and 5'-CGTCGGTCAATCTTCTCG-3') using the following PCR condition (annealing temperature: 55 ^{0}C, extension: 45 sec, cycles: 40). Only RNA samples not contaminated with DNA were used for realtime PCR. Integrity of the RNA samples was examined by gel electrophoresis at multiple steps during this process. The first strand cDNA synthesis was carried out using SuperScript III kit (Invitrogen) according to the manufacturer's instructions. KAPA SYBR FAST qPCR master mix was used for performing realtime PCR. Gene expression levels were normalized based on the *TEF1* expression level as previously described [157] [9]. Primers are listed as follows.

TEF1 (Lin lab 329/330)

(5'-CGTCACCACTGAAGTCAAGT-3') and (5'-AGAAGCAGCCTCCATAGG-3')

[9]

*MF***a**1 (Lin lab 1269/1270)

(5'-ACGCCTTCACTGCTATCTT-3') and (5'-TAAGCAATAACGCAAGAGTAA-3').

MFα1 (Lin lab 1267/1268)

(5’-ATCTTCACCACCTTCACTTCT-3’) and (5’-CTAGGCGATGACACAAAGG-3’).

2.3 Results

2.3.1 Uniparental mitochondrial DNA inheritance is determined in the original zygote prior to the formation of mating hyphae

Previous studies on mitochondrial DNA inheritance in *C. neoformans* demonstrated that inter-variety mating (hybrid matings between strains of two different serotypes) or intra-variety mating (matings between strains of the same serotype) both lead to uniparental mtDNA inheritance from the **a** parent [2, 137, 138]. Here, we also chose to use intervarietal matings between serotype A and serotype D strains to investigate the factors involved in determining mtDNA inheritance in this fungus for the following reasons. The intervarietal mating shows the same hallmarks as does the intravariety mating (see Fig 2.2); the intervarietal mating also displays uniparental a mtDNA inheritance. The meiosis-associated problems due to genome divergence occur later at basidia during the late stage of sexual development, which is long after the mtDNA inheritance pattern is established [1, 135, 158-160]. Hybrid mating occur commonly in nature (18–22), and studying mtDNA inheritance in hybrid mating would help our understanding of the genetic makeup of cryptococcal natural populations. Importantly, AD hybrid mating allows us to track the origin of the progeny’s mtDNA based on the serotype-specific size polymorphism of the gene residing in the mitochondria that encodes cytochrome b subunit 1 (*COB1*) [1, 161].

.

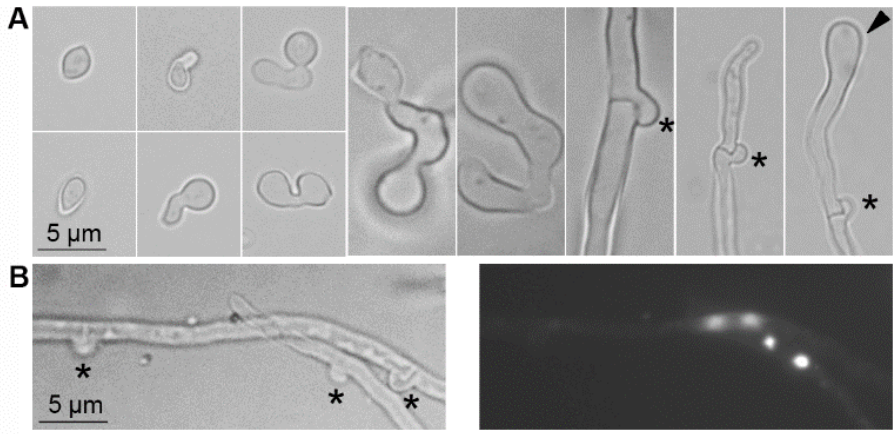

Figure 2.2 AD hybrid matings exhibit the same hallmarks as do intravarietal matings.

(A) The hybrid mating between Aa and Dα strains was examined at multiple time points during sexual development. At early stage, yeast cells become shmoo cells (first column) and then send conjugation tubes (second column). The length of the conjugation tubes depends on the distance between the mating partner cells. The mating partners fuse to produce the original zygote cells (third, fourth, and fifth columns). The original zygote then sends out a heterokaryotic dikaryon with fused clamp cells (sixth column). Some dikaryotic hyphae develop into aerial hyphae (seventh column) and generate swollen basidia (eighth column) where spore chains form. Asterisks, clamp cells; black arrow, basidium. (B) The dikaryotic hyphae with fused clamp cells contain two parental nuclei as visualized through the 4′,6-diamidino-2-phenylindole (DAPI) stain. Asterisks, clamp cells.

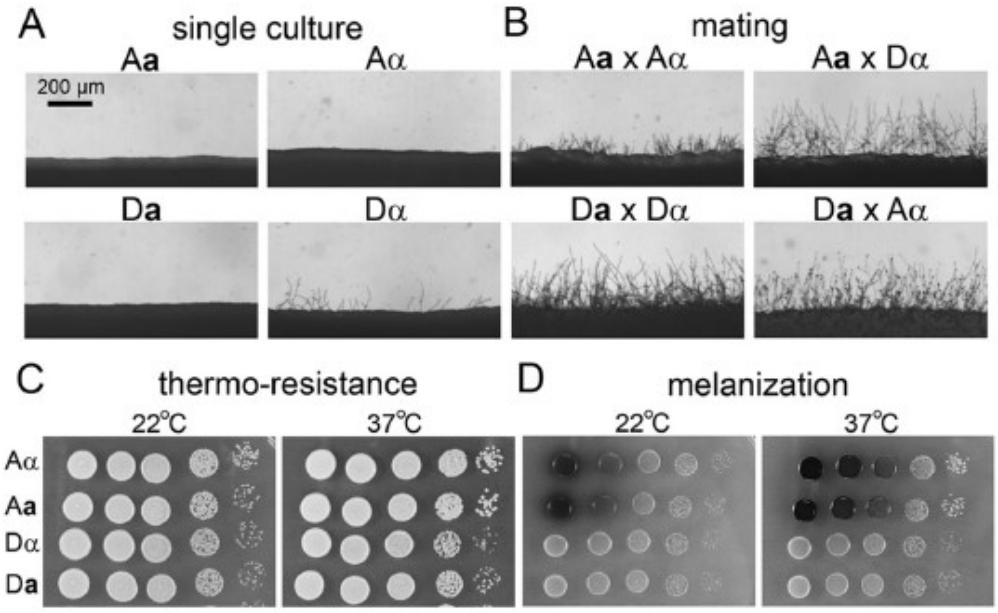

Figure 2.3 Phenotypic differences of the strains used.
(A) Incubation of individual strain on V8 media for 48 hours. A and D represent serotype A and serotype D variety respectively of *C. neoformans* whereas **a** and α represent their mating type. (B) Co-culture of cells of opposite mating types on V8 plate for 48 hours to visualize their filamentation ability. Filamentation produced during mating between same serotypes and for hybrid crosses are shown.

The serotype A congenic pair KN99**a** and KN99α are designated as A**a** and Aα, and the serotype D congenic pair JEC20**a** and JEC21α are designated as D**a** and Dα in this study. The A**a**/Aα strains do not self-filament and they mate poorly with each other (Figure 2.3). The Dα strain does self-filament sporadically after long incubation and the D**a** strain does not self-filament. However, the D**a** and Dα strains mate with each other robustly and they also mate with the Aα or the A**a** strains robustly (Figure 2.3). These strains also differ in other phenotypes, such as thermo-tolerance, melanization, and capsule production [148] (Figure 2.2).

Previous studies have shown that mtDNA inheritance pattern was established at an early but unidentified stage of sexual development. Sexual spores, hyphae, cells budded from the hyphae, or diploids derived dikaryons all inherit mtDNA predominantly from the **a** parent [2, 3, 138]. Here, we used previously established methods and tested the mtDNA of cells derived from the hybrid crosses. As shown in the table, cells derived from the reciprocal hybrid matings showed mtDNA inheritance predominantly from the **a** parent (Table 2.2 crosses 1 and 4).

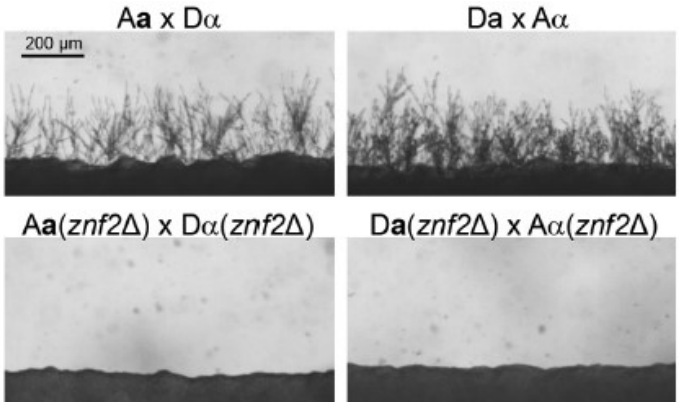

Figure 2.4 Deletion of Znf2 abolishes filamentation.
Robust filamentation is produced during hybrid mating after 48 hours of co-culture. Production of filamentation is completely eliminated in znf2 deletion strains.

Previous studies proposed that the postzygotic control of uniparental mtDNA inheritance could be caused by the incomplete cytoplasmic mixing and subsequent filamentation from the **a** parental side of the original zygote [138]. This hypothesis is reasonable given that in *Saccharomyces cerevisiae*, mtDNA inheritance in daughter cells depends on the budding position on the zygote. If the first bud arises from either end of the zygote, then those cells contain mtDNA from only one parent depending on which parental side the bud arises from. If the first bud arises from middle of the zygote then it contains mtDNA from both the parents [162, 163]. If such a position effect is critical in mtDNA inheritance *C. neoformans*, one would predict that progeny would more likely to inherit mtDNA from the parental strain with enhanced ability to filament. Alterations of the ability to undergo filamentation in the parental strains then could affect the mtDNA inheritance pattern.

Table 2.2 Mitochondrial inheritance from crosses involving *znf2* mutant strains.

	Crosses	mtDNA from the α parent	mtDNA from the **a** parent
1.	A (α) × D (**a**)	4%; (2/50)	82%; (41/50)
2.	A (α) × D (**a**) *znf2*Δ	0%; (0/50)	100%; (50/50)
3.	A (α) *znf2*Δ × D (**a**) *znf2*Δ	2%; (1/48)	87.5%; (42/48)
4.	D (α) × A (**a**)	4%; (2/49)	92%; (45/49)
5.	D (α) *znf2*Δ × A (**a**)	2%; (1/49)	98%; (48/49)
6.	D (α) *znf2*Δ × A (**a**) *znf2*Δ	13%; (6/45)	87%; (39/45)

Note: A minor portion of the progeny in certain crosses were found to inherit mtDNA from both the a and the α parent. Such phenomenon was also observed previously [1-3]. The number of progeny examined from each cross is indicated in parenthesis. Inheritance of mitochondrial DNA from a and α parent in znf2 deletion strains in unilateral crosses or bilateral crosses is not statistically different from the respective wild type cross.

We decided to examine the impact of alterations in the ability to undergo self-filamentation on the mtDNA inheritance pattern through genetic mutations of the *ZNF2* gene. Znf2 is the master regulator of filamentation and it does not control cell fusion events during mating [4, 9]. Deletion of *ZNF2* completely abolishes *C. neoformans* ability to filament (Figure 2.4) [4, 9].

To examine the position effect of mating hyphal formation, we analyzed mtDNA inheritance in crosses involving *znf2*Δ mutants in the **a** or the α mating partner. If the position effect controls the mtDNA inheritance, one would predict a decrease in the inheritance from the **a** parent when Znf2 is deleted in the **a** parental strain. However,

blocking the filamentation ability in the D**a** parental strain did not diminish the predominance of **a** mtDNA inheritance in the unilateral cross A(α) × D(**a**) *znf2*Δ (Table 2.2, crosses 2 and 1, Figure 2.4.A). Similarly, we did not observe any significant change in the mtDNA inheritance pattern in the unilateral cross D(α) *znf2*Δ × A(**a**) where the *ZNF2* gene was deleted in the α parent compared to the control cross (Table 2.2, crosses 5 and 4). Thus, it appears that the position of hyphal formation does not affect the uniparental mtDNA inheritance pattern.

However, because the *ZNF2* gene is deleted only in one parent, the *ZNF2* gene (the wild-type) from the other parent could compensate the loss once the two parental cells are fused. It is shown previously that the deletion of *ZNF2* abolishes mating hypha formation only in bilateral crosses (*znf2*Δ x *znf2*Δ) but not in unilateral crosses (*znf2*Δ x wild-type). Thus we decided to examine mtDNA inheritance in crosses where the *ZNF2* gene is deleted in both parental strains. If the position effect of mating hypha formation is responsible for the uniparental mtDNA inheritance from the **a** parent, abolishing the formation of mating hyphae from the zygote should result in a biparental mtDNA inheritance pattern. Interestingly, bilateral crosses with Znf2 disrupted in both parents yielded uniparental mtDNA inheritance from the **a** parent (Table 2.2, crosses 3 and 6), a pattern similar to the wild-type crosses (Table 2.2, crosses 1 and 4). Again, the results suggest that formation of mating hyphae is not important for the establishment of mtDNA inheritance pattern. Consequently, the position of mating hyphal formation does not determine the uniparental mtDNA inheritance in *C. neoformans*.

Taken together, these results refute the original hypothesis and indicate that mtDNA inheritance is not dependent on subsequent mating hypha formation from the original zygotes. These results also suggest that the pattern of mtDNA inheritance is established in the original zygotes prior to the formation of mating hyphae. This new hypothesis offers a plausible explanation for previous observations that various intermediate cell types obtained from bisexual matings predominantly inherited the mitochondria from the **a** parents [2, 137, 138].

2.3.2 Prezygotic control of uniparental mitochondrial DNA inheritance

The results presented in the previous section indicate that uniparental mtDNA inheritance pattern is established in the original zygote prior to the generation of dikaryotic hyphae. Previous studies demonstrated that the homeodomain protein complex Sxi1α/Sxi2**a**, which is required for the formation of dikaryotic hyphae [140, 141], controls the uniparental mtDNA inheritance in *C. neoformans* [2, 3]. Because this intact protein complex can only form after the cell fusion event as Sxi1α comes from α cells and Sxi2**a** comes from **a** cells, deletion of either the *SXI1*α gene from the α parent or the *SXI2***a** gene from the **a** parent (unilateral matings) has the same effect as the deletion of both genes (bilateral mating). In these unilateral or bilateral crosses, the mtDNA inheritance shows a biparental pattern, and surprisingly with modestly more progeny inheriting the α parental mtDNA [2, 3]. We further confirmed these previous observations in our study (see the next section for details). These observations suggest that the original zygote contains ample mitochondria originated from the α parent.

The idea of existence of modestly more α mitochondria than **a** mitochondria in the original zygote appears to be conflicting to our earlier conclusion that *C. neoformans* establishes the uniparental **a** mtDNA inheritance in the zygote prior to the formation of the mating hypha, which emerges after the zygote formation (Figure 2.2). We envision that rapid and selective degradation of α mitochondria in the zygote could achieve the uniparental **a** mtDNA inheritance and be consistent with the presence of both **a** and α

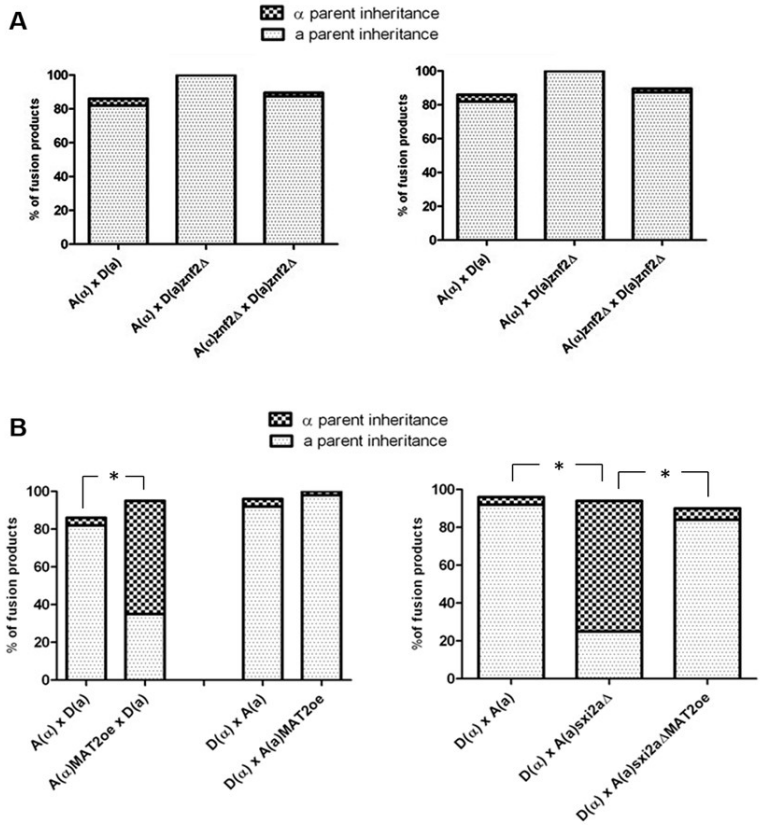

Figure 2.5 Graphic representation of mitochondrial inheritance in the crosses. (A) Inheritance of mitochondrial DNA from **a** and α parents in unilateral crosses or bilateral crosses involving *znf2*Δ mutant strains is not statistically different from that in the respective wild-type crosses. (B) Graphic representation for the effect of *MAT2*^{oe} on the mitochondrial inheritance. *, the inheritance of mtDNA from **a** and α parents is statistically significant across the groups (P value, <0.05).

mitochondria in the newly formed zygote. Such selectively retaining **a** mtDNA in the zygote can be achieved by either prezygotically marking the **a** mitochondria for preservation or the α mitochondria for annihilation followed by rapid degradation of the α mitochondria in the zygote after the Sxi1α and Sxi2**a** form the functional protein complex.

Such a model predicts that efficient selective elimination of the α mtDNA from the zygote relies on selective marking of parental mitochondria (or parental mtDNA) prior to the cell fusion event. Thus, some prezygotic factors must be involved in the control of mtDNA inheritance in *C. neoformans*. We decided to investigate the role of Mat2 in mtDNA inheritance based on its essential role in early stages of mating. Mat2 is the key transcription factor in the pheromone sensing and response cascade [4, 97]. It directs the conjugation process and is required for the cell fusion event during α-**a** mating [4, 9]. A functional *MAT2* gene must be present in both mating partners for cell fusion to occur [4]. The essential role of Mat2 in cell fusion presents a challenge as no zygote can be generated even in unilateral matings where Mat2 is disrupted only in one parent. Hence, we decided to use *MAT2* overexpression ($MAT2^{oe}$) strains where the *MAT2* gene is placed under the control of the constitutively active promoter from the *GPD1* gene [9]. We generated $MAT2^{oe}$ strains in both Aα and A**a** backgrounds. As shown in Figure 2.5, overexpression of *MAT2* confers robust self-filamentation and enhances production of mating hyphae in α-**a** crosses on V8 juice agar media. This is consistent with the established roles for Mat2 [4, 9]: stimulating pheromone production,

driving the formation of mating competent shmoo cells, and enhancing self-filamentation.

Surprisingly, when *MAT2* was overexpressed in the α parent, a modest dominance of α mtDNA inheritance (60%) was observed (Table 2.2., cross 2, A(α)*MAT2*^{oe} × D(a)). Thus, it appears that overexpression of MAT2 in the α parent was able to change the progeny inheritance pattern from predominantly a mtDNA to biparental with modest dominance of α mtDNA. When *MAT2* was overexpressed in the **a** parent, mtDNA inheritance remains uniparental from the a parent (Table 2.3, crosses 5 and 6). To determine whether the dominance of the mtDNA originating from the parental *MAT2*^{oe} strain is caused by an increased number of copies of mtDNA in the *MAT2*^{oe} strains, we compared the ratio of mtDNA (the *COB1* gene) and nuclear DNA (the *TEF1* gene) between the *MAT2*^{oe} strains and the wild-type strains. No difference in the *COB1/TEF1* ratio was observed between the *MAT2*^{oe} strains and the wild-type strains when cells were cultured in either yeast extract-peptone-dextrose (YPD) medium or V8 juice medium (Figure 2.5). Similarly, the deletion of the *MAT2* gene did not alter the ratio of *COB1/TEF1* either (Figure 2.5). Thus, mutations of Mat2, either disruption or overexpression, do not appear to alter the copy number of mtDNA per cell. Furthermore, we found no apparent alterations in mitochondrial morphology in the *MAT2*^{oe} strain compared to the wild type based on microscopic examination (Figure 2.6). Thus, Mat2 promotes the mtDNA inheritance through a means other than increasing the copy number of mtDNA in the cell. The data implicate that Mat2 controls mtDNA inheritance in *C. neoformans*.

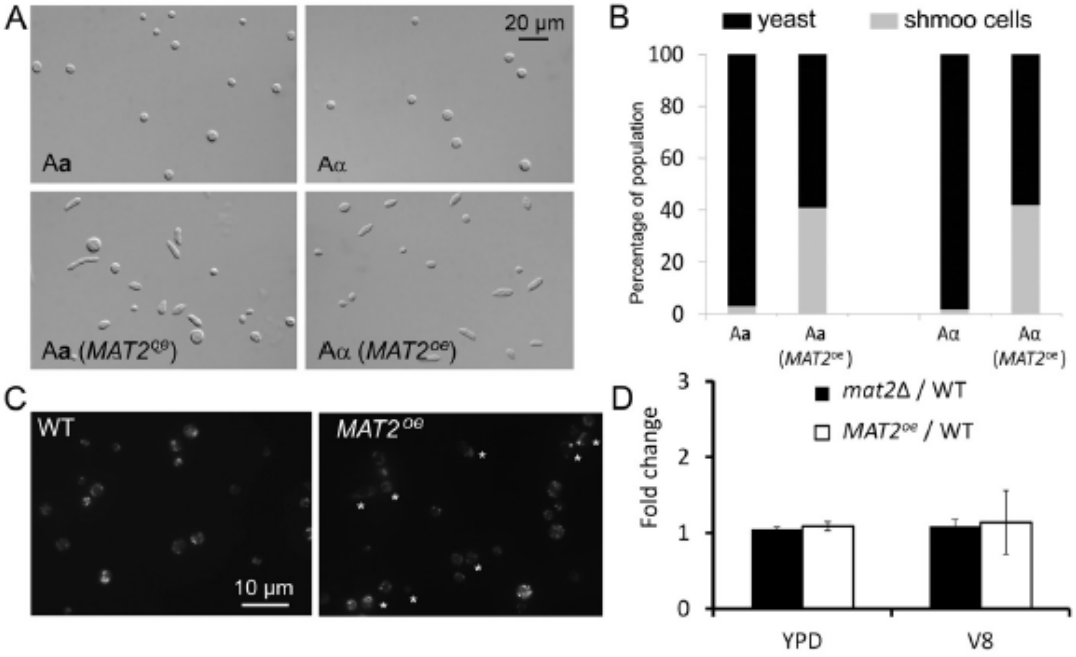

Figure 2.6 Overexpression of *MAT2* drives shmoo cell formation but does not alter mitochondrial morphology or the mtDNA copy number.
(A) The images in the top panel show the round yeast cells of the wild-type (WT) Aa and Aα strains after incubation in V8 medium for 48 h. The images in the bottom panel show the cell morphology (round yeasts and pear-shaped or elongated shmoo cells) of Aa and Aα strains when *MAT2* is overexpressed. (B) Quantification of the distribution of yeast cell morphology and shmoo cell morphology in different populations as shown in panel A. (C) Mitotracker CMXRox-labeled wild-type cells and the *MAT2*^{oe} cells. Stars indicate shmoo cells. (D) The comparison of the *COB1/TEF1* ratios between the wild type, the *MAT2*^{oe} strain, and the *mat2*Δ mutant cultured in YPD and V8 media. All strains shown here were in the Aα background. Similar results were obtained for strains in the A**a** background.

Table 2.3 Effect of mutations of *SXI1*α, *SXI2*a and *MAT2* on mitochondrial inheritance.

	Crosses	mtDNA from the α parent	mtDNA from the **a** parent
1.	A (α) × D (**a**)	4%; (2/50)	82%; (41/50)
2.	A (α) *MAT2*^{oe} × D (**a**)	60%; (52/87)	35%; (31/87)
3.	A (α) × D (**a**) *sxi2***a**Δ	67%; (20/30)	20%; (6/30)
4.	A (α) *MAT2*^{oe} × D (**a**) *sxi2***a**Δ	84%; (36/44)	12%; (5/44)
5.	D (α) × A (**a**)	4%; (2/49)	92%; (45/49)
6.	D (α) × A (**a**) *MAT2*^{oe}	2%; (1/46)	98%; (45/46)
7.	D (α) *sxi1*αΔ × A (**a**)	75%; (36/48)	25%; (12/48)
8.	D (α) *sxi1*αΔ × A (**a**) *MAT2*^{oe}	23.8%; (10/42)	73.8%; (31/42)
9.	D (α) × A (**a**) *sxi2***a**Δ	69.38%; (34/49)	24.5%; (12/49)
10.	D (α) × A (**a**) *sxi2***a**Δ *MAT2*^{oe}	6%; (3/49)	83.6%; (41/49)

The control crosses 1 and 5 are the same as the crosses 1 and 4 in Table 2.2. They are included here for easy comparison and are listed in grey.

2.3.3 Prezygotic control and postzygotic control cooperate to determine mitochondrial DNA inheritance

Next we decided to investigate whether the prezygotic control of mtDNA inheritance regulated by Mat2 is dependent on the postzygotic control regulated by Sxi1α/Sxi2**a**. As observed in previous studies [2, 3], we found that deletion of either the *SXI1*α gene in the α parent or the *SXI2***a** gene in the **a** parent results in biparental mtDNA inheritance in the unilateral matings (Table 2.3, crosses 3, 7, and 9). A modest domination by the α mtDNA inheritance was observed in all these crosses (67%, 75%, and 69% respectively). Modest dominance of α mtDNA among the progeny was also observed previously when either the *SXI1*α gene or the *SXI2***a** gene was disrupted in the parental strains. We found that **s**uch altered mtDNA inheritance pattern is independent of the serotype or the mating type where the mutation occurs. This is consistent with our hypothesis that the newly formed zygote contains both **a** and α mtDNA, with α mtDNA being modestly more abundant.

To examine whether mtDNA inheritance controlled by Mat2 is dependent on the Sxi1α/Sxi2**a** complex, we analyzed mtDNA inheritance pattern of crosses involving one parent overexpressing *MAT2* and the other parent disrupted with the homoedomain complex (Table 2.3, crosses 4 and 8). When *MAT2* is overexpressed in the **a** parent, crossing with the *sxi1*αΔ α strain produced a modest dominance of **a** mtDNA inheritance among the progeny (74%), compared to the mere 25% **a** mtDNA inheritance in the cross between A**a** and D(α) *sxi1*αΔ strains (Table 2.3, crosses 7 and 8). Thus, it appears that *MAT2* overexpressed in the **a** parent can restore partially the dominance of **a** mtDNA

inheritance pattern, although the restoration is not to the level comparable to the wild-type cross where 92% progeny inherited the **a** mtDNA (Table 2.3, cross 5). In contrast, overexpression of *MAT2* in the α parent appears to worsen the alteration caused by the deletion of *SXI2***a**. Predominantly α mtDNA inheritance pattern (84%) was observed in the cross A(α) *MAT2*^{oe} × D(**a**) *sxi2***a**Δ, which is slightly more than the 67% observed in the cross A(α) × D(**a**) *sxi2***a**Δ (Table 2.3, crosses 3 and 4). Thus, it appears that the parental origin of the *MAT*2 overexpression determines the type of mitochondria to be preserved. If Mat2 is constantly active in the **a** parent, then **a** mtDNA is preserved in the progeny; if Mat2 is constantly active in the α parent, then α mtDNA is preserved in the progeny. The Sxi1α/Sxi2**a** complex likely helps more efficiently degrade the mtDNA not marked for preservation.

To further confirm the cooperation between Mat2 and Sxi1α/Sxi2**a** on the control of mitochondrial inheritance, we constructed a *MAT2*^{oe} strain in the *sxi2***a**Δ mutant background. Consistent with our hypothesis, the mtDNA inheritance pattern in the cross D(α) × A(**a**) *sxi2***a**Δ *MAT2*^{oe} is similar to the cross D(α) *sxi1*αΔ × A(**a**)*MAT2*^{oe} (Table 2.3, crosses 8 and 10; Figure 2.4 (B)), where modestly predominant proportion of the progeny (84% and 74% respectively) inherited mtDNA from the **a** parent where *MAT2* is overexpressed. This again supports our hypothesis that the parental origin of the *MAT*2 overexpression determines the type of mitochondria to be preserved in the progeny, and tighter uniparental mtDNA inheritance pattern can be achieved with the cooperation between Mat2 and Sxi1α/Sxi2**a**.

2.4 Discussions

Previous studies have demonstrated the predominantly uniparental **a** mtDNA inheritance pattern in α-**a** crosses, and such inheritance pattern is suggested to be established during early stages of sexual development [137, 138]. This study identified Mat2 as a novel candidate contributing to the prezygotic control of mitochondrial DNA inheritance. It is shown previously that under appropriate conditions, wild-type **a** cells express pheromone even in the absence of the α partner. In contrast, α cells produce pheromone as a response to the pheromone produced by **a** cells [134]. Therefore, **a** cells likely initiate the mating process and their mitochondria are preserved to be inherited in the progeny.

To confirm that Mat2 is differentially regulated in **a** and α cells when they are cultured alone and when they are cocultured together during mating, we measured the expression level of the *MAT2* gene and the pheromone genes controlled by Mat2 (*MF**a*** and *MFα*) at multiple time points during the process. The pheromone genes were included as they are highly sensitive to the change of the *MAT2* expression level [9] and thus can robustly reflect the activity of Mat2 even when the change in the *MAT2* expression level is subtle. As shown in Figure 2.7 (A), the expression level of *MF***a** increased more than 70 fold by 4 hours in the culture of **a** cells alone. In contrast, the expression level of *MF*α increased less than 3 fold by 4 hours in the culture of α cells alone and the level gradually increased to about 18 fold by 10 hours. The patterns of *MF***a** and *MF*α expression level are largely correlated with the *MAT2* expression level in these cultures Figure 2.7 (A-B). In the **a**-α coculture, the expression levels of both *MF***a**

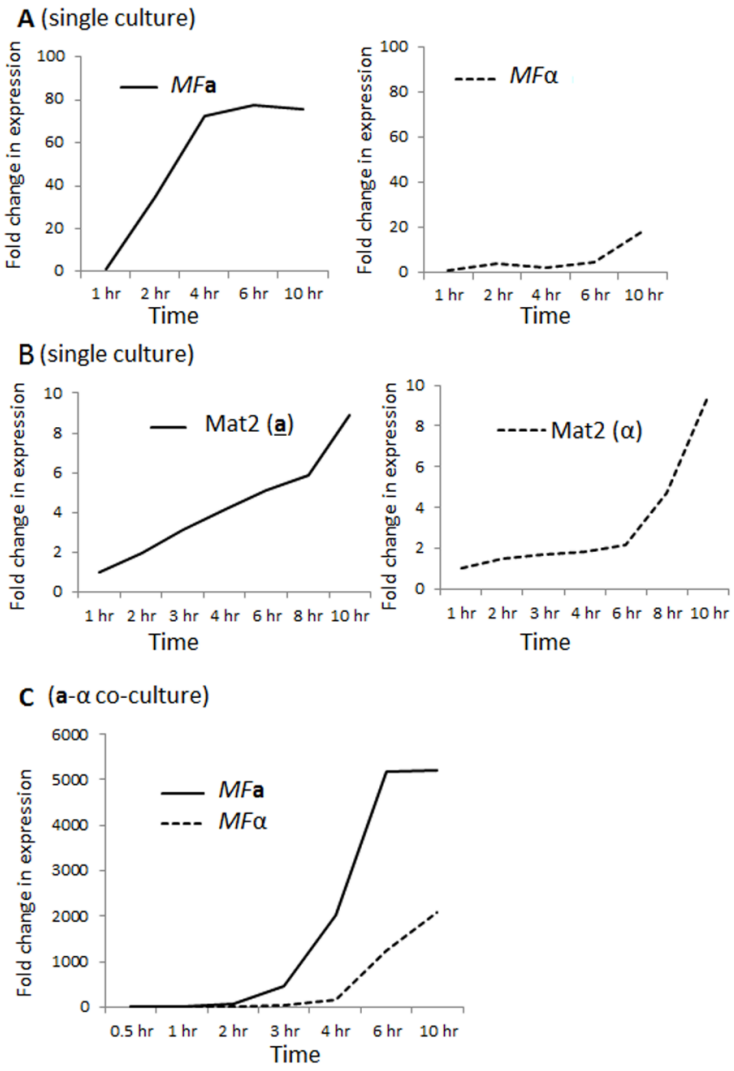

Figure 2.7 *MF**a*** is induced earlier and to a higher level than is *MFα*. (A) The pheromone expression level of the a and α cells at various time points when cultured alone on V8 agar medium. (B) The *MAT2* expression level of the a and α strains at various time points when cultured alone on V8 agar medium. (C) The expression level of the pheromone *MF***a** and *MFα* at various time points during **a**-α coculture (mating) on V8 medium.

and *MF*α were drastically higher due to the positive feedback regulation of the pheromone sensing and response cascade in both α and **a** cells. However, the expression

level of *MF***a** again increased earlier and stronger compared to *MF*α during the mating process (Figure 2.7.C). Thus, **a** cells initiate the mating process through activation of pheromone pathway controlled by Mat2.

Based on these observations, we proposed the following model to explain mtDNA inheritance in *C. neoformans* (Figure 2.8). During natural α-**a** matings, the activation of Mat2 in **a** cells leads to the marking of **a** mitochondria for preservation. In response to the pheromone produced by **a** cells, α cells also activates its Mat2 and send conjugation tubes towards **a** cells. After the α cell fuses with the **a** cell, the nuclei and mitochondria from both parental cells coexist in this newly formed zygote. Simultaneously, the cell fusion event allows the formation of the Sxi1α/Sxi2**a** complex in the zygote, which directs downstream factors to help eliminate α mitochondria before the zygote matures and sends out the dikaryotic hyphae. Thus, the cooperation between Mat2 and the Sxi1α/Sxi2**a** complex ensures stricter uniparental mtDNA inheritance from the **a** parent. Based on this model, one would predict that variations on the relative level of the initial Mat2 activity between the mating pair, due to genetic differences or environmental factors, might cause variations in the tightness of the uniparental mtDNA inheritance. For instance, high temperatures inhibit the expression of *MAT2* in both α and **a** cells [9] and may diminish the differences in the initial Mat2 level between the mating pair, this could lead to the leakage of the uniparental mtDNA inheritance as observed previously [139]. Further investigation with a large number of natural isolates with different levels of Mat2 expression or with strains where Mat2 expression level and timing can be precisely controlled is necessary to validate this model.

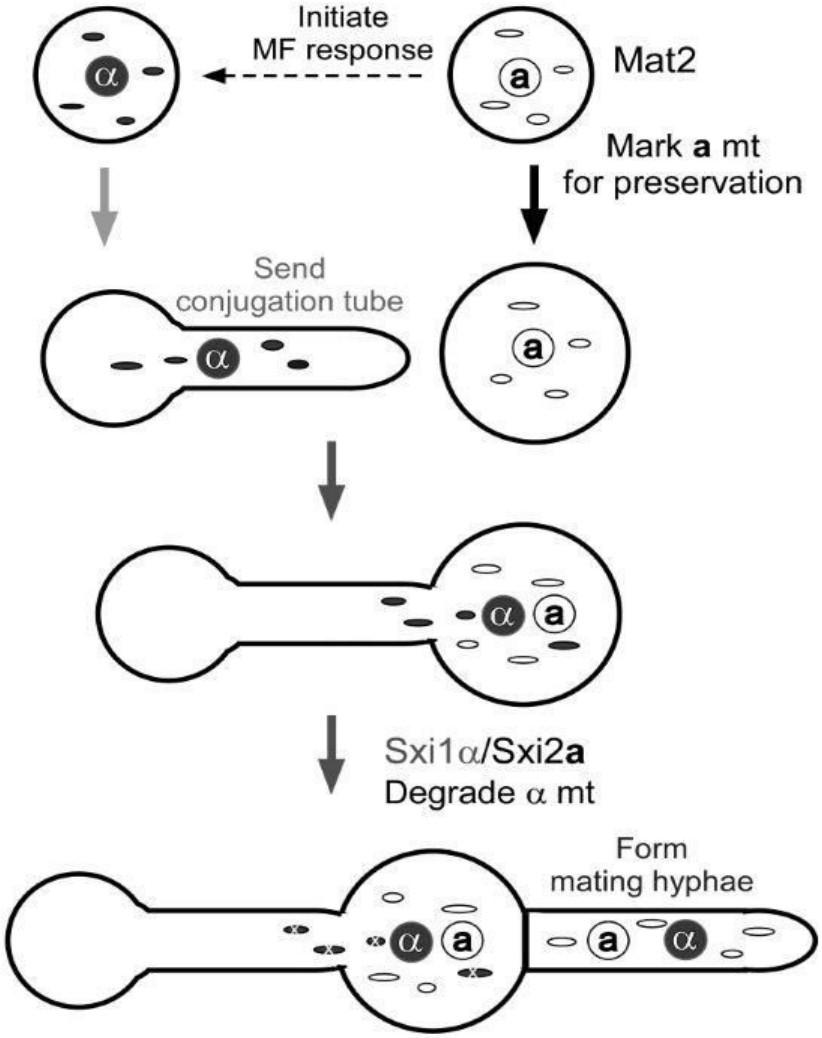

Figure 2.8 Model of mtDNA inheritance in *C. neoformans*.
Under mating-inducing conditions, the **a** cell activates Mat2 and produces high levels of the *MF**a*** pheromone. In response to *MF**a***, the α cell activates Mat2 and produces a conjugation tube. The earlier induction of Mat2 at a higher level in the **a** cell marks its mitochondria for preservation. Immediately after cell fusion, the Sxi1α/Sxi2a complex forms, and it helps degrade the unprotected α mitochondria in the newly formed zygote. Thus, the **a** mitochondria dominate in the mature zygote and cells subsequently generated from that zygote (e.g., hyphae and spores)

The cooperation between the prezygotic and postzygotic control to ensure a stricter uniparental mtDNA inheritance have been studied in other systems, although

there are cases where either the prezygotic control or the postzygotic control prevails. In mammals, sperm mitochondria were tagged with ubiquitin during spermatogenesis (the process of the production of mature sperm cells) and they rapidly disappear during zygote development [164]. In the fish *Oryzias latipes*, the abundance of sperm mtDNA decreases 5-fold during spermatogenesis and rapid elimination of remaining paternal mtDNA takes place within 2 hours after fertilization [165]. A 10-fold reduction in paternal mtDNA occurs during mouse spermatogenesis [166]. The size difference between sperm and oocyte in these systems results in unequal contribution of paternal and maternal mtDNA in the zygote that facilitates a highly stringent uniparental mtDNA inheritance pattern [128, 164, 167]. In fruit fly *Drosophila melanogaster*, paternal mtDNA is completely eliminated during sperm development [168], and thus the prezygotic control is sufficient to guarantee a uniparental mtDNA inheritance pattern.

The high mobility group (HMG)-domain transcription factors are critical regulators controlling sexual development in fungi (Mat2 in *C. neoformans* and *sexP*/*sexM* in *Phycomyces*) [169], and they are critical factors controlling mtDNA inheritance during sexual reproduction (this study and personal communication with Alexander Idnurm). Sex is proposed to enhance species fitness under changing and stressful environments. Uniparental mitochondrial inheritance is proposed to enhance the co-adaptation of mitochondrial and nuclear genomes and therefore improve species fitness more rapidly [170]. Thus, intricate connections between the regulation of sexual development and mitochondrial inheritance might have coevolved during the development of different eukaryotes. The highly virulent *C. gattii* strains responsible for

the cryptococcosis outbreak in British Columbia and Northwest US might have increased their fitness (virulence) in the temperate climate due to changes in their mitochondrial and nuclear genomes [171, 172]. Given the robust genetic and molecular tools available in *C. neoformans*, and the vast ecological and epidemiological knowledge regarding its natural distribution and genotypes, *C. neoformans* could serve as an excellent model to study the evolution of uniparental mitochondrial inheritance, the ecological and medical importance of this phenomenon, and the underlying molecular mechanisms.

3 CHARACTERIZING A FAMILY OF SECRETORY PROTEINS ASSOCIATED WITH DIFFERENT MORPHOTYPES IN *CRYPTOCOCCUS NEOFORMANS*

3.1 Introduction

Adhesins are cell surface proteins which are required for microbes to adhere to the substrate as well as to other cells [173-175]. Adhesins in pathogenic fungi play a role in a wide variety of functions such as host-pathogen interactions, biofilm formation, filamentation, and mating [174, 176, 177]. The expression of adhesins is responsive to environmental cues [173]. For instance, adhesins of *Saccharomyces* (Flo proteins) are activated during nitrogen or carbon source starvation, and they are required for cell-cell adherence and cell-substrate adherence [178-180]. Many fungal adhesins show a cell-type specific expression pattern. For instance, *Candida albicans* Hwp1 and Hwp2 are hyphal specific and they are also upregulated in opaque cells during mating. Hwp1 and Hwp2 are required for *Candida* adhesion to host cells and the formation of biofilms [181-183]. On the other hand, *Candida* Ywp1 is yeast cell specific cell wall protein which inhibits adhesin [184, 185]. Candidalysin, the hypha specific secreted protein is required for *Candida* to cause damages to epithelial cells but it does not have any effect on *Candida* hyphal morphogenesis [186]. Bad1, the adhesin and an important virulence factor characterized in *Blastomyces dermatitidis*, is yeast specific [187]. Understanding the regulation of cell surface proteins thus can help us understand fungal development and how it interacts with its environment and the host.

Cell flocculin 1 (Cfl1), a hyphal specific protein of *C. neoformans,* is the first adhesin identified in the phylum Basidiomycota [9, 188, 189]. *CFL1* is one of the most induced genes during *C. neoformans* sexual development [9, 189]. *C. neoformans* adhesin Cfl1 is unique in that it does not contain a common domain structure present in known ascomycetes fungal adhesins such as a C-terminal GPI anchor, an N-terminal carbohydrate or peptide binding domain, or the middle domain containing serine/threonine rich repeats [178, 190]. However, consistent with the function of adhesins, overexpression of Cfl1 leads to wrinkled colony morphology (biofilm) as well as increased flocculation [9]. Furthermore, Cfl1 is a secretory protein and its secretion is required for its adhesin function. Cfl1 is both cell-wall associated and the released Cfl1 acts as a signal to regulate the colony morphology in an autocrine and paracrine manner [189]. Therefore, cells expressing Cfl1 can induce the expression of endogenous Cfl1 in the neighboring cells, which leads to the formation of biofilm and the production of hyphae [189].

Domain organization of Cfl1 shows that it contains an N-terminal EGF motif and an amylogenic region which has a predicted function in cell-cell adhesion [189]. The C-terminal region containing 80 amino acid residues is highly conserved among Cfl1 homologs across different basidiomyceteous species and is named the SIGC domain (signal C-terminal domain) [189]. Interestingly, the *C. neoformans* genome has four additional Cfl1 homologs. The aim of this study is to characterize these homologs and to understand their role in the development of *Cryptococcus neoformans*.

3.2 Materials and Methods

3.2.1 Strains and growth conditions

Strains used in this study are listed in Table 2.1. *C. neoformans* strains are stored in -80 °C and grown on YPD (Yeast Extract Peptone Dextrose) media for routine culture. Mating assays were performed on V8 pH7 media at 22 °C in dark.

3.2.2 Generation of gene disruption and overexpression strains

Gene deletion was conducted using the split marker recombination strategy as described previously [191]. Briefly, the 5' and 3' flanking region of the gene of interest was fused to two third of the fragment of the NAT or the NEO dominant drug resistance marker using overlap PCR. Two split fragments were mixed and introduced into *Cryptococcus neoformans* using biolistic transformation as described previously [192]. Transformants with gene deletion were confirmed through PCR and genetic linkage assay by phenotyping / genotyping of the dissected meiotic progeny from a genetic cross between the mutant α strain and the congenic wild type **a** strain [193]. Gene deletion mutants in the **a** mating type were obtained through genetic crosses between a mutant in the α mating type and a wild-type partner in the **a** mating type as described previously [193]. For the construction of the overexpression vector, amplified fragment of the ORF of the gene was digested and ligated into the pXL1-mCherry vector after the *GPD1* promoter or the *CTR4* promoter [9]. The *GPD1* promoter was used for the constitutive expression. The *CTR4* promoter was used as an inducible system with the copper chelator BCS inducing the expression of the gene and copper repressing the expression

of the gene. The vector also contains the m-Cherry tag towards the C-terminus of the gene as described previously [9]. The overexpression construct was then introduced into *Cryptococcus neoformans* using biolistic transformation as described previously [192].

3.2.3 Construction of mCherry-tagged proteins

The mCherry-tagged proteins driven by their native promoters were constructed as described previously [9]. 1 kb upstream of the gene's ORF together with its ORF was amplified through PCR and ligated into the pXL1 vector containing m-Cherry such that mCherry is fused in frame with the C-terminus of the gene. The construct was introduced into *C. neoformans* cells using biolistic transformation.

3.2.4 Phenotypic assays

Phenotypic assays were performed as described previously [194]. Briefly, strains to be tested were grown overnight in YPD liquid media. The cells were washed and adjusted to the same density (OD_{600} = 3). For thermo-tolerance assays, cells were serially diluted and spotted onto YPD agar-medium and incubated at 30 $^{\circ}$C, 37 $^{\circ}$C, or 39 $^{\circ}$C. For the capsule formation assay, cells were cultured in liquid fetal bovine serum or RPMI medium for 48 hours at 37 $^{\circ}$C with 5% CO_2. The capsule was visualized as a halo surrounding the yeast cell under light microscope through Indian ink exclusion. Melanin production was visualized by spotting the cells onto L-DOPA (L-dihydroxyphenylalanine) media. For mating assays, cells were incubated on V8 media in the dark at 22 $^{\circ}$C for 3 days before the mating filaments images were taken. Colony images were taken 5 days after incubation at 22 °C with stereoscope Olympus

SZX16. To visualize basidia and spore chains, cells were incubated on V8 media for 10-14 days and images were taken using Zeiss Axiocam 506 camera. For examining protein subcellular localization, strains were grown on YPD or V8 media. The cells were visualized using a Zeiss Imager M2 fluorescent microscope with a Axiocam 506 camera. The filter used for visualizing mCherry was the FL filter set 43 HE cy3 (Carl Zeiss Microscopy). To observe protein localization at various stages of cryptococcal development, cells were visualized at different time points after incubation on V8 agar media.

3.2.5 RNA purification and qPCR

RNA extraction and quantitative real time PCR (RT-PCR) were performed as described previously [9]. Cells undergoing unisexual development on V8 media were harvested at various time points as indicated in the figures, washed with cold ddH_2O, and lyophilized. Total RNA was extracted using the Purelink RNA mini kit from Life Technology according to the manufacturer's instructions. After DNase I treatment, the samples were analyzed on formaldehyde agarose gel to assess the RNA quality and concentration. The first strand cDNA synthesis was carried out using Superscript III cDNA synthesis kit (Life Technology) following the manufacturer's instructions. Constitutively expressed housekeeping gene *TEF1* was used as an internal control for the normalization of other genes as we described previously [9].

3.2.6 Colony immunoblot

Immunoblot was performed as we described previously [189]. Respective strains were grown overnight in YPD. Three microliters of cell suspension of density $2x10^7$ cells / ml were spotted onto V8 media and incubated for 5 days at 22°C. Then, a sterile nitrocellulose membrane (Millipore) was laid over the colonies and the cells were incubated for additional 3 days. Membrane was then removed and washed with 1x Tris buffer saline to remove the attached cells. The blot was then incubated with anti-mCherry primary antibody (1/2000 dilution, Clontech). Then a rabbit anti-mouse secondary antibody coupled with HRP was used (1/10,000 dilution, Clontech Inc.). For detection, enhanced chemiluminescence (ECL) system was used according to the manufacturer's instruction (Pierce).

3.2.7 Phagocytosis assay

Mouse macrophage cell line J774A.1 (ATCC® TIB-67™) were used for the phagocytosis assay as described previously [195]. Macrophage cells were culture in Dulbecco's modified Eagle's medium (DMEM; catalog no. 30-2002) with 10% fetal bovine serum (FBS). *C. neoformans* WT H99 cells and *DHA1* deletion mutant in H99 background were used for the study. Freshly grown J774A.1 cells were seeded in 24-well microtiter plate overnight at 37 °C + 5% CO_2 with each well containing 2.5×10^5 *C. neoformans* cells per 500 microliters. Next day, each well was replaced with fresh media containing 2.5×10^6 *C. neoformans* cells in 500 microliters of media. The cells were mixed well with the macrophage by rocking for 30 seconds and were incubated at 37 °C

+ 5% CO_2. After 2 hours, the co-cultures were washed with phosphate saline buffer (500 µl per well) for 6 times to remove non-adherent cells. Co-cultures were further incubated in fresh media (DMEM with 10% FBS) containing fluconazole (5µg/ml) for 24 hours. Fluconazole was added so that it inhibits the extracellular replication of *C. neoformans* [196]. After 24 hours, intracellular and extracellular population of *C. neoformans* was measured. For measuring extracellular population, the co-cultures were washed 6 times with PBS. This extracellular fluid was plated at different dilution in YNB (Yeast Nitrogen Base) agar media and colony forming unit (c.f.u) was measured after 48 hourss of incubation. Intracellular population of *C. neoformans* was measured by lysing the macrophage cells after the extracellular population of *C. neoformans* was collected. To lyse macrophage, 100 µl of 0.5% tween-20 was added to the culture and incubated at 37 °C for 10 minutes. The suspension was made up to 200 µl through addition of YPD, serially diluted, and plated on YNB agar plates. C.f.u was counted 48 hours after incubation at 30°C. Growth assay of the cells in the same medium without macrophage was carried out as a control. WT and the mutant cells were incubated in the macrophage medium for 24 hours. They were then serially diluted and plated on YNP plates. C.f.u was counted 48 hours post incubation at 30 °C. There was no significant difference in growth between WT and the mutant cells grown in macrophage medium (data not shown).

3.3 Results

3.3.1 Identification of genes encoding Cfl1 homologs

Based on the previous study [9], the *C. neoformans* genome has four additional homologs of Cfl1. Blast search of Cfl1 against *Cryptococcus neoformans var. neoformans* translated genome using FungiDB led to identification of these four

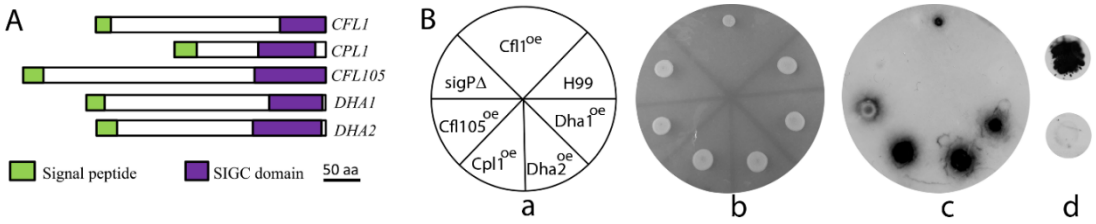

Figure 3.1 Schematic diagram for amino acid sequence alignment of *CFL1* homologs and their secretion.
SignalP 4.1 Server was used for the prediction of signal peptide and the location of signal peptide cleavage site. Position of the SIGC domain among the homologs was predicted based on the blast search of the *CFL1* SIGC domain against each homolog. All of the Cfl1 homologs have an N-terminal signal peptide for secretion and the C-terminal SIGC domain. Similarity in sequence among the homologs mostly lies in the SIGC domain. (B) Cfl1 homologs are secretory proteins and are released extracellularly. The strains P*CTR4*-*CFL1*::mCherry (Cfl1 ^{oe}), P*CTR4*-*DHA1*::mCherry (Dha1^{oe}), P*CTR4*-*DHA2*::mCherry (Dha2 ^{oe}), P*CTR4*-*CPL1*::mCherry (Cpl1^{oe}), and P*CTR4*-*CFL105*::mCherry (Cfl105^{oe}) were grown overnight in liquid YPD. Cells of same OD (OD600=3) were spotted onto V8+BCS plates. Proteins released from the colony onto the membrane was detected by using antibody against mCherry. a: Plate layout of the strains grown on V8 agar medium. b: Colony images of the strains on V8 agar medium. Since Cfl1 is known to be secreted abundantly during mating, Cfl1 overexpressing cells were spotted three days later than other strains to avoid potential interference of the signal from Cfl1oe cells with signals from other cells. Colony immunoblot detects secreted products from all the strains overexpressing Cfl1 homologs. No signal was detected from the WT H99 cells or the SigPΔ-Cfl1^{oe} cells with Cfl1's signal peptide deleted. d: Colony immunoblot of the Cfl1^{oe} cells (top) and SigPΔ-Cfl1^{oe} cells with signal peptide deletion (bottom). Here both strains were cultured for 5 days before the membrane was laid over the colonies.

additional *CFL1* homologs as *DHA1* (CND04870), *DHA2* (CNM00910), *CPL1* (CNC04160), and *CFL105* (CNG01330). All Cfl1 homologs have an N-terminal signal peptide and are predicted to be secretory proteins by the WoLFPSORT program. All Cfl1 homologs have the C-terminal SIGC domain that is the most conserved region (Figure 3.1.A). Among all Cfl1 homologs, Dha1 and Dha2 are most similar, sharing 72% identities and 83% similarities. This suggests that Dha1 and Dha2 might be paralogs. In comparison, the identities shared between other Cfl1 homologs are lower than 40%. Dha1 has been previously shown to elicit delayed-type-hypersensitivity (DTH) reaction in mice. Mice that were immunized with culture filtrate of serotype A strain (184A) were shown to elicit DTH which was measured based on mouse footpad swelling assay [197]. *CPL1* has also been shown to affect capsule formation and the gene deletion mutants had reduced virulence in a systematic study of around 1201 gene deletion mutants [198]. In a recent study, Cpl1 was shown to be secreted into culture supernatant and was also detected in serum of mice infected with *Cryptococcus neoformans* [199]. The role of these homologs on *C. neoformans* development has not been studied.

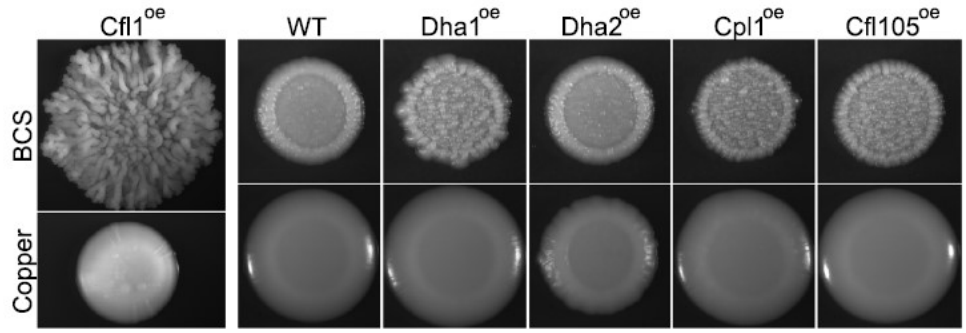

Figure 3.2 Colony morphology of strains with the expression of the *CFL1* homologs driven by the *CTR4* promoter.
The *CFL1* homolog genes are highly expressed in the presence of BCS and are repressed in the presence of copper in the medium. All the strains except Dha2^{oe} showed wrinkled colony morphology on medium with BCS. All strains appear to be similar to the wild type control on medium with copper, as expected.

3.3.2 All Cfl1 homologs are secreted proteins

Cfl1 is known to be released extracellularly [189]. We also know that mCherry tagged Cfl1 at its C-terminus is functional [189]. To test if the homologs of Cfl1 are released extracellularly like Cfl1, we applied the same approach and tagged all the homologs of Cfl1 with mCherry and drive their expression using the inducible promoter of the copper transporter gene *CTR4* [189]. Then we performed colony immunoblot assay with these strains cultured under copper-limiting condition where the expression of these genes was induced. As expected, we detected extracellular released Cfl1 in this assay (Figure 3.1.B). Because Cfl1 is secreted abundantly (panel d in Figure 3.1.B), we spotted Cfl1 overexpressing cells three days later than other strains so that the signal from Cfl1^{oe} cells would not interfere with signals from other colonies (hence the Cfl1^{oe} colony is smaller in (Figure 3.1.B). We did not detect signals from the strain LW295

(Cfl1-sigPΔ) where the Cfl1's signal peptide was deleted, or from the WT strain without the mCherry tag (Figure 3.1.B), as expected. By contrast, we detected signals from colonies where the four Cfl1 homologs were tagged with mCherry by the colony immunoblot (Figure 3.1.B). The result indicates that all four homologs of Cfl1 are indeed released to the milieu like Cfl1.

3.3.3 Impact of overexpression of the Cfl1 homologs on colony morphology

We previously demonstrated that overexpression of Cfl1 promotes the formation of wrinkled colony morphology similar to that of the formation of biofilm [9, 189]. The P_{CTR4}-*CFL1*-mCherry cells formed a complex colony embedded with a layer of matrix when the strain was cultured under an inducing condition in the presence of the copper chelator BCS, while the strain formed a smooth colony under a repressing condition in the presence of copper (Figure 3.2), as expected based on our previous studies [9, 188, 189]. The P_{CTR4}-*DHA2*-mCherry strain (Dha2^{oe}) formed a round and smooth colony on YPD medium with BCS, similar to the WT XL280 colony (Figure 3.2). Interestingly, the P_{CTR4}-*DHA1*-mCherry strain, the P_{CTR4}-*CPL1*-mCherry strain, and the P_{CTR4}-*CFL105*-mCherry strain colonies showed increased wrinkledness in the colony morphology in the presence of BCS, but to a much lesser degree compared to the Cfl1^{oe} colony under the same inducing condition (Figure 3.2). These results suggest that Dha1, Cpl1, Cfl105, and Cfl1 promote biofilm formation.

3.3.4 Expression profile of *CFL1* homologs

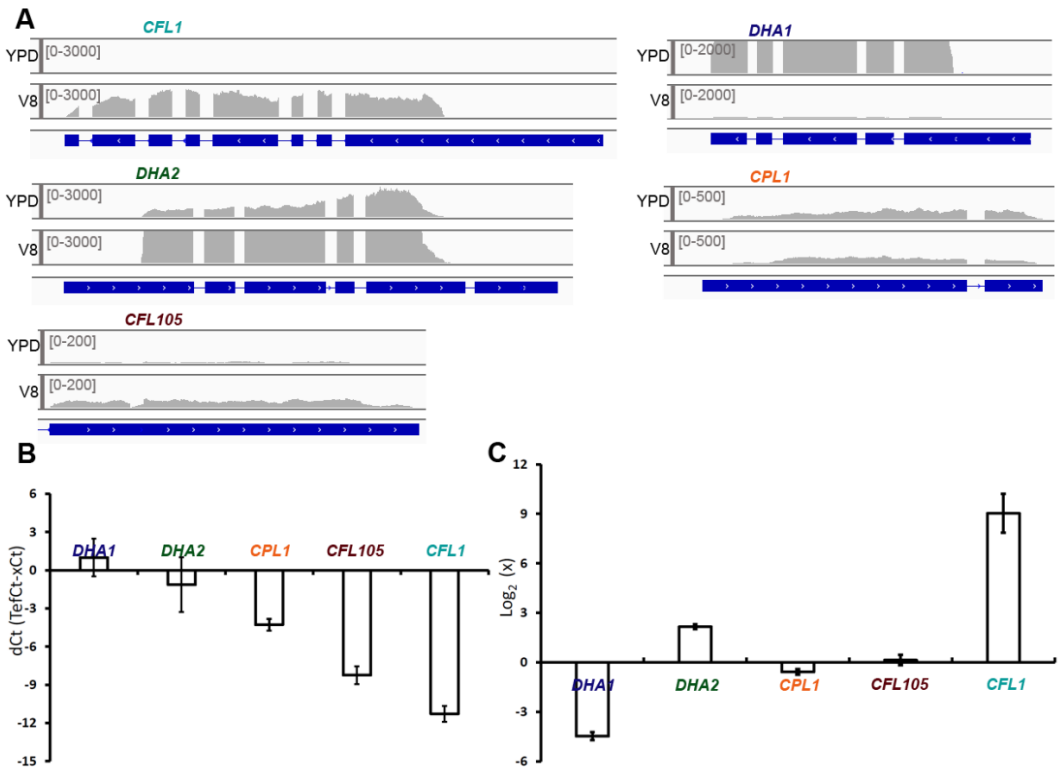

Figure 3.3 Transcript level of *CFL1* homologs.
Transcript level (FPKMs) of the *CFL1* homologs when the wild type XL280 strain was cultured in YPD or on V8 medium for 24 hours based on the RNA-seq data [8]. For transcript analysis, IGV software was used. Reads count scale was set to different threshold value for each gene so that the transcript level of each gene can be easily visualized. We can see that the *DHA1* transcript level is high in YPD media whereas the *CFL1* and *DHA2* transcript levels are high under mating conditions (V8 media). The *CFL105* and *CPL1* transcript levels are low under both conditions. (B) The relative transcript level of *CFL1* homologs based on RT-PCR. RNA samples for the yeast phase growth were collected by growing WT XL280 cells in liquid YPD media overnight. RT-PCR graph showing the dCt values of the *CFL1* homologs. The dCt value was calculated based on the comparison of Ct value of the respective gene with that of the *TEF1* gene. (C) RNA samples for the mating samples were collected on V8 agar media for 24 hours. The relative transcript level of the genes on mating media is based on their transcript level in YPD media. *CFL1* and *DHA2* are significantly induced on V8 medium whereas *DHA1* is repressed compared to its level in YPD medium.

To understand their role in the development of *C. neoformans*, we examined the expression pattern of *CFL1* homologues in wild type XL280 during the yeast phase growth in YPD media and during sexual development on V8 media by analyzing RNA-seq data that we recently published [8]. During the yeast phase growth in YPD, *CFL1* showed the lowest transcript level whereas *DHA1* showed the highest transcript level (Figure 3.3.A). This pattern is consistent with our quantitative RT-PCR results (Figure 3.3.B). The high expression level of *DHA1* during yeast growth is consistent with a previous study where Dha1 protein was easily detected in the supernatant of *C. neoformans* yeast cultures [197]. The transcript level of *DHA2* is ranked in second in YPD, followed by *CPL1*, *CFL105*, and *CFL1* (Figure 3.3.A-B).

C. neoformans can undergo unisexual development on mating-inducing media such as V8 juice agar medium [68, 81]. During unisexual development on V8 media at 24 hours post inoculation, the transcript levels of *CFL1* and *DHA2* are significantly higher than other genes based on the RNA-seq data (Figure 3.3) The increase in the transcript level of these two genes on V8 compared to that in YPD was confirmed with our RT PCR results (Figure 3.3.B-C). The finding indicates that the *CFL1* and *DHA2* transcript level drastically increased during unisexual development on V8 compared to that in YPD (Figure 3.3.A-B). The high level of *CFL1* transcripts during unisexual development is expected given that Cfl1 is a hypha-specific protein [9]. Because *DHA2* was also significantly induced during unisexual development on V8 medium, we speculate that *DHA2* might also be specifically induced in the hyphal subpopulation like

CFL1. On the other hand, no drastic change in transcript levels was observed for *CPL1* or *CFL105* during sexual development on V8 media compared to yeast growth in YPD.

By contrast, the *DHA1* transcript level was drastically reduced on V8 medium, suggesting that *DHA1* might encode a yeast-specific product. The expression data of some of these *CFL1* homologs genes showed that some of these genes have higher transcript during yeast phase growth while some are induced during sexual development. Thus, we hypothesize that some of these homologs, particularly Dha1, Dha2, and Cfl1, likely play a role in *C. neoformans* development.

3.3.5 Impact of the deletion of *CFL1* homologs on *C. neoformans* classic virulence traits

To examine if Cfl1 homologs play any role in *C. neoformans* virulence traits and morphology, we deleted these genes in the serotype D XL280 background. We then used these deletion mutants for phenotypic assays, including assays for thermo-tolerance, melanization, and capsule production. Deletion of most of the *CFL1* homologs in XL280 did not have any apparent effect on thermo-tolerance or melanin production (Figure 3.4.A-B). Likewise, no defect on melanization or growth at high temperature was observed for the gene deletion mutants made in the serotype A H99 background (Figure 3.5). We also did not observe obvious impact on capsule production by the disruption of most of the *CFL1* homologs except *CPL1* in XL280 background (Figure 3.4). Smaller capsule size of the *cpl1*Δ mutant in H99 background was also observed (Figure 3.5).

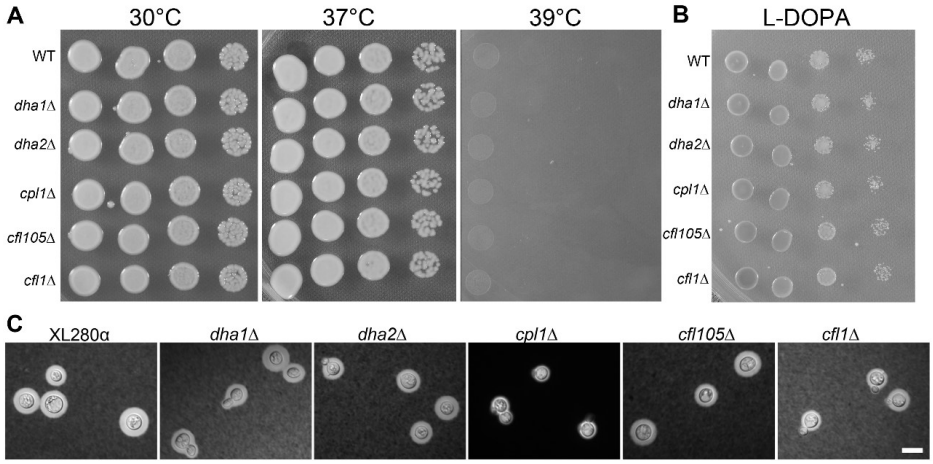

Figure 3.4 Effect of gene deletion on thermo-tolerance, melanin production, and capsule production.

Cells of the wild type XL280, the *dha1*Δ mutant, the *dha2*Δ mutant, the *cpl1*Δ mutant, the *cfl105*Δ mutant, the *cfl1*Δ mutant of the same OD (OD600=3) were serially diluted (10x) and spotted onto YPD or L-DOPA agar medium. To examine capsule, cells were cultured in liquid RPMI media. (A) To test the thermo-tolerance, cells on YPD medium were incubated at 30 °C, 37 °C, or 39 °C. (B) To test melanization, cells on L-DOPA medium were incubated at 22 °C in the dark. (C) Indian ink exclusion assay of capsule production of the cells cultured in RPMI medium at 37 °C with 5% CO_2. Scale bar: 10 μm.

This is consistent with a previous observation of the *cpl1*Δ mutant made in the H99 background [198].

3.3.6 Impact of the deletion of *CFL1* homologs on *C. neoformans* development

Given that Cfl1 plays an important role in promoting yeast to hyphal morphological transition in *C. neoformans*, we decided to examine if the Cfl1 homologs also plays a role in filamentation and sporulation during cryptococcal development. *C. neoformans* can undergo filamentation and sporulation during both **a**-α bisexual

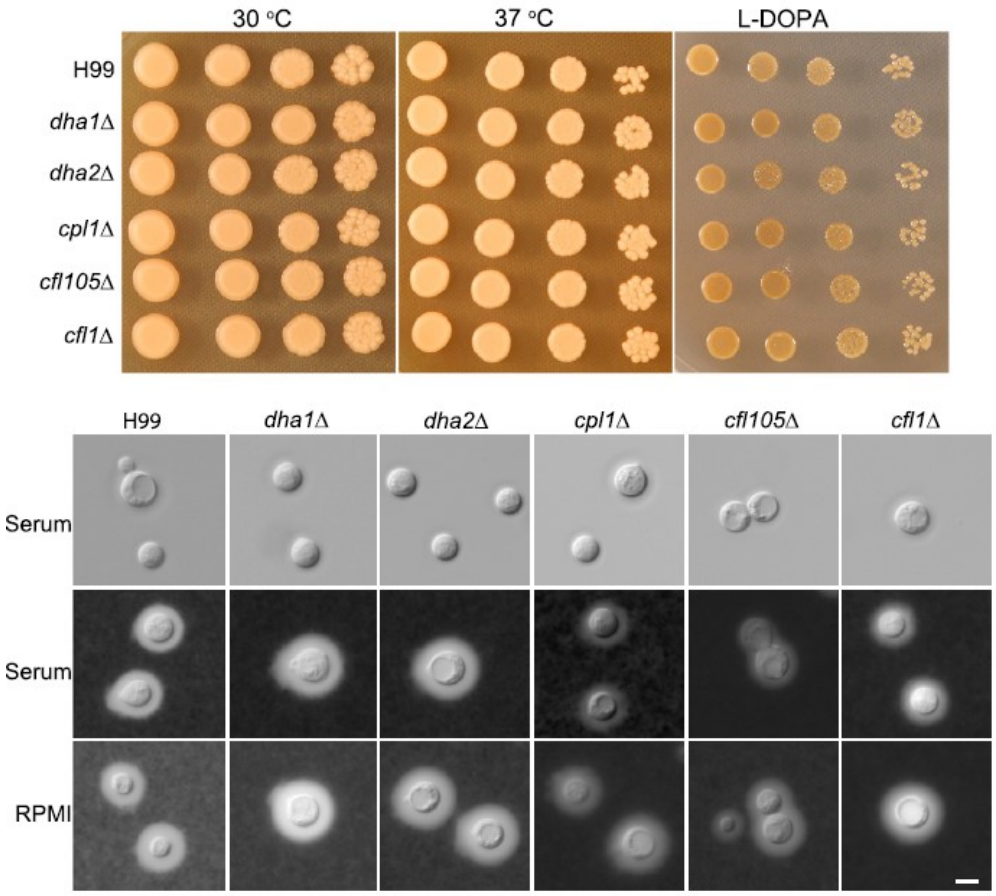

Figure 3.5 Effect of gene deletion of *CFL1* homologs in H99 background on thermo-tolerance, melanization, and capsule formation.
The *cpl1*Δ mutant showed apparent defect in capsule formation. Scale bar: 5 μm.

reproduction or during unisexual reproduction with cells of one mating type [68, 81, 200]. We chose to use strains in the wild type XL280α for such investigation as XL280 has been widely used for morphogenesis studies [142]. We first examined the effect of deletion of these genes during unisexual development where α cells alone were cultured under mating-inducing condition (V8 juice agar medium). Deletion of the *CFL1* gene substantially reduced aerial hypha formation (Figure 3.6), as shown previously [189].

Even though no spores could be detected when WT strain had already produced spores, the *cfl1*Δ mutant can eventually sporulate. Surprisingly, no obvious defect in filamentation or sporulation was observed in the *dha1*Δ mutant, the *dha2*Δ mutant, the *cpl1*Δ mutant, or the *cfl105*Δ mutant (Figure 3.6.A).

To examine the effect of the disruption of *CFL1* homolog genes on bisexual mating, we first obtained the gene deletion mutants in the mating type **a** background by dissecting the meiotic progeny from a cross between the gene deletion α strain and the congenic WT **a** strain [142]. Then we performed crosses with the mutant α cells with the corresponding mutant **a** cells. As expected, the cross of *cfl1*Δ α x *cfl1*Δ **a** showed reduced production of aerial hyphae as well as sporulation. However, no apparent defect in bilateral bisexual mating was detected for any of the other gene deletion mutants (Figure 3.6.B).

The fact that the deletion of *DHA2* did not yield any obvious phenotype during cryptococcal development was surprising given that its transcript level is drastically induced during mating. One possible explanation is that Dha2 might not directly play a role in hyphal production or hyphal elongation *per se*, but its production is associated with cryptococcal development. For instance, it may sense or respond to other environmental cues that are typically present under mating conditions. Such was the case with the secreted protein *ECE1* of *Candida albicans*. *ECE1* is highly expressed by

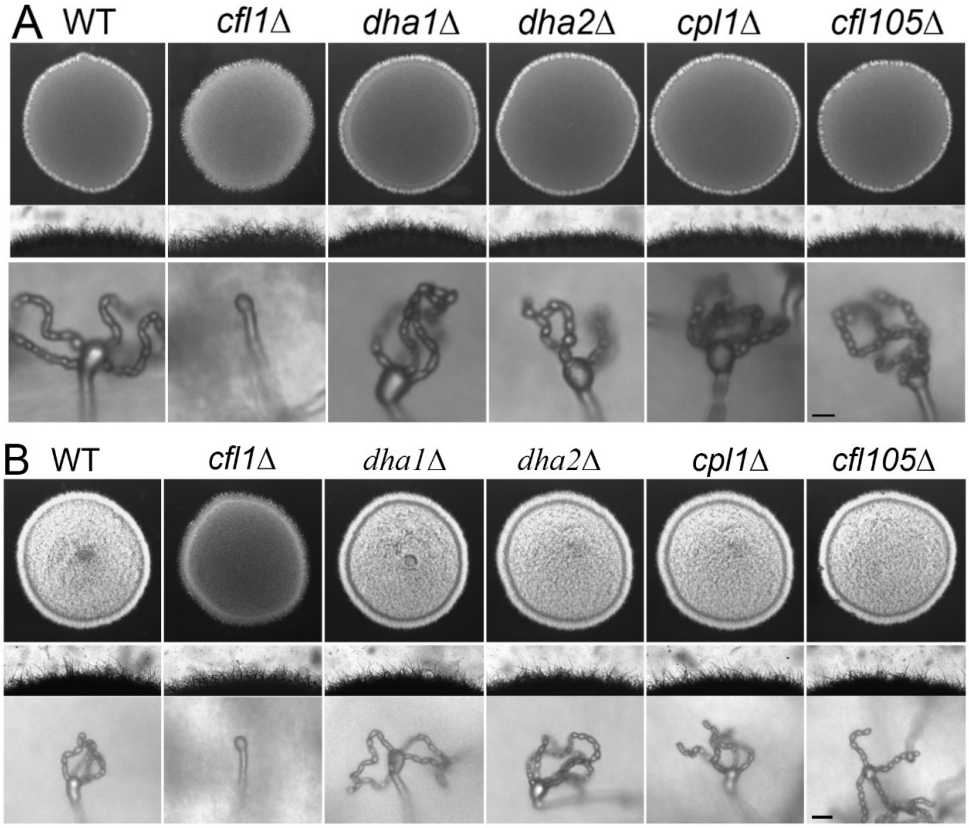

Figure 3.6 Effect of gene deletion on unisexual and bisexual reproduction. Cells of the wild type XL280, the *dha1*Δ mutant, the *dha2*Δ mutant, the *cpl1*Δ mutant, the *cfl105*Δ mutant, the *cfl1*Δ mutant (all in the α mating type) at the same density were spotted onto V8 agar media and incubated in dark at 22 °C for 5 days either alone for unisexual reproduction (A) or mixed together with the corresponding mutant in the mating type **a** for bisexual reproduction (B). The white fluffy appearance of the colony reflects the production of aerial hyphae. Deletion of *CFL1* led to reduced aerial hyphal formation in both unisexual and bisexual reproduction. Sporulation is significantly reduced and delayed, however, they do eventually sporulate. Scale bar for spore chains: 10 μm.

Candida hyphal cells during epithelial infection, but the deletion of *ECE1* does not affect hyphal morphology, adherence, or *Candida* invasion to human epithelial cells [186]. Interestingly, the secretion of the encoded protein is crucial for *Candida* to cause

damages to epithelial cells [186]. Another possible reason for the lack of phenotype in cryptococcal development of the *dha2*Δ mutant might be due to functional redundancy. Functional redundancy has been shown to prevail in the *FLO* gene family of *Saccharomyces* during various processes like mating, filamentation, and flocculation [180]. Alternatively, it is possible that increased *DHA2* gene expression level during cryptococcal development does not correlate with its protein level and there is a dichotomy in the *DHA2* gene expression and Dha2 protein production.

3.3.7 Dha1 and Dha2 have distinct localization patterns during cryptococcal development

Based on the expression profile, the *DHA2* and *CFL1* genes have high transcript levels during cryptococcal sexual development, whereas the *DHA1* gene is highly expressed during yeast phase growth. Hence, we decided to test their protein expression and localization pattern during yeast growth and during sexual development on V8 agar media. For this purpose, we tagged these proteins with m-Cherry at the C-terminus and used their own native promoters to drive their gene expression. Cfl1 fused with m-Cherry driven by its own promoter (P_{CFL1}-*CFL1*-mCherry) was used as a positive control for a hyphal specific protein [9, 189]. When the P_{CFL1}-*CFL1*-mCherry strain was grown on YPD media, we could not detect the Cfl1-mCherry signal at the colony level or with individual yeast cells (Figure 3.7.A-B). This observation is consistent with its smooth colony morphology as well as the extremely low transcript level of *CFL1* under this condition (Figure 3.6.A, Figure 3.3.A). When the P_{DHA1}-*DHA1*-mCherry strain was

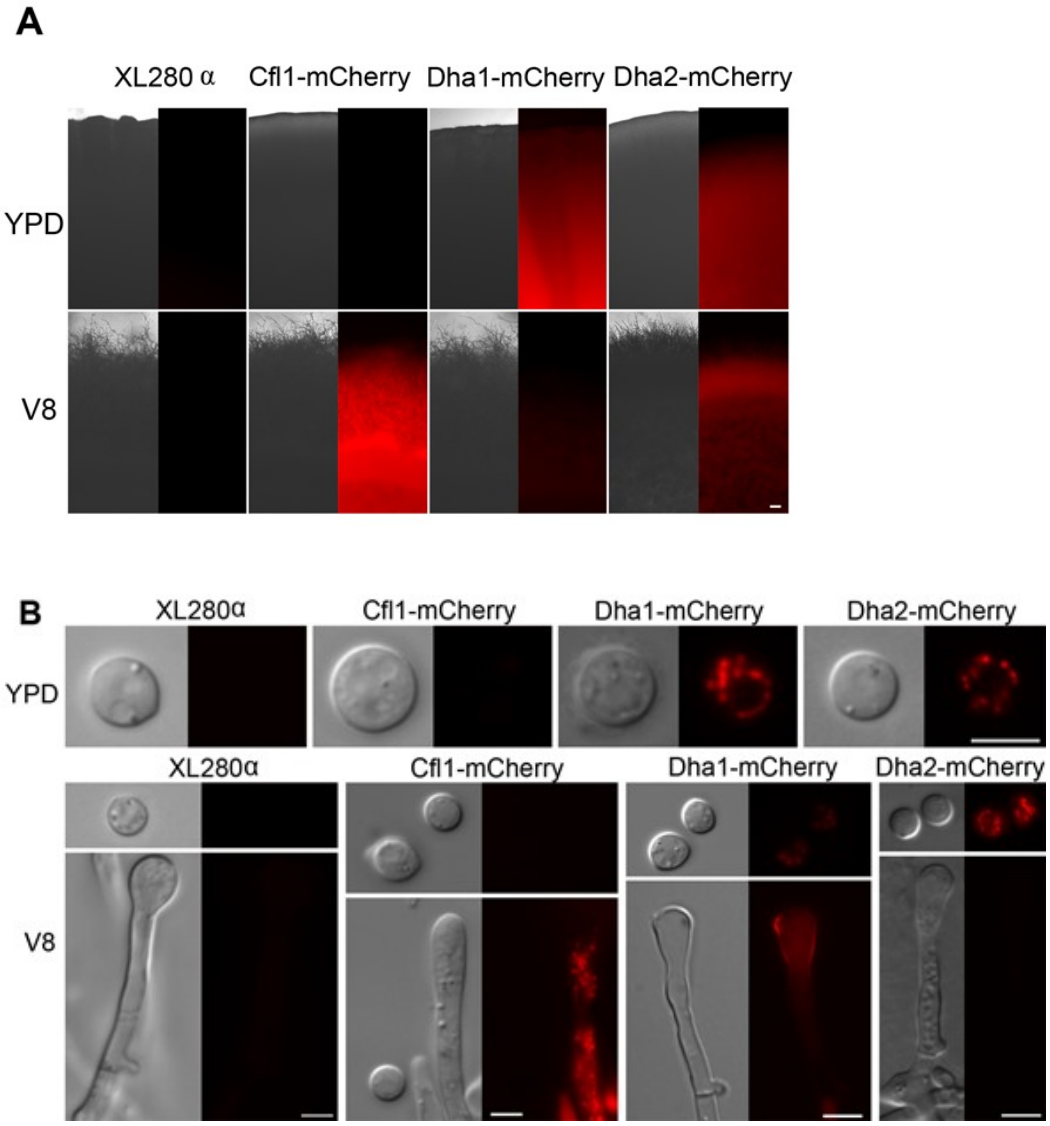

Figure 3.7 Protein expression pattern of Cfl1, Dha1, and Dha2 during yeast phase growth and during cryptococcal development.
Each protein is fused with mCherry at its C-terminus and the gene expression was driven by its native promoter. (A) Colony images of the unlabeled wild type XL280, the P_{CFL1}-*CFL1*-mCherry strain, the P_{DHA1}-*DHA1*-mCherry strain, and the P_{DHA2}-*DHA2*-mCherry strain grown in YPD media and on V8 media. Scale bar: 100 µm (B) Expression and subcellular localization of Cfl1, Dha1, and Dha2 in yeast cells during growth in YPD media and on V8 media. DIC and fluorescence images of the unlabeled wild type XL280, the P_{CFL1}-*CFL1*-mCherry strain, the P_{DHA1}-*DHA1*-mCherry strain, and the P_{DHA2}-*DHA2*-mCherry cells in YPD (yeast cells only) and on V8 media (yeast cells and hyphae). Scale bar: 5 µm

grown on YPD media, we could easily detect Dha1-mCherry signal in yeast intracellular punctate structures that are consistent with secretory vesicles (Figure 3.7.B). This is consistent with the high transcript level of *DHA1* in yeast growth (Figure 3.3.A). Likewise, we could easily detect the Dha2-mCherry signal in vesicles in yeast cells (Figure 3.7.B).

Next we examined their localization during sexual development on V8 agar media. *C. neoformans* mating colony is heterogeneous in morphology, and it consists of cell types including yeast, aerial hyphae, and invasive hyphae. Later during sexual development, some of the aerial hyphae go on to produce basidia where meiosis and sporulation take place. Based on the fluorescence image of the mating colony, Cfl1 and Dha2 proteins were abundantly produced when cells were grown on V8 medium, whereas a much reduced signal of Dha1 was detected at the colony level under the same conditions (Figure 3.7.A). At the cellular level, Cfl1 was highly expressed in hyphae but rarely in yeasts, and Cfl1 was observed in structures consistent with secretory vesicles (Figure 3.7.B). Surprisingly, although *DHA2*, like *CFL1*, had high transcript level when *C. neoformans* cells were cultured on V8 media, the Dha2 protein was mostly detected in yeast cells (Figure 3.7.B) and rarely in hyphal cells. This Dha2 protein expression pattern on V8 media is opposite of Cfl1. Thus, our data indicate that gene expression profile at the population level is not always indicative of the behaviors of individual cell types within the heterogeneous population. The transcript level for *DHA1* is low on V8 medium. Consistently, only some yeast cells showed the weak signal of Dha1-mCherry in intracellular punctate structures during early developmental stage of *C. neoformans*

(Figure 3.7.B). Interestingly, Dha1-mCherry was localized at the basidium neck and in spores at a later stage during sexual development (Figure 3.7.B). This suggests that Dha1 is also a spore protein.

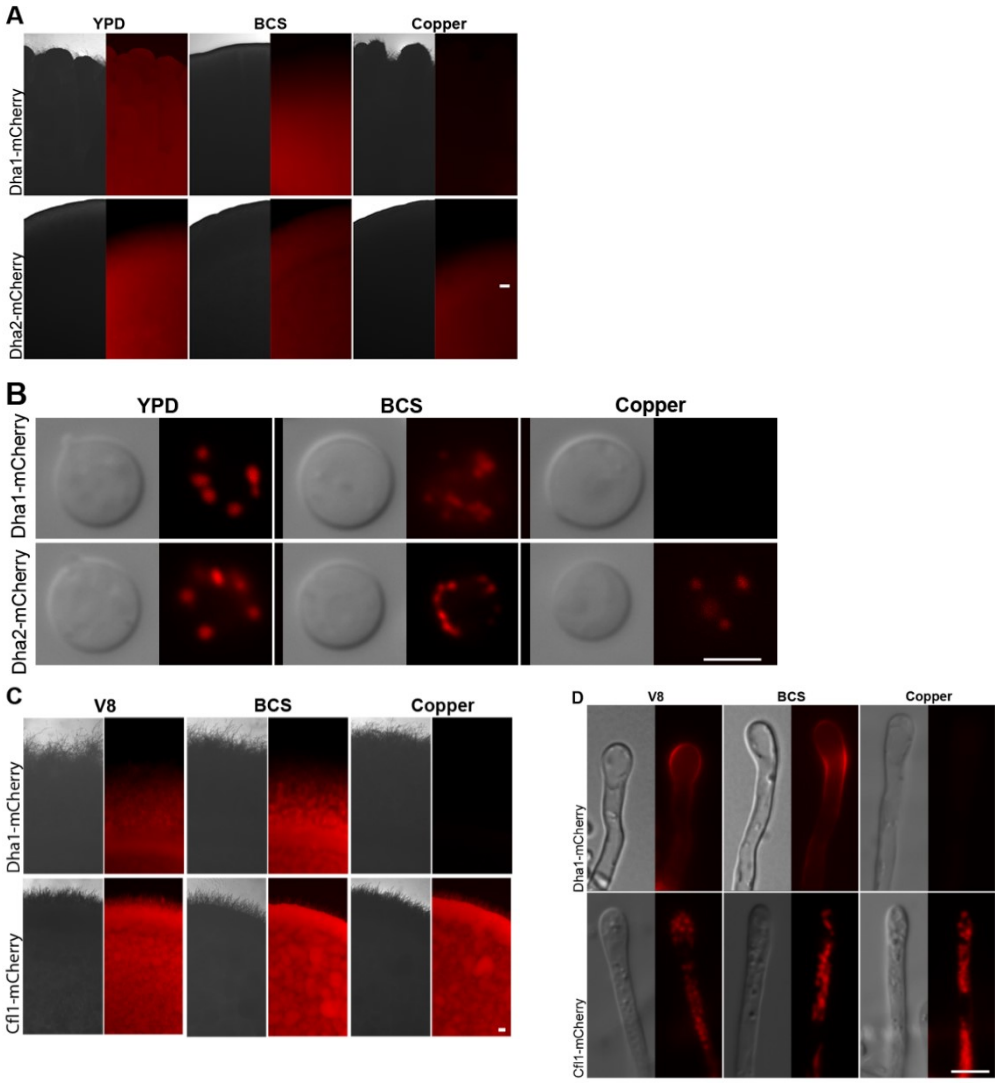

Figure 3.8 Dha1 is repressed by copper.
Cells of the P$_{CFL1}$-*CFL1*-mCherry strain, the P$_{DHA1}$-*DHA1*-mCherry strain, and the P$_{DHA2}$-*DHA2*-mCherry strain were spotted onto YPD or V8 agar medium with or without the addition of copper or the copper chelator BCS (A). Images of the yeast cells cultured in YPD were shown in (B). Images after 10 days for strains grown on V8 medium (C). Images of the hyphal cells from colonies on V8 medium were shown in (D). Scale bar: 100 μm.

Our observations indicate cell-type specific expression patterns of the Cfl1 family proteins. Cfl1 is specific to hyphae, whereas Dha1 is enriched in yeasts, basidia, and spores. In contrast, Dha2 is specific to yeast cells. Hence, the unique expression pattern of Dha1, Dha2, and Cfl1 may contribute to the heterogeneity in cell surface and physiology within a mating population of *C. neoformans*. Our data also suggest that gene expression data from a whole population should be interpreted with caution due to the existence of heterogeneous subpopulations.

3.3.8 Dha1 is responsive to copper limitation

Dha1 is highly expressed by yeast cells in YPD medium but not by yeast cells cultured on V8 medium. We previously found that YPD medium is copper-limiting to *C. neoformans* as the copper transcription factor mutant *mac1*Δ/*cuf1*Δ grows poorly on YPD medium without copper supplement [87]. By contrast, copper in V8 medium is a known factor to stimulate cryptococcal filamentation [88]. Thus, we decided to examine the influence of copper availability on Dha1 protein production. Here we cultured the P_{DHA1}-*DHA1*-mCherry strain on YPD medium supplemented with copper or the copper chelator BCS. Remarkably, the Dha1-mCherry fluorescence signal was drastically repressed by even 50 μM of copper on YPD medium (Figure 3.8). Consistently, closer examination at cellular level showed similar reduction of the Dha1-mCherry signal in the yeast cells in YPD medium supplied with extra copper (Figure 3.8.B). Drastic repression of Dha1-mCherry by copper was also seen on V8 media during mating (Figure 3.8.C). At the colony level, the Dha1-mCherry signal was not detected in the presence of copper and it was slightly induced by BCS on the V8 medium (Figure

3.8.C). At the cellular level, we could not detect Dha1-mCherry on the neck of basidium when there is addition of copper (Figure 3.8.D). We also noticed a reduction in basidium production in the presence of extra copper in the medium even though filamentation was increased [88].

To test if fluorescence reduction seen in the P_{DHA1}-*DHA1*-mCherry strain is a non-specific effect of copper, we examined the impact of copper on the Dha2-mCherry signal from the P_{DHA2}-*DHA2*-mCherry strain cultured in YPD medium. We did not observe dramatic copper- dependent repression (Figure 3.8.A-B). We also examined the effect of copper on the expression of the hyphal specific protein Cfl1-mCherry. The Cfl1 signal from the P_{DHA1}-*DHA1*-mCherry strain cultured on V8 medium was not affected by either the presence of copper or the copper chelator (Figure 3.8.C). Collectively, these results indicate that Dha1 is responsive to the copper level in the medium and it may play a role in sensing copper limitation.

3.3.9 The *dha1*Δ mutant has reduced intracellular replication within the macrophage

C. neoformans experiences a copper limiting environment within the macrophage and during brain infection, but not in the lungs [201]. Since our results showed that Dha1 is highly produced by copper limitation, we wanted to examine if deletion of *DHA1* has any effect on the intracellular replication within macrophages. For the phagocytosis assay, cryptococcal cells were co-incubated with macrophages for 2 hours before the non-adherent *C. neoformans* cells were removed by thorough washing. We then added the fungistatic drug fluconazole to inhibit the replication of extracellular cryptococcal

cells as described previously [196, 202]. After 24 hours of co-incubation, we measured the intracellular and extracellular fungal burden by counting cryptococcal CFUs present in the medium alone *versus* cryptococcal CFUs from lysed macrophages. We found no difference between the *dha1*Δ mutant and the wild type in fungal burden at 2 hours post co-culture with macrophages (Figure 3.9.A). This suggests that the deletion of the *DHA1* gene does not affect cryptococcal phagocytosis or adherence. By contrast, we detected a slight reduction of the *dha1*Δ fungal burden in the extracellular pool after 24 hours of co-culture with macrophages and a significant reduction in the intracellular pool of the *dha1*Δ mutant than the wild type at this time point (Figure 3.9.B-C). This suggests that the *dha1*Δ mutant likely have reduced ability to replicate or survive within macrophages.

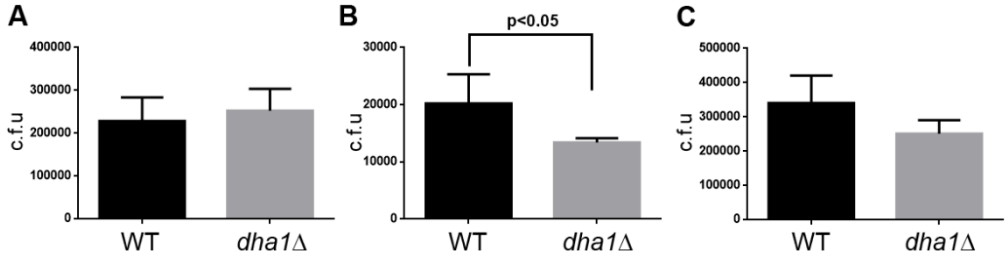

Figure 3.9 *The dha1*Δ mutant has reduced intracellular survival or replication. *Cryptococcus* cells of the wild type and the *dha1*Δ in mutant were incubated with macrophages for 2 hours or 24 hours at 37 °C+ 5% CO2. Adherent and the original phagocytosed *C. neoformans* cells were determined based on initial 2 hours incubation with the macrophage (A). The intracellular count of cryptococcal cells at 24 hours of co-culture with macrophages (B). The extracellular count of *C. neoformans* cells 24 hours of co-culture with macrophages was obtained from the extracellular medium containing the fungistatic drug fluconazole (C).

3.4 Discussions

In this study, we showed that all four homologs of Cfl1 in *C. neoformans* are secretory proteins and are released extracellularly, similar to Cfl1 [189]. This family of secretory proteins might be involved in diverse biological functions of this fungus. For instance, the deletion of *CPL1* affects cryptococcal capsule formation, a major virulence factor of this pathogen. The deletion of *DHA1* affects cryptococcal interaction with macrophages.

The cell type specific expression shown by Cfl1 homologs is shown in Figure 3.10. The cell-type specific expression shown by cell surface proteins is not uncommon. Morphological transitions in microbes are associated with change in the expression of cell surface proteins [178]. The changes in the expression of cell surface proteins contribute to the physiology diversity in cells of different morphotypes [178]. The observation that high levels of Dha2 are only present in yeast cells during sexual development suggests that it might be important for maintaining heterogeneity in the community. We noticed that all the cells that express Dha2 are round yeast cells and not shmoo cells or germ tubes. This intriguing observation suggests that the Dha2-producing cells might not be producing or responding to pheromones. This might allow some cells to further differentiate into hyphae while maintaining a subpopulation of yeast cells in a mating colony. Combining the high expression of Dha1 in yeast cells and in spores, Dha2 in yeasts, and Cfl1 in hyphae, the expression pattern of multiple surface and secretory proteins confer diverse properties to the mating colony of *C. neoformans* that

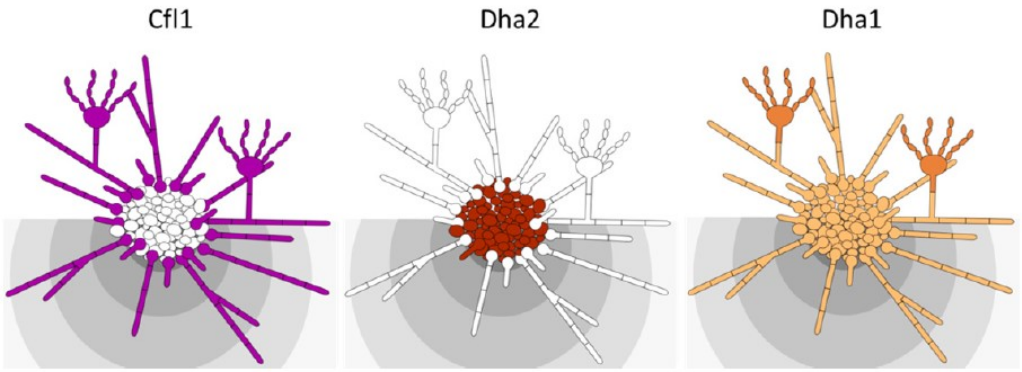

Figure 3.10 Cell type specific expression pattern shown by Cfl1, Dha1, and Dha2 during sexual development. Cfl1 is produced by hyphae, whereas Dha2 is mostly produced by yeast cells. Dha1 is weakly expressed in yeast cells during mating on V8 medium. However, it is enriched in basidia and spores.

contains a population with heterogeneous morphotypes. This bet hedging might be a strategy for the population to cope in unforeseen environmental conditions. It is interesting that the secretory protein Dha1 is induced by copper limitation and repressed by copper. It is known that *C. neoformans* experiences an environment of copper limitation during brain infection, while it needs to detoxify excessive copper during lung infection [201]. Within macrophages, however, *C. neoformans* experiences copper limitation based on the induction of its copper transporter genes [201]. It is tempting to hypothesize, given that Dha1 is induced by copper limitation and that the *dha1*Δ mutant is defective in intracellular survival or replication, that Dha1 might help *C. neoformans* acquire copper or sense copper-limitation within the macrophage. Amino acid sequence

analysis shows that Dha1 protein is cysteine rich, with 22 out of 327 of its residues being cysteine (6.7%). By contrast, the house keeping proteins Tef1 (8/459), Gpd1 (4/344), or Act1 (5/377) only have 1.7%, 1.16%, or 1.3% of residues being cysteine respectively. It is possible that Dha1 plays a role in sensing redox status of its environment, which connects to its response to the copper level in the environment. The hypothesis of secretory protein plays a role in sensing metals/redox status in fungal environment warrants further investigation.

4 PHEROMONE INDEPENDENT SEXUAL REPRODUCTION IN *CRYPTOCOCCUS NEOFORMANS*

4.1 Introduction

Sexual development can be achieved either through bisexual mating (compatible mating partner required) or unisexual mating (self-fertile). Unisexual reproduction is a form of homothallism. More details about homothallism is mentioned in Chapter 1. Term bisexual reproduction is used in the fungus *Cryptococcus neoformans* to represent heterothallism. Bisexual reproduction is best known in higher eukaryotes. Each reproduction mode has its own costs and benefits. Bisexual reproduction promotes outcrossing, but, finding the compatible mating partner can be challenging. Unisexual reproduction promotes inbreeding, but it avoids the cost associated with locating the mating partners. The latter might be critical for non-motile species, or species where compatible partners are rare.

The human fungal pathogen *Cryptococcus neoformans* can undergo both bisexual (**a**-α) as well as unisexual (mostly α) under laboratory conditions. Similar environmental factors, such as nutrient limitation, dehydration, and copper, are known to influence both modes of reproduction,[87, 88]. Both modes of sexual development include yeast-hypha transition and the formation of fruiting bodies known as basidia and meiotic basidiospores (Figure 4.1). Bisexual reproduction is by far much more efficient in terms of robustness in filamentation and sporulation [13, 19, 68], and their **a** and α progeny are comparable in terms of fitness [142, 203, 204], with the obvious exception

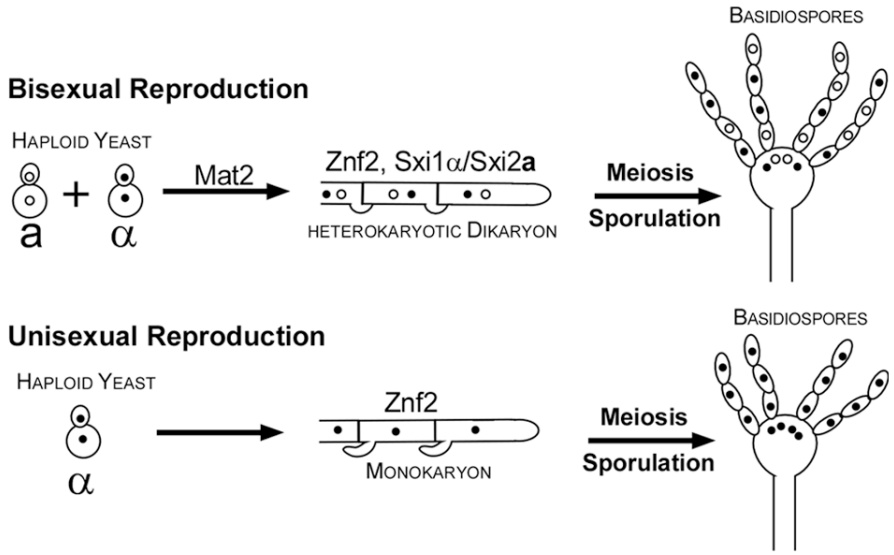

Figure 4.1 *C. neoformans* can undergo bisexual (a-α) reproduction as well unisexual (α) reproduction.
Both bisexual and unisexual reproduction culminates with the formation of fruiting structure basidium where meiosis and sporulation take place. However, they differ in the route they take to achieve sexual development (early developmental stages). Bisexual mating proceeds through cell fusion between **a** and α cells for which Mat2 is essential. Sxi1α and Sxi2**a** are required for maintaining the heterokaryotic dikaryon stage where the parental nuclei remain unfused. Znf2 is required for subsequent filamentation. Karyogamy (nuclear fusion) followed by meiosis takes place in the basidium. Unisexual reproduction can proceed either through cell-cell fusion between two α cells or through endoduplication. Here, nuclear fusion takes place to form a diploid before the formation of the monokaryotic hyphae. In this case also, Znf2 is required for filamentation. Znf2 and features downstream of Znf2 is conserved in both types of sexual development

that the α mating type enhances unisexual reproduction [68, 87, 142] The enhanced ability of α isolates to undergo unisexual reproduction can at least partly explain the predominance of the α mating type (99.9%) among clinical and environmental isolates [23, 79, 80, 203]. However, the predominance of the α mating type in nature and the inefficiency of unisex observed under laboratory conditions presents a conundrum.

So far, no genetic factor that specifies the cryptococcal commitment to unisexual versus bisexual reproduction has been identified. Based on the features of cryptococcal sexual development (Figure 4.1), the decision in committing to a particular mode of sexual reproduction has to occur very early during mating. Bisexual mating proceeds through cell fusion, and formation of dikaryotic hyphae whereas unisex proceeds to form a monokaryotic hyphae. Diploidization during unisex is highly plastic and could be derived from cell fusion or mostly endoreplication at any stage of the development prior to meiosis and sporulation [51, 52, 205]. Decision in choosing bisexual reproduction likely occurs prior to cell fusion. The Sxi1α-Sxi2**a** homeodomain proteins are specific to bisexual reproduction to maintain the dikaryotic state of the hyphae post cell fusion [6, 7]. Because Sxi1α/Sxi2**a** are not necessary for **a-** α conjugation [6, 7], this homeodomain complex functions after the choice of bisexual reproduction mode has been made. The master regulator of filamentation, Znf2, functions downstream of the pheromone sensing pathway. It is required for filamentation and subsequent development to complete the life cycle during both unisexual and bisexual reproduction [4, 9]. The transcription factor Mat2 induces transcription of multiple components of the pheromone sensing pathway by binding to the PRE elements in the promoter region of the respective genes [4, 97]. Consequently, the *mat2*Δ mutant cannot undergo cell fusion even with a compatible wild-type partner [4]. We previously showed that this transcription factor of the pheromone pathway plays an important role in deciding which parental mitochondrial DNA will be inherited in the progeny even prior to cell fusion [206]. This finding indicates that Mat2 could greatly influence the behavior of the mating partner prior to

actual cell fusion, making it a likely candidate involved in early decision making process for sexual development. However, contradictory to this is the observation that Mat2 is shown to be necessary for both unisexual and bisexual mating [4, 9].

Previous studies have presented some intriguing observations that the pheromone pathway might not be essential for unisexual reproduction despite their critical role in bisexual reproduction [83, 93, 98, 99]. For instance, deletion of the pheromone receptor gene *CPRα* (*STE3*) reduces the bisexual mating frequency to 0.3% (measured as the number of **a**-α cell fusion products) compared to that of WT [98]. However, for unisexual reproduction, the abundance of hyphae produced by WT and *ste3*Δ mutant was similar, suggesting that the pheromone receptor does not play a significant role in unisexual reproduction [98]. Likewise, bisexual mating was impaired for the *ste6*Δ mutant disrupted in the pheromone transporter gene, but the gene deletion did not affect unisexual reproduction [99]. Similarly, when the G-protein α subunit genes *GPA2* and *GPA3*, which are involved in pheromone sensing, were both deleted, the *gpa2*Δ*gpa3*Δ mutant was found to be sterile in bisexual mating but was unaffected for unisex reproduction. In fact, the *gpa2*Δ*gpa3*Δ double mutants were hyper-filamentous during unisexual development [93].

The prerequisite for meiosis (reduction division) is polyploidization. This is achieved by **a**-α cell fusion during bisexual reproduction. However, unisexual reproduction can proceed through cell fusion or endoreplication [52, 68]. Lin et al. 2005 found that the frequency of cell fusion during unisexual mating was very low [68] and evidence from population genetics studies indicates that endoreplication might be the

major route for ploidy increase [80]. Thus it is conceivable that the pheromone pathway, which is designed for non-self-recognition, might not be as important for unisex. We conducted this study to resolve the conflict and to investigate if the role of the pheromone pathway is priming *C. neoformans* to choose one versus the other sexual reproduction mode.

4.2 Methods and Materials

4.2.1 Strains

The strains used in this paper are listed in the Supplemental Table 1. *C. neoformans* strains were maintained as glycerol stocks in -80 °C. Yeast cells were grown on YPD (Yeast extract Peptone Dextrose). Mating assays were performed on V8 pH7 medium in the dark at 22 °C with or without the addition of copper or other metal ions as indicated in the texts and figures. Copper at 400 μM was used in most experiments unless indicated otherwise. Other media used for filamentation assays include MS medium, YNB medium, and Filament Agar medium as described previously [81, 86].

4.2.2 Gene disruption, complementation, and overexpression

Gene deletion was carried out using the split marker recombination approach as we previously described [191]. Briefly, the 5' and 3' flanking sequences of the gene of interest were fused to two third of the NAT or NEO drug resistance marker respectively using overlap PCR. Dominant markers NAT and NEO were amplified from plasmid the plasmids pPZP-NATcc and pPZP-NEO1 [207]. The gene deletion construct was

introduced to the recipient strains through biolistic transformation as described previously [192]. Gene deletion was confirmed through PCR. The linkage between the gene deletion and the observed phenotypes was also established through genetic linkage assay as described previously [193]. Briefly, meiotic progeny was dissected from genetic crosses for the strains if bisexual mating was possible and these progeny were analyzed for the interested phenotype, mating type, and the presence of the gene deletion at the correct genetic locus. For complementation of the deletion strains, ORF and 1-1.5 kb upstream of the gene was amplified using the wild type genomic DNA as the template. The amplicon was then inserted into the pPZP-NEO1 plasmid. The wild type allele of the gene together with the drug selection marker was then introduced into the corresponding gene deletion strain through biolistic transformation. To construct overexpression strains, ORFs of the genes of interest were amplified by PCR, digested, and then ligated into the pXL1 plasmid after the *GPD1* promoter region of *Cryptococcus neoformans* as we described previously [9]. This generates constitutive overexpression. For inducible system, we replaced the P_{GPD1} region of the plasmid with the $P_{CRT4\text{-}2}$ to generate copper inducible system as described previously [9, 208]. All primers used for generating gene deletion, complementation, or overexpression were listed in the Supplemental Table 2.

4.2.3 Mating assay and microscopy

For self-filamentation, WT and mutant cells of equal density (OD_{600} = 3) were plated onto V8 or V8+copper medium and incubated in the dark at 22°C for 6 days or as specified in the figures. For most of the phenotypic assay, 400 μM of $CuSO_4$ was added

to the V8 juice medium. For visualization of fluorescent proteins and sporulation, 150-200 μM of $CuSO_4$ was used. For bisexual mating, equal number of cells of mating type **a** and α were mixed together on V8 juice agar medium and incubated in the dark. For visualizing basidia and spores, cells were incubated for extended period of time till 16 days. Images of the colony were acquired through GO21 camera connected to the stereoscope Olympus SZX16 as we described previously [8]. Yeast, hyphae, basidia, and spores were captured by a Zeiss Axiocam 506 camera connected to a Zeiss Imager M2 epifluorescence microscope as we described previously [209]. The filter used for visualizing mCherry was the FL filter set 43 HE cy3 (Carl Zeiss Microscopy).

4.2.4 RNA extraction, qPCR and northern blot

RNA extraction and qPCR was performed as we described previously [9]. For extraction of RNA from cells grown on V8 and V8+copper, an equal number of cells were plated and incubated in the dark at 22 °C. For the control samples, cells were grown overnight in liquid YPD. At the indicated time points, cells were collected, washed with cold ddH_2O, and lyophilized. Total RNA was extracted using Purelink RNA minikit (Life Technologies) followed by DNase treatment (Ambion). The quality and quantity of the RNA samples were analyzed by electrophoresis on a denaturing formaldehyde agarose gel. First strand cDNA synthesis was performed using Superscript III cDNA synthesis kit (Life Technology) following the manufacturer's instructions. Gene expression levels were normalized using constitutively expressing housekeeping gene *TEF1* as we described previously.

The procedures for northern blot analyses were the same as we described previously [4]. Briefly, total RNA was extracted from cells grown on V8 and V8+copper for 16 hours. Poly (A) tailed RNAs were purified using PolyATtract mRNA isolation System IV (Promega) following manufacturer's instructions. The random primers DNA labeling System (Life technologies) was used for generating probes for *MF*α and *ACT1*.

4.2.5 RNA-seq analysis

WT strain XL280 and the *mat2*Δ mutant were cultured on YPD, V8, and V8+Copper (400 μM) media. Cells were collected at 16 hours for isolation of total RNA. Strand specific RNA-seq was performed at TAMU genomic facility following the standard protocol for Illumina Genome Analyzer IIx (http://www.txgen.tamu.edu/?s=sequencing) as we described previously [8]. Sequence reads were aligned to the XL280 reference sequence using Tophat [73, 210]. Cufflinks was used for gene expression quantification [211]. Gene expression normalization and differential gene expression analysis was done similarly to what we described previously [8]. RNA-seq is deposited at NCBI.

4.2.6 Insertional mutagenesis via *Agrobacterium*-mediated transformation and mutant screen

Insertional mutagenesis was performed in the *mat2*Δ mutant of the XL280 background (NAT^R). *Agrobacterium tumefaciencs* strain EHA105 containing the Ti-plasmid pPZP-NEO1 was used for the insertional mutagenesis as described previously [4, 207]. *A. tumefaciencs* was grown overnight in Luria-Bertani containing

medium kanamycin at 22 °C. Cells were washed twice with sterile water and grown on induction medium containing 100 µM Acetosyringone for additional 6 hours. *Cryptococcus neoformans* cells grown overnight in liquid YPD was washed and resuspended in induction medium to get $1x10^7$ cells/ml. Equal aliquots of fungal and bacterial cells were mixed and co-cultured on the induction medium (200 µl per drop) for 3 days at 22 ^{0}C in the dark. The cocultured cells were then collected and plated onto V8 + cefotaxime + G418 + NAT + copper medium. This selective medium will kill *Agrobacterium* cells (cefotaxime) and selected for the transformants with T-DNA (G418). Most colonies, like the *mat2*Δ mutant parental strain, were able to filament on the V8+copper medium. After 2 weeks of incubation, mutants that only grow in the yeast form were selected. To identify insertion sites through inverse PCR coupled with sequencing, genome DNA from the selected candidates was digested with a restriction enzyme, purified, and self-ligated as we described previously [4]. Primers AI076/Ai077 were used for inverse PCR and sequencing as we described previously [4, 207]. After sequencing, flanking region sequences were used for blast search against *C. neoformans* serotype D genome database at Genebank to identify the insertion sites and the genetic loci affected by the insertion.

4.2.7 Sequencing and identification of the insertional sites

All 47 candidate insertional mutants selected above were grown overnight in YPD liquid medium. Genomic DNA was extracted following cetyltrimethylammonium bromide (CTAB) extraction protocol as previously described [212, 213]. Genomic DNA from 47 individual selected mutants was pooled into four groups with each group

consisting DNA from 11-12 mutants. 10 µg of total DNA from each pool was submitted to the TAMU AgriLife, Centre for bioinformatics and genomic systems engineering for sequencing (Illumina Miseq 175 bp x 175 bp, paired end reads). Each group yielded $1.1x10^8$ to $1.75x10^8$ reads pairs (129.5 M pairs), yielding an average 12x coverage of *Cryptococcus neoformans* genome per strain. Analysis of the insertion sites was performed using the AIMHII approach as previously described for *C. neoformans* [214].

4.3 Results

4.3.1 The *mat2*Δ mutant is able to undergo filamentation

Mat2 regulates the pheromone response MAPK pathway and is required for cell fusion during bisexual (**a**-α) mating in *Cryptococcus neoformans* [4, 9, 97]. The failure in **a**-α cell fusion blocks further development of dikaryotic hyphal growth. Consequently, no yeast to hypha differentiation was observed when the *mat2*Δ mutant was co-cultured with an opposite mating partner that only produces hyphae during bisexual mating (Figure 4.2). The *mat2*Δ mutant strains made in the otherwise self-filamentous wild-type backgrounds (e.g. JEC21 or XL280) also failed to undergo yeast to hypha differentiation when cultured alone under all mating-inducing conditions tested so far (V8, YNB, Filament Agar, and MS media). Thus, Mat2 was considered crucial for both unisexual and bisexual reproduction. Previous studies have shown that the pheromone pathway promotes **a**-α bisexual outcross, but it is unlikely to be critical for unisexual development (see introduction for details). If this statement is valid, then we would predict that the disruption of the master regulator of the pheromone sensing

pathway should not abolish the ability of *Cryptococcus neoformans* to undergo unisexual reproduction. Accordingly, the *mat2*Δ mutant should be able to undergo filamentation under certain conditions.

We previously found that copper (≤ 100 μM) enhances self-filamentation [87]. Copper is also one of the components in the mating-inducing V8 juice medium [88]. Thus, we decided to test the impact of copper addition at various concentrations on the *mat2*Δ mutant. The colony of the *mat2*Δ mutant on V8 medium was smooth and round due to the presence of only yeast cells (Figure 4.3.A), as expected based on previous studies [4, 97]. We found copper at 400 μM induced robust filamentation in the *mat2Δ* mutant. Even copper at 200 μM induced visible filamentation in the *mat2*Δ mutant (Figure 4.3**.**A). Therefore, the colony of the *mat2*Δ mutant on the V8+copper medium

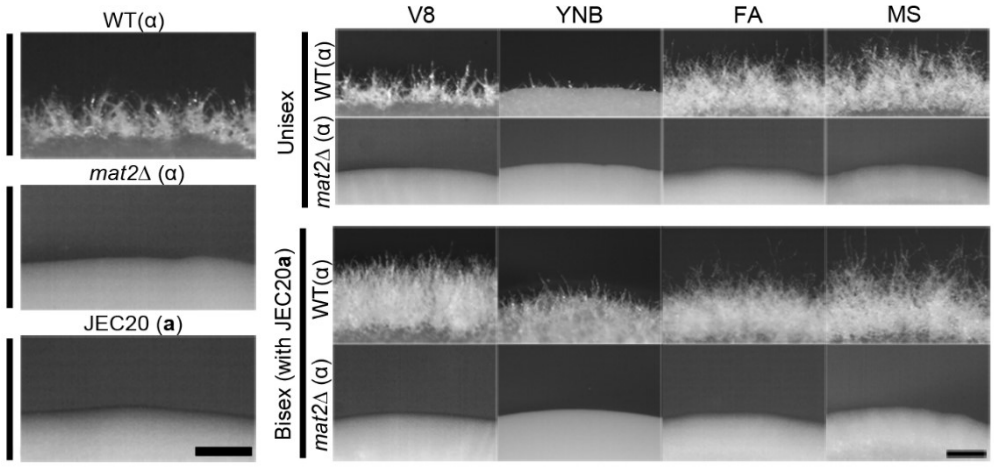

Figure 4.2 *mat2*Δ mutant is unable to undergo bisexual and unisexual mating under known mating inducing conditions.
An Equal number of cells of WT and *mat2*Δ mutant were incubated alone in the dark at 22°C for 4 days for unisexual mating. For bisexual mating equal number JEC20**a** cells were mixed with either XL280α or *mat2*Δα and incubated in the dark at 22°C. Four different mating media were used.

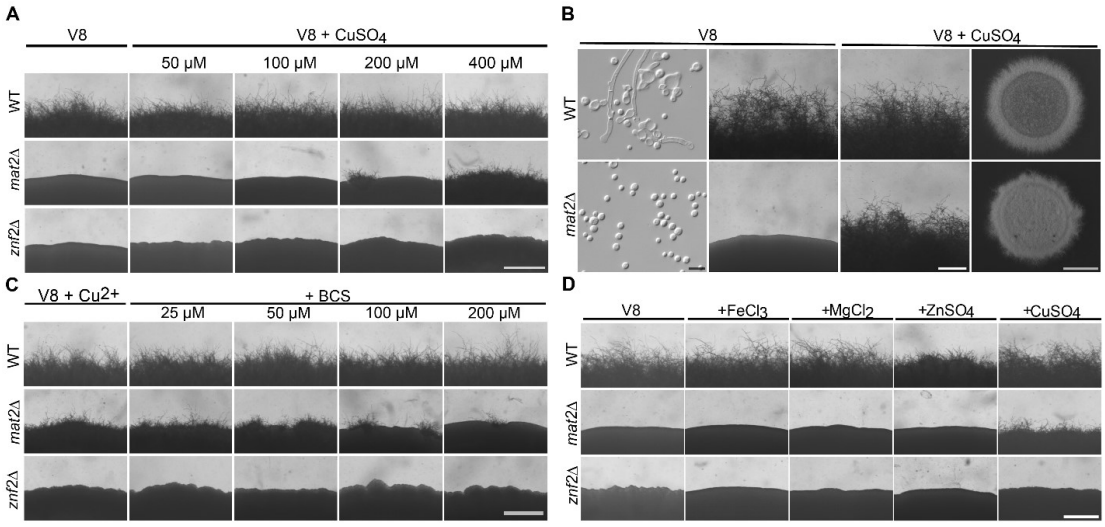

Figure 4.3 *mat2*Δ mutant can filament in copper.
(A) WT, *mat2*Δ and *znf2*Δ mutants were cultured in V8 medium or V8 medium supplemented with different concentrations of copper. WT can filament well at all conditions whereas *znf2*Δ cannot. *mat2*Δ mutant starts to show filamentation at 200 µM. (B) *mat2*Δ mutant looks smooth and round on V8 media but can produce profuse filamentation with the addition of 400 µM copper. (C) Addition of copper chelator to the 400 µM copper can reduce the robustness of filamentation shown by *mat2*Δ mutant. (D) *mat2*Δ mutant cannot filament on V8 media supplemented with 400 µM of other metal ions as shown in the figure. Scale bar: 500µm. Scale bar for light microscope image of the cells: 10µm

appeared fluffy due to profuse production of filaments all over the colony (Figure 4.3.B). Consistently, addition of copper chelator BCS to the V8 medium with 400 µM of copper reduced the robustness of filamentation shown by the *mat2*Δ mutant (Figure 4.3.C). To understand if the induction of filamentation in the *mat2*Δ mutant is specific to copper or a general response to metal ions at high concentrations, we tested a variety of metal ions including iron, magnesium, and zinc. WT cells filamented well under all tested

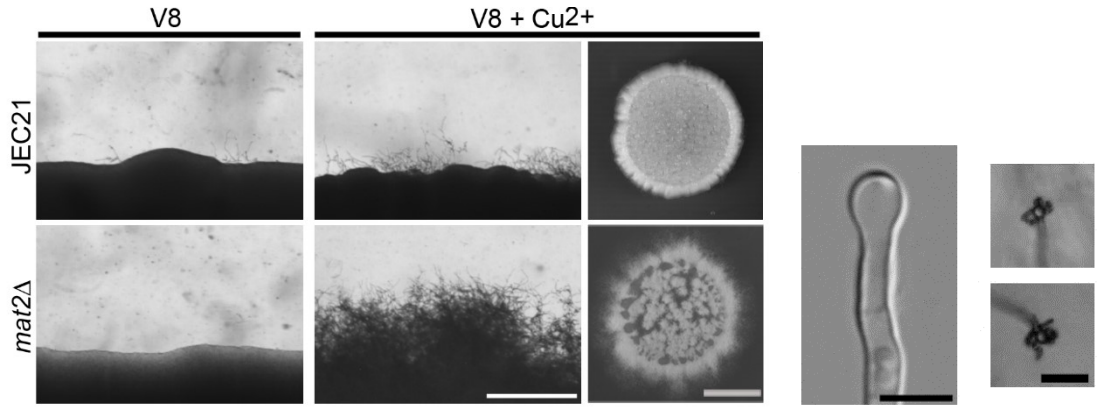

Figure 4.4 *mat2*Δ can filament independent of the strain background.
(A) JEC21 filaments a little better in V8+Cu2+ compared to that in V8. mat2Δ strain cannot filament in V8 but can produce robust filamentation in V8+Cu2+.
(B) mat2Δ mutant has the ability to produce fruiting structure as well as spores.

conditions. None of the other metal ions tested induced filamentation in the *mat2*Δ mutant (Figure 4.3.D).

To examine if the ability of the *mat2*Δ mutant to filament in response to copper is specific to the XL280 background, we tested the *mat2*Δ mutant made in the JEC21 background. WT JEC21 produces sporadic filaments on V8 medium after relative long incubation and filamentation was slightly increased on V8+copper medium. By contrast, the *mat2*Δ mutant filamented robustly on V8+copper medium **(**Figure 4.4.A). Hence, these data show that *mat2*Δ can filament in response to copper. We also found that the *mat2*Δ mutant was able to produce basidia and spores on V8+copper medium, although at a lower frequency (Figure 4.4.B). This is documentation of filamentation and sporulation in the *mat2*Δ mutant.

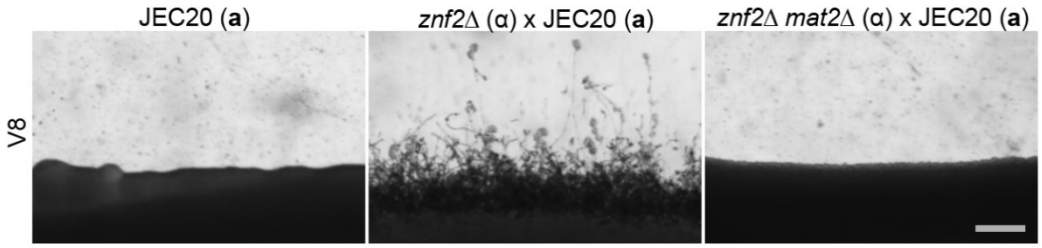

Figure 4.5 *znf2*Δ mutant can undergo unilateral mating unlike *znf2*Δ*mat2*Δ. JEC20 on its own does not produce filamentation, but can produce filaments while mated with JEC20. However, *znf2*Δ*mat2*Δ double deletion mutant produce filaments cannot consistent with role of Mat2 in cell fusion.

4.3.2 Filamentation shown by the *mat2*Δ mutant still requires Znf2

Mat2 controls multiple components of the pheromone sensing pathway. Deletion of *MAT2* abolishes the ability of the cells to produce pheromone or to respond to pheromone. Thus, the *mat2*Δ mutant does not produce mating projections on V8 medium [4, 97]. Because Znf2 is activated by Mat2 to initiate filamentation during mating, the *mat2*Δ mutant consequently does not produce hyphae on V8 medium either. Znf2 is the master regulator of filamentation in *C. neoformans* [4, 9]. Unlike the *mat2*Δ mutant, the pheromone sensing pathway is not impaired in the *znf2*Δ mutant. Accordingly, deletion of *ZNF2* does not impair cell fusion during bisexual mating [4].

To determine if the copper evoked filamentation of the *mat2*Δ mutant still requires Znf2, we deleted both the *MAT2* and the *ZNF2* genes. For this purpose, the *MAT2* gene deletion cassette was introduced into the *znf2*Δ mutant background to create the *mat2*Δ*znf2*Δ double mutant. Although the *znf2*Δ mutant cannot self-filament, the *znf2*Δ mutant can mate with a WT partner of a compatible mating type to produce

filaments during bisexual mating on V8 medium (Figure 4.5). In contrast, the *mat2*Δ mutant cannot mate with a wild type partner due to its defect in the pheromone pathway. We found that the *mat2*Δ*znf2*Δ double mutant failed to filament when crossing with the WT partner on V8 medium (Figure 4.5), consistent with the essential role of Mat2 in cell fusion. We then tested self-filamentation of this *znf2*Δ*mat2*Δ double mutant on V8+copper medium. As expected, the *mat2*Δ single mutant filamented on V8+copper

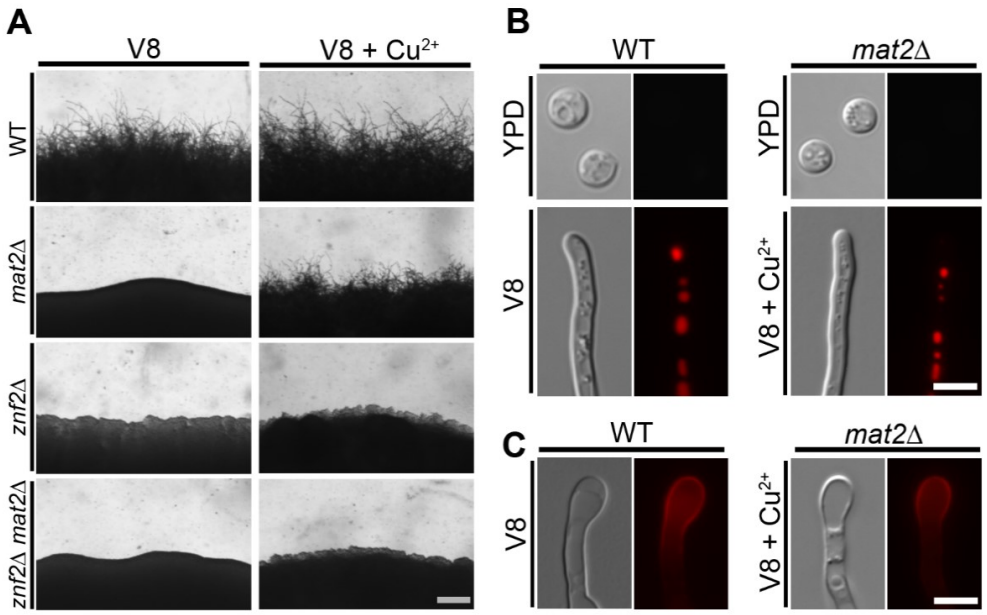

Figure 4.6 Filamentation shown by *mat2*Δ mutant requires Znf2.
(A) WT, *mat2*Δ, *znf2*Δ and *znf2*Δ *mat2*Δ strains were cultured on V8 and V8+ Cu media for 7 days before the pictures were taken. WT can filament in V8 and V8+ Cu^{2+}. *mat2*Δ mutant cannot filament on V8 but can filament in presence of copper. When *ZNF2* is deleted, the double deletion *mat2*Δ *znf2*Δ mutant cannot filament. Scale bar: 200µm. (B) Localization of hyphal specific proteins. Cfl1 is not expressed in both WT and *mat2*Δ mutant in the yeast cells. In hyphae, localization of Cfl1 in *mat2*Δ mutant on V8 + Cu^{2+} is similar to its localization in WT cells on V8. (C) Localization of surface protein Dha1 tagged with mCherry at its C-terminus in *mat2*Δ mutant on V8 + Cu^{2+} is similar to its localization in WT on V8 media. Scale bar: 5 µm.

medium and the *znf2*Δ single mutant did not filament under any conditions tested. The *znf2*Δ*mat2*Δ double mutant was unable to filament on V8+copper medium, similar to the *znf2*Δ single mutant (Figure 4.6**.**A). These data indicate that filamentation in the *mat2*Δ mutant stimulated by copper still requires Znf2. The finding further corroborates Znf2 as the master regulator of filamentation.

To examine if filamentation by the *mat2*Δ mutant on V8+copper shares the same molecular feature as filamentation by wild type, we examined the expression pattern of a few proteins known to be expressed in hyphae (Cfl1 and Dha1). We first examined the hypha-specific protein Cfl1. We previously discovered that *C. neoformans* wild-type hypha cells, but not yeast cells, express Cfl1 [9]. Consistently, the production of Cfl1 protein by hyphae was detected when wild-type cells were plated on V8 medium but not when the wild-type strain was cultured in YPD medium in the yeast form (Figure 4.6**.**B). To examine if Cfl1 by is similarly expressed by hyphae produced by the *mat2*Δ mutant on V8+copper, we fused Cfl1 with mCherry at its C-terminus (Cfl1-mCherry) and expressed the fusion protein with its native promoter ectopically in the *mat2*Δ mutant. No Cfl1-mCherry could be detected when this strain was cultured on YPD or on V8 medium growing only in the yeast form (Figure 4.6**.**B). By contrast, Cfl1 could be clearly detected on the hyphae produced by this *mat2*Δ mutant when grown on V8 + copper. We then decided to examine another protein, Dha1, which is enriched in basidia produced by wild-type hyphae (Gyawali et al. under review). We found that Dha1-mCherry showed similar localization in the basidia produced by either the wild type cultured on V8 or the *mat2*Δ mutant cultured on V8+copper (Figure 4.6.C). These results

suggest filamentation produced by the *mat2*Δ mutant shares the same molecular features with that of the wild type.

4.3.3 Filamentation in the *mat2*Δ mutant is independent of the pheromone sensing pathway

The ability of the *mat2*Δ mutant to filament on V8+copper could be caused by cryptic activation of pheromone under this condition. If true, then the *mat2*Δ mutant still requires the pheromone pathway for filamentation to occur. Alternatively, filamentation can take place in the *mat2*Δ mutant independent of the pheromone pathway. To distinguish these hypotheses, we examined the transcript level of the pheromone gene *MFα1* in WT cells and the *mat2*Δ cells on V8 and V8+copper at various time points. *CFL1*, the hyphal specific gene downstream of Znf2 is used as a marker of filamentation [9]. On V8 medium, WT XL280 is filamentous, as expected (Figure 4.2). Accordingly, the transcript level of *CFL1* was increased when WT was cultured on V8 medium compared to that on YPD medium (Figure 4.7.A). The transcript level of *MFα1* was also induced in WT cells on V8 medium (Figure 4.7.A), consistent with the known induction of pheromone under this condition [4, 87]. Consistent with the non-filamentous phenotype of the *mat2*Δ mutant on V8 medium, there was no induction in the *CFL1* transcript level (Figure 4.7.A). There was also no increase in the *MFα1* transcript level in the *mat2*Δ mutant on V8 medium (Figure 4.7.A), consistent with the established role of Mat2 in the pheromone pathway. Consistent with the real-time PCR results, northern blot analysis also indicated no induction for the *MFα1* transcript in the *mat2*Δ mutant cultured on V8 medium (Figure 4.7.C). On V8+copper medium, the transcript level for

both *CFL1* and *MFα1* were increased in WT cells compared to that in YPD medium (Figure 4.7.B). For the *mat2*Δ mutant cultured on V8+copper medium, the transcript level of *CFL1* was increased (Figure 4.7.B), consistent with its filamentous phenotype under this condition. However, there was no induction of the *MFα1* transcript on V8+copper. We also did not detect any *MFα1* transcript in the *mat2*Δ mutant on V8+copper medium by Northern blot (Figure 4.7.C). Thus, regardless of the conditions used, there was no detectable induction of pheromone in the *mat2*Δ mutant. These results further support the key role of Mat2 in regulating the pheromone pathway. The result supports the idea that filamentation in the *mat2*Δ mutant is independent of pheromone.

To further attest pheromone-independent filamentation in the *mat2*Δ mutant, we decided to compare the transcript level of other components of the pheromone sensing pathway in WT and the *mat2*Δ mutant on V8 and V8+copper medium using RNA-seq. Regardless of the condition used, we found that the transcript levels for many gene components in the pheromone pathway were low in the *mat2*Δ mutant, including the pheromone transporter gene *STE6* and the pheromone receptor gene *STE3* (Figure 4.7.D). By contrast, the transcript level of *CFL1* was induced in the *mat2*Δ mutant on V8+copper medium, consistent with the filamentous phenotype. Deletion of pheromone gene (*mfα1,2,3*Δ) or pheromone transporter (*ste6*Δ) in JEC21 could still filament in V8+copper (Figure 4.8). Collectively, these results demonstrate that filamentation in *mat2*Δ on V8+copper medium is independent of pheromone or the components of the pheromone sensing pathway.

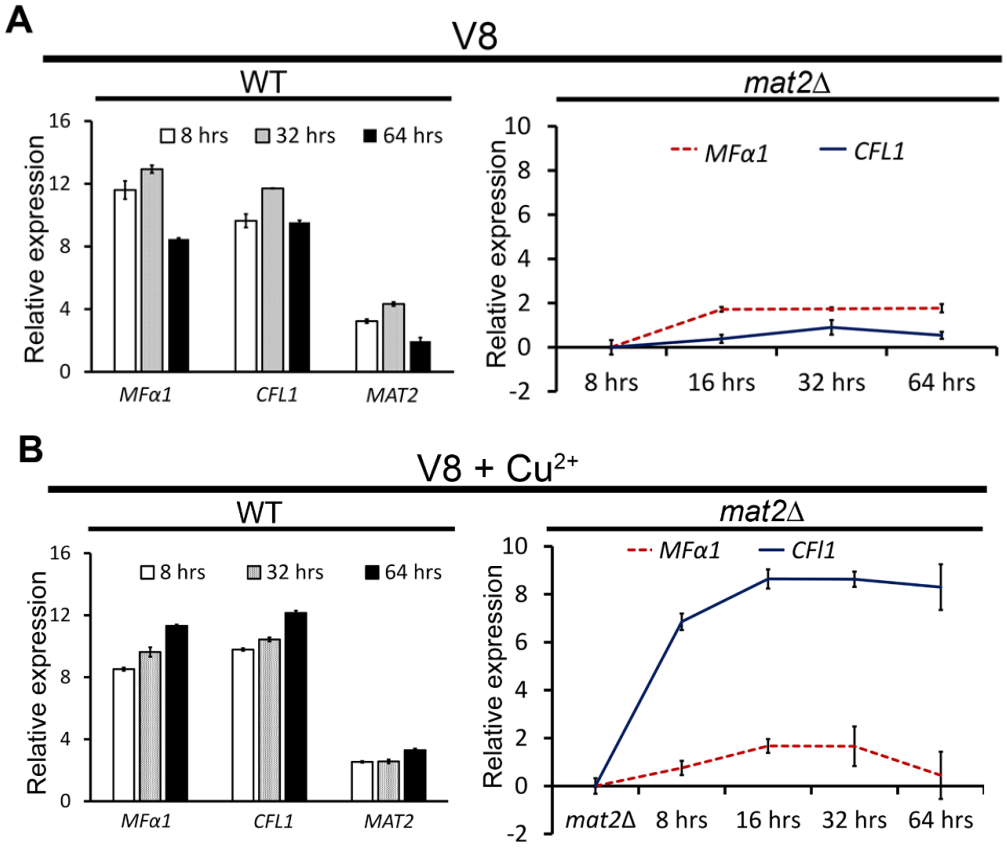

Figure 4.7 Filamentation shown by *mat2*Δ is independent of pheromone. WT and *mat2*Δ mutant samples were grown on V8 and V8 + Cu $^{2+}$ for different time points as indicated in the figure after which the samples were collected for RNA extraction. (A) RT-PCR graphs showing the relative expression level of pheromone gene *MFα1*, *CFL1* and *MAT2* in WT and *mat2*Δ mutant on V8 media at different time points. All three genes are induced in WT whereas they have low transcript in *mat2*Δ mutant. (B) Graphs showing the relative expression level of *MFα*, *CFL1* and *MAT2* in WT and *mat2*Δ mutant in V8 + Cu^{2+}. In WT cells, all of them are induced. In *mat2*Δ mutant, there is no induction in the transcript level of *MFα*, however, *CFL1* is induced. (C) Northern blot showing there is no induction in the transcript level of *MF*α in *mat2*Δ mutant either in V8 or V8 + Cu^{2+}. (D) Transcript level (FPKMs) of the *CFL1,* pheromone receptor *STE3* and pheromone transporter *STE6* in WT and *mat2*Δ mutant cultured on V8 or V8+ Cu^{2+} for 16 hours based on RNA-seq data. IGV software was used for transcript analysis. Reads count scale was set to different threshold value for each gene based on their transcript level. *CFL1*, *STE3* and *STE6* are induced in WT grown on V8. On *mat2*Δ mutant, transcript level is very low. For the samples on V8 + Cu^{2+}, only *CFL1* is induced in both WT and *mat2*Δ mutant.

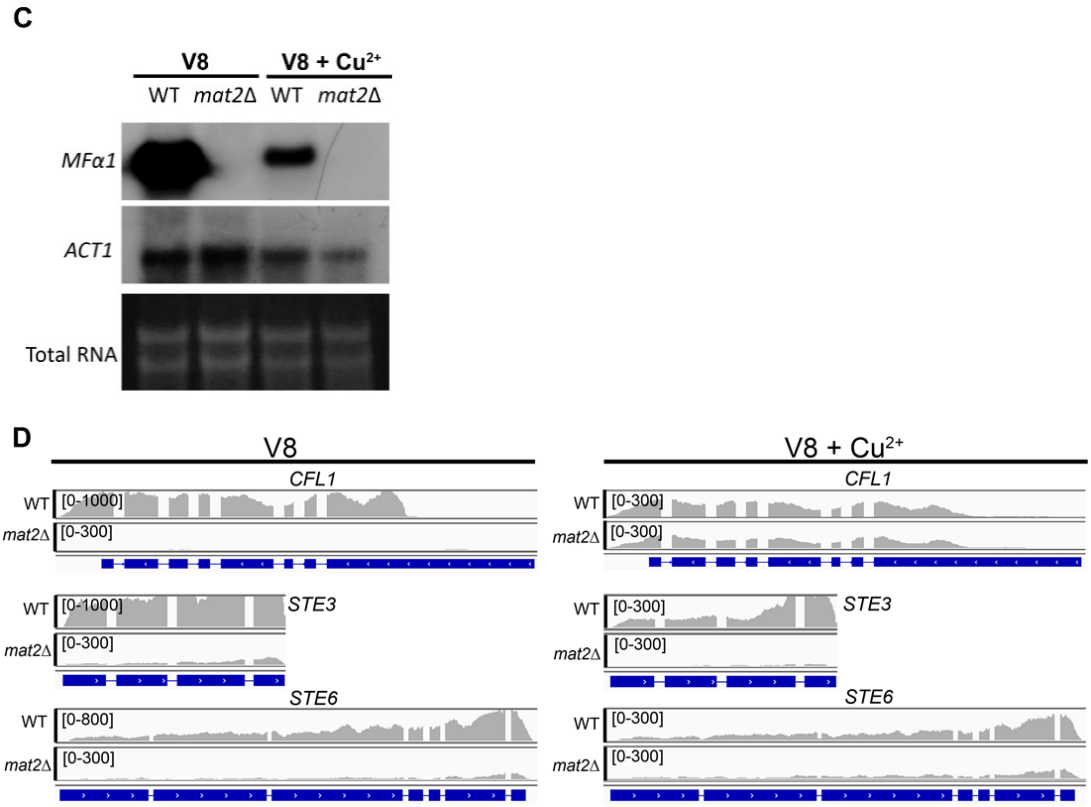

Figure 4.7 Continued.

If the *mat2*Δ mutant can filament independent of the pheromone pathway on V8+copper medium, then one would predict that factors affecting pheromone production should not affect *mat2*Δ filamentation. Light is known to inhibit *C. neoformans* mating by repressing the pheromone genes like *MFα1* through the light sensor complex [82]. We hypothesize that if light primarily inhibits mating through inhibition of the pheromone sensing pathway, then filamentation shown by the *mat2*Δ mutant on copper medium should not be affected by light. To test this hypothesis, we cultured the WT and the *mat2*Δ strains on V8 or V8+copper medium in dark or under constant light. WT cultured on V8 medium showed drastic reduction in filamentation when it was exposed

to constant light (Figure 4.9). The *mat2*Δ strain grown on V8 did not show any filamentation either in light or in dark, as expected. Surprisingly, both WT and the *mat2*Δ mutant filamented equally well on V8+copper medium in dark or in the presence of light (Figure 4.9.A). These results suggest that light does not inhibit filamentation on V8+ copper medium, consistent with it being pheromone independent.

A previous study by Fu et al. 2013 showed that prior growth at high temperature can prime self-filamentation in *C. neoformans* once cells are transferred to filamentation-inducing conditions. We tested if filamentation induced by high temperature is independent of pheromone. Here, we first cultured WT, the *mat2*Δ mutant, and the *znf2*Δ mutant at 22 °C, 30 °C, and 37 °C on YPD medium for 36 hours. Then we collect cells from cultures at different temperatures and plated them onto V8 medium. These cells were incubated on V8 medium at 22 °C for 10 days. As expected, the WT strain showed filamentation and the *znf2*Δ mutant showed no filamentation

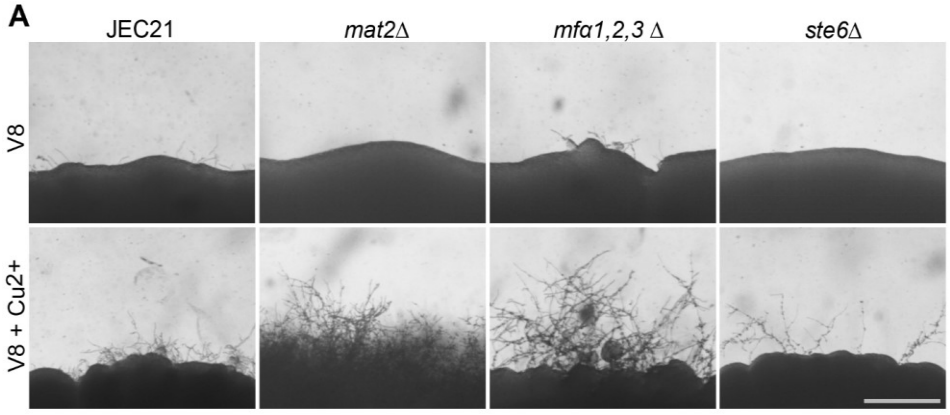

Figure 4.8 Filamentation shown by *mat2*Δ is independent of the pheromone transporter.
The mutants of pheromone pathway can filament in V8+Cu^{2+}.

under all three conditions tested. The *mat2*Δ mutant transferred from prior cultures at 22 °C or 30 °C on YPD medium did not show any filamentation (Figure 4.9.B). Interestingly, the *mat*2Δ strain transferred from the prior culture at 37 °C filamented (Figure 4.9.B). This finding indicates that high temperature-induced filamentation can be also independent of pheromone.

4.3.4 Suppressor screen to identify factors critical for *mat2*Δ filamentation

To identify components required for the pheromone independent filamentation in *mat2*Δ, we decided to perform forward genetic screen in the *mat2*Δ mutant background via *Agrobacterium* mediated insertional mutagenesis. This T-DNA insertional mutagenesis has been successfully used in *C. neoformans* to identify novel genes regulating different processes [4, 207, 214, 215]. Here we utilized the unique ability of

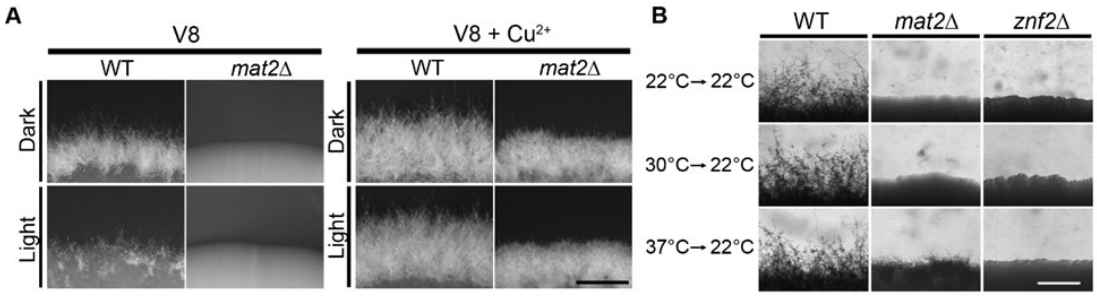

Figure 4.9 Pheromone independent filamentation is not affected by light. WT and *mat2*Δ mutant strains were cultured on V8 or V8 + Cu^{2+} and incubated at 22 °C in dark or at constant light. On V8 media, filamentation shown by WT is dramatically reduced in presence of light. On V8 + Cu, WT and *mat2*Δ mutant filaments well in dark and as well as in light. (B) Heat shock induced filamentation can take place independent of pheromone. WT, *mat2*Δ, and *znf2*Δ mutant strains were grown on YPD at different temperatures and after 36 hours, were transferred to V8 media and incubated in dark at 22°C for 8 days. WT can filament under all conditions whereas *znf2*Δ mutant cannot filament at any conditions. *mat2*Δ mutant cannot filament when transferred from 22 °C and 30 °C. However, when transferred from 37 °C, filamentation could be seen in *mat2*Δ mutant.

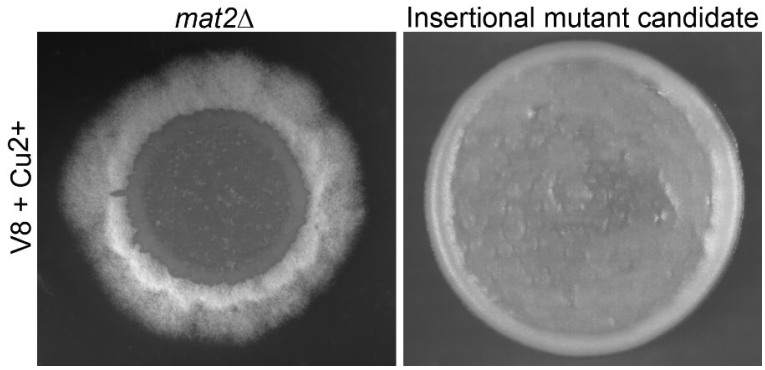

Figure 4.10 Insertional mutant candidate.

Insertional mutant candidate. Insertional mutagenesis was performed in *mat2*Δ background. *mat2*Δ mutant produces robust filamentation in V8+Copper. Candidate genes of interest were the one that cannot produce filaments as shown above.

the *mat2*Δ mutant to filament on V8+copper medium to perform a suppressor screen to identify genetic components required for Mat2-independent filamentation. We generated and screened 77,000 insertional mutants on V8+copper medium for isolates that could not filament (Figure 4.10). We isolated 47 insertional mutants that showed only yeast growth on V8+copper medium. Genomic DNA of these selected insertional mutants were pooled into four groups and sequenced. Sequences bordering the T-DNA construct were used to perform BLAST search against the *Cryptococcus neoformans* (Serotype D) genome database to identify the insertion sites. Some of the insertion sites were also identified through inverse PCR as previously described [4]. Genetic loci affected by the T-DNA insertions from the 47 mutants were identified and are included in the Table 4.1. Because the parental strain *mat2*Δ is sterile in bisexual mating, we could not perform genetic linkage analysis by crossing.

To work around this problem, a few candidate genes were confirmed independently through targeted gene deletion. Deletion of the coding sequences recapitulated the phenotype caused by the insertion (see the next section for details).

Table 4.1 Insertion sites identified through insertional mutagenesis.

Chromosome #	XL280 insertion sites	H99	JEC21
10	CNXL_056820	CNAG_04891	CNJ03160
11	CNXL_058570	CNAG_07533	CNK01380
13	CNXL_066220	CNAG_06203	CNM02020
13	CNXL_066760	CNAG_07009	CNM02560
14	CNXL_069460	CNAG_06508	CNN02320
2	CNXL_011610	CNAG_03772	CNB02680
4	CNXL_024340	CNAG_01060	CND01910
7	CNXL_107240	N/A	N/A
9	CNXL_052770	CNAG_05267	CNH03630
3	CNXL_017360	CNAG_01736	N/A
3	CNXL_017370	CNAG_01737	CNC02410
5	CNXL_031740	CNAG_02281	CNE02650
5	CNXL_031750	CNAG_02280	CNE02660
7	CNXL_041540	CNAG_03401	CNG01820
7	CNXL_041550	CNAG_03400	CNG01830
11	CNXL_060650	CNAG_02007	CNK03420
12	CNXL_062200	CNAG_05520	CNH01720
13	CNXL_066220	CNAG_06203	CNM02020
14	CNXL_069460	CNAG_06508	CNN02320
2	CNXL_014100	CNAG_04027	CNB05100
3	CNXL_019210	CNAG_02783	CNC04010
4	CNXL_022810	CNAG_00888	CND00260
10	CNXL_109310	N/A	N/A
9	CNXL_049990	N/A	CNL06260
9	CNXL_050000	CNAG_04989	CNL06250
9	CNXL_051420	CNAG_05130	CNL04910
9	CNXL_051430	CNAG_05131	CNL04900
1	CNXL_004080	CNAG_00408	CNA03970
1	CNXL_101190	N/A	N/A

Table 4.1 Continued

Chromosome #	XL280 insertion sites	H99	JEC21
10	CNXL_056170	CNAG_04836	CNJ02610
13	CNXL_066220	CNAG_06203	CNM02020
3	CNXL_021810	CNAG_01529	CNC06530
4	CNXL_022810	CNAG_00888	CND00260
4	CNXL_026510	CNAG_01279	CND04010
8	CNXL_048700	CNAG_04243	CNI03840
10	CNXL_054740	CNAG_04699	CNJ01290
10	CNXL_054750	CNAG_04700	CNJ01300
14	CNXL_068260	CNAG_06400	CNN01260
14	CNXL_111850	N/A	N/A
3	CNXL_019740	CNAG_07517	CNC04530
3	CNXL_019750	CNAG_02838	CNC04540
3	CNXL_021550	CNAG_01555	N/A
3	CNXL_021560	CNAG_01554	CNC06300
5	CNXL_031740	CNAG_02281	CNE02650
5	CNXL_031750	CNAG_02280	CNE02660
5	CNXL_034280	CNAG_02028	CNE05060
9	CNXL_049990	N/A	CNL06260
9	CNXL_050000	CNAG_04989	CNL06250
11	CNXL_060490	CNAG_01991	CNK03240
13	CNXL_065940	CNAG_06172|CNAG_06173	CNM01730|CNM01740
13	CNXL_066220	CNAG_06203	CNM02020
14	CNXL_066940	CNAG_06276	CNN00100
14	CNXL_068720	CNAG_06446	CNN01710
3	CNXL_015600	CNAG_03012	CNC00730
10	CNXL_055800	CNAG_04801	CNJ02280
11	CNXL_060490	CNAG_01991	CNK03240
3	CNXL_019140	CNAG_02773	CNC03940
3	CNXL_019150	CNAG_02775	CNC03950
9	CNXL_051910	CNAG_05179	CNL04470
9	CNXL_051920	CNAG_05180	CNL04460
4	CNXL_023270	CNAG_00938	CND00780
10	CNXL_054510	CNAG_04676	CNJ01080
1	CNXL_002690	CNAG_07114	CNA02690
11	CNXL_058410	CNAG_07548	CNK01220
2	CNXL_014550	CNAG_04073	CNB05560
8	CNXL_044960	CNAG_04539	CNI00150

Table 4.1 Continued

Chromosome #	XL280 insertion sites	H99	JEC21
8	CNXL_045350	CNAG_04500	CNI00570
9	CNXL_052740	CNAG_05264	CNH03660|CNL03660
1	CNXL_006290	CNAG_00624	CNA06040
4	CNXL_022560	N/A	N/A
5	CNXL_031240	CNAG_07988	CNE02180
10	CNXL_054510	CNAG_04676	CNJ01080
11	CNXL_057230	CNAG_06924	CNK00060
11	CNXL_060650	CNAG_02007	CNK03420
11	CNXL_060650	CNAG_02007	CNK03420
13	CNXL_065760	CNAG_06157	CNM01590
6	CNXL_040810	CNAG_03479	CNG01140
8	CNXL_045350	CNAG_04500	CNI00570
3	CNXL_019780	CNAG_02841	CNC04570
7	CNXL_040800	CNAG_03480	CNG01130
7	CNXL_040820	CNAG_03476	CNG01150
8	CNXL_048630	CNAG_04236	CNI03770
8	CNXL_048640	CNAG_04237	CNI03780
1	CNXL_002720	CNAG_00284	N/A
10	CNXL_053370	N/A	N/A
10	CNXL_109340	N/A	N/A
14	CNXL_069640	N/A	CNE00100|CNN02460
2	CNXL_008720	CNAG_06877	N/A
2	CNXL_010270	CNAG_03644	CNB01440
4	CNXL_103540	N/A	N/A
5	CNXL_029000	N/A	N/A
5	CNXL_034430	N/A	N/A
7	CNXL_039600	N/A	N/A
8	CNXL_045350	CNAG_04500	CNI00570
8	CNXL_045800	CNAG_04455	CNI01020
1	CNXL_007250	CNAG_00715	N/A
3	CNXL_017280	CNAG_01729	CNC02340
6	CNXL_035610	CNAG_05874	CNF00980
6	CNXL_105640	N/A	N/A
7	CNXL_044790	N/A	CNG04710
3	CNXL_015600	CNAG_03012	CNC00730
3	CNXL_015600	CNAG_03012	CNC00730

Table 4.1 Continued

Chromosome #	XL280 insertion sites	H99	JEC21
5	CNXL_029040	CNAG_02552|CNAG_02553	CNE00130|CNE00140
7	CNXL_042090	CNAG_03346	N/A
8	CNXL_045350	CNAG_04500	CNI00570
1	CNXL_004680	CNAG_00473	CNA04550
1	CNXL_004690	CNAG_00474	CNA04560
6	CNXL_034740	CNAG_05965	CNF00170
6	CNXL_105500	N/A	N/A

4.3.5 Calcineurin is required for pheromone-dependent and pheromone-independent filamentation

One of the candidate genes that was identified through DNA sequencing and inverse PCR sequencing was *CNB1*. Cnb1 is the regulatory subunit of calcineurin, which is a serine threonine specific phosphatase [216-218]. Calcineurin is a heterodimer composed of the catalytic subunit Cna1 and the regulatory subunit Cnb1. Calcineurin is required for fungal adaptation to different environment conditions such as ion stress, pheromone response, morphogenesis, and growth at 37 °C [217].

To confirm that the deletion of *CNB1* caused defects in filamentation, we made an independent deletion of the *CNB1* gene in the WT XL280 background. The deletion of *CNB1* caused severe growth defect at 37 °C (Figure 4.11), similar to what was reported previously of the *cnb1*Δ mutant made in the JEC21 background [216]. To examine the effect of the *CNB1* gene deletion on unisexual reproduction, we cultured the *cnb1*Δ strain on V8 medium. No filamentation could be observed. The *cnb1*Δ mutant

cultured on V8+copper medium also did not produce any filaments (Figure 4.12). This finding suggests that the Cnb1 is required for filamentation regardless of the pheromone response. To see if the pheromone response pathway is functional in the *cnb1*Δ mutant made in XL280 background, we crossed the *cnb1*Δ α cells with JEC20 (**a**). Because JEC20 is a wild type mating type **a** strain that does not self-filament, any filaments observed from the cross would be the result of cell fusion between *cnb1*Δ α mutant and JEC20 (**a**). Robust filamentation was observed from the cross between *cnb1*Δ α and JEC20 (**a**) (Figure 4.12), indicating that Cnb1 is not required for the pheromone response. This is again consistent with previous studies in JEC21 background indicating that the deletion of *CNB1* does not have any defect in pheromone production or cell fusion [219].

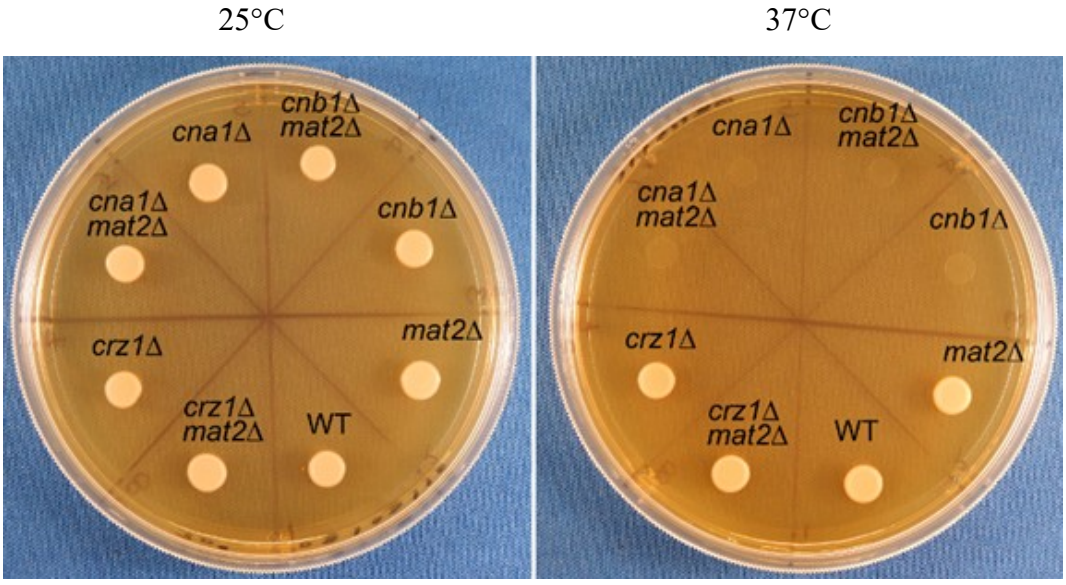

Figure 4.11 High temperature sensitivity of the calcineurin mutants.
tested for their growth at 37 °C. Calcineurin mutants *cna1*Δ and *cnb1*Δ can grow at 22 °C but have a growth defect at 37 °C. However, *crz1*Δ mutant can grow at 37 °C and so does *crz1*Δ *mat2*Δ mutant. Complementation of *CNA1* restores the growth at 37°C.

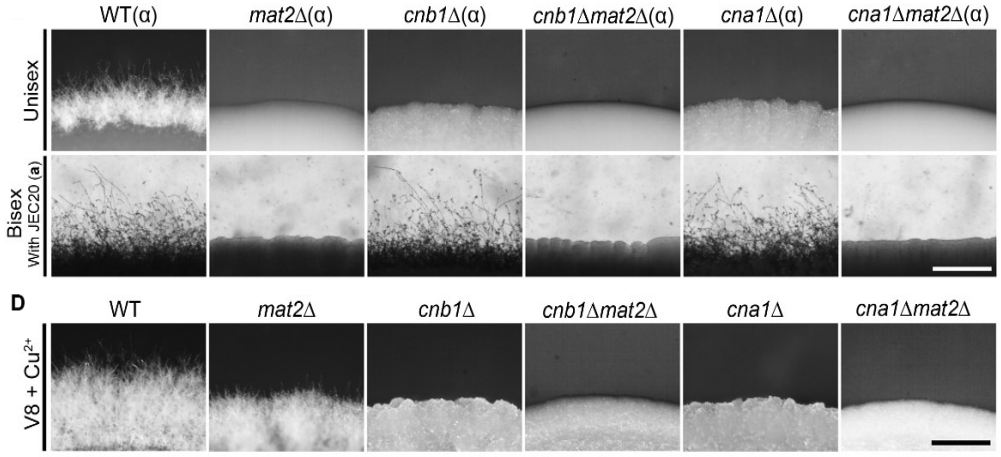

Figure 4.12 Calcineurin is required for filamentation.
Deletion of calcineurin subunit 1 (*CNA1*) or regulatory subunit B (*CNB1*) causes defect in filamentation in V8. Double deletion of calcineurin mutants with *mat2*Δ mutant also abolishes filamentation. Similar defect in filamentation is seen for the mutants when grown V8 + Cu^{2+} for 6 days. Scale bar: 500 μm.

To further confirm that the deletion of *CNB1* is responsible for the blocked filamentation of *mat2*Δ on V8+copper medium, we introduced the *MAT2* gene deletion construct into the *cnb1*Δ mutant background to generate the *cnb1*Δ *mat2*Δ double mutant. The *cnb1*Δ*mat2*Δ double mutant did not produce any filaments when crossing with JEC20 (**a**) (Figure 4.12) This is consistent with the cell fusion defect phenotype of *mat2*Δ mutant, as we reported previously [4]. The *cnb1*Δ*mat2*Δ double mutant failed to undergo self-filamentation on either V8 or V8+copper medium Figure 4.12). The results support the idea that Cnb1is required for both pheromone-dependent and pheromone-independent filamentation.

To further test if the requirement for filamentation is specific to *CNB1* or a general requirement for calcineurin, we made a gene deletion of the catalytic subunit of calcineurin, *CNA1*. Similar to the deletion of *CNB1*, the deletion of *CNA1* did not prevent crossing with a compatible wild-type mating partner during bisexual mating, but it blocked self-filamentation (Figure 4.12). The double mutant *cna1*Δ*mat2*Δ, similar to the double mutant *cnb1*Δ*mat2*Δ, was unable to filament on V8 or V8+copper medium (Figure 4.12).

We then tested if high temperature induced filamentation also requires calcineurin. Because deletion of the *CNA1* or the *CNB1* gene results in a severe growth defect at 37°C, we chose to use the immunosuppressive drug FK506, which inhibits calcineurin and is widely used in testing the effect of calcineurin inhibition [219]. Here, we cultured the WT and the *mat2*Δ mutant strains at 37 °C and then transferred the cells onto V8 medium containing FK506 (1μg/ml). No filamentation was observed in either the wild type or the *mat2*Δ mutant (Figure 4.13), indicating that FK506 abolished filamentation. Hence, thermo-induced filamentation also requires calcineurin. Collectively, these data confirm that filamentation, be it pheromone-dependent or pheromone-independent, requires calcineurin.

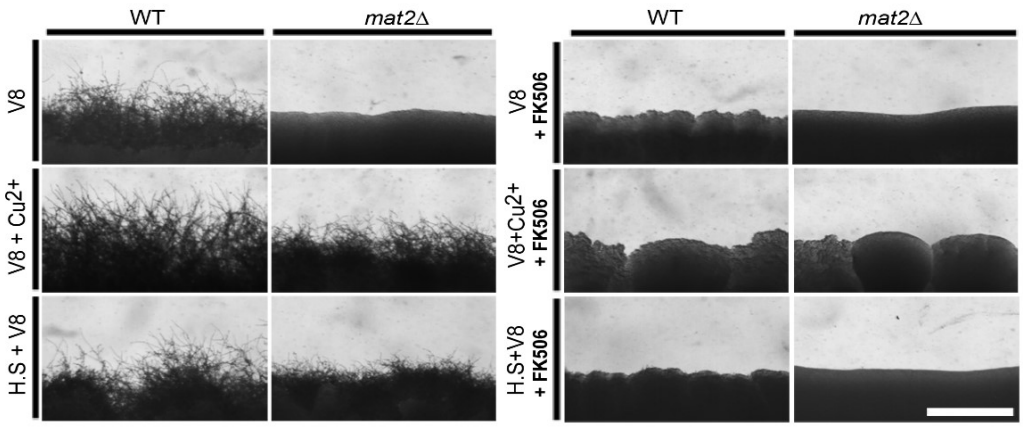

Figure 4.13 Pheromone dependent, pheromone independent and heat shock induced filamentation requires calcineurin.
WT and *mat2*Δ strains were grown at 37 °C and 30 °C for 36 hours. The strains from 37°C were transferred to V8 or V8 containing 1 µg /ml FK506 (calcineurin inhibitor). The strains from 30 °C were transferred to V8 or V8 + Cu^{2+} with or without the addition of 1 µg /ml FK506. Images were taken 1 week after incubation in dark at 22 °C. Addition of FK506 abolished filamentation under all three conditions tested above. Pheromone dependent filamentation represented by WT grown on V8 media requires calcineurin. Pheromone independent filamentation shown by *mat2*Δ on V8 + Cu^{2+} and heat shock induced filamentation also requires functional calcineurin.

4.3.6 Znf2 and calcineurin work together to for filamentation

Znf2 is required for cryptococcal yeast-to-hypha transition. So far no factor has been identified that can override the need for Znf2 in terms of filamentation. This morphogenesis regulator is expressed at low levels under various conditions except conditions that induce filamentation. Znf2 functions downstream of the pheromone sensing pathway controlled by Mat2, but Znf2 itself is not critical for pheromone response [4]. As demonstrated in this study, Znf2 is required for both Mat2-dependent and Mat2-independent filamentation. It is thus not surprising that overexpression of Znf2

can enable filamentation in various mutants (e.g. *mat2*Δ). Znf2 is a specific regulator for hyphal morphogenesis and is not critical for adaptation to many other stresses tested [4, 9]. In contrast to Znf2, calcineurin is involved in various stress responses in *C. neoformans* (e.g. thermo-tolerance in Figure 4.11). However, in terms of filamentation, calcineurin is also essential, be it Mat2-dependent or Mat2-independent (this study and previous studies) [4, 219]. Therefore, we examined if the defect in filamentation caused by the disruption of calcineurin can be overcome by Znf2. For this purpose, we introduced the *ZNF2* overexpression construct into the *mat2*Δ*cnb1*Δ double mutant and the *mat2*Δ single mutant. Overexpression of *ZNF2* in the *mat2*Δ mutant background enabled filamentation (Figure 4.14), as we reported previously [9]. However, overexpression of *ZNF2* in the *mat2*Δ*cnb1*Δ double deletion mutant failed to confer filamentation (Figure 4.14). Furthermore, we found that when the *CNA1* gene was deleted from the hyper-filamentous *ZNF2*^{oe} strain, filamentation was abolished on V8 medium (Figure 4.14). No filamentation was observed when the *ZNF2*^{oe}*cna1*Δ strain was grown on V8+copper medium either (Figure 4.14). These results indicate that both Znf2 and calcineurin are required for pheromone-dependent and pheromone-independent filamentation.

4.4 Discussions

We demonstrate that *C. neoformans* can undergo sexual development without the need for pheromone or other components of the pheromone sensing pathway. One of the major events that happens during the initial phase of bisexual mating is pheromone mediated non-self-recognition and cell fusion. Thus, the efficiency of bisexual mating is

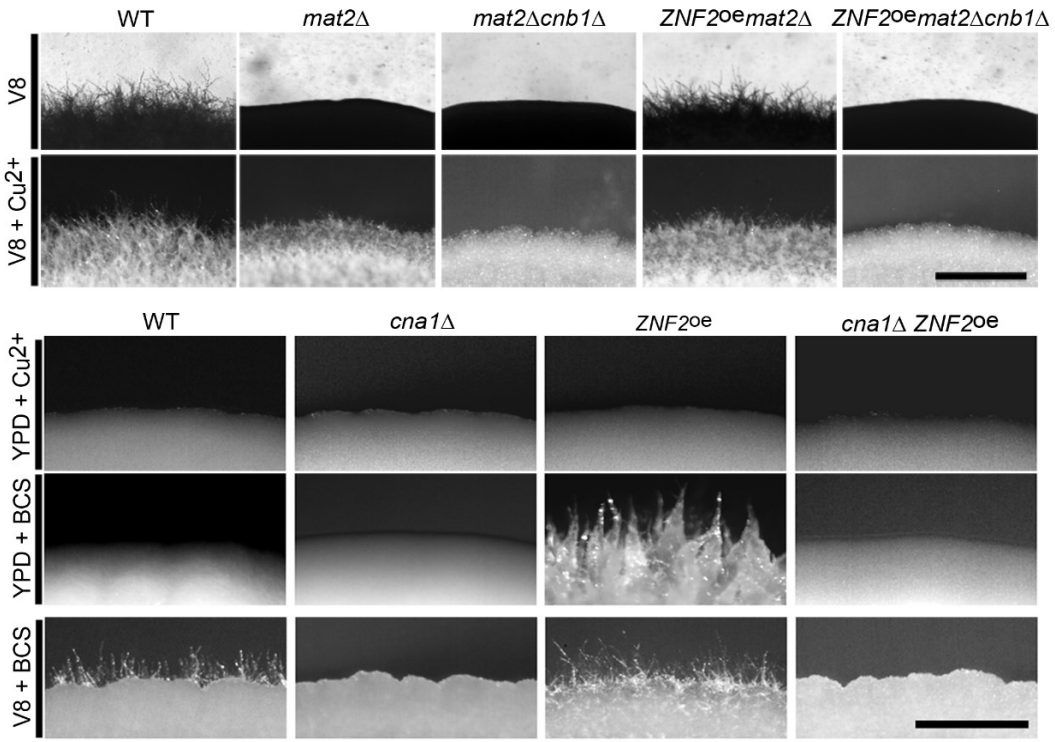

Figure 4.14 Znf2 and calcineurin is required for filamentation. Overexpression of Znf2 in *mat2*Δ mutant is sufficient to restore filamentation. However, overexpression of *ZNF2* in *mat2*Δ *cnb1*Δ deletion mutant is unable to restore filamentation. Deletion of *CNA1* from *ZNF2* ^{oe} strain abolishes filamentation. *ZNF2* is kept under the control of inducible promoter *CTR4*. Induction of *ZNF2* through the addition of copper chelator BCS, makes the cells filamentous even on YPD media. When *CNA1* is deletion from this hyperfilamentous strain, no filamentation can be observed under inducing condition in YPD or in V8.

often measured by the quantity of the cell fusion products [98]. However, for unisexual development in *C. neoformans*, Lin et. al in 2005 found that the frequency of cell fusion among α cells was very low, suggesting that other processes/mechanisms such as endoduplication (replication of the genome without cell division) might play more important role during unisexual development. Consistently, most of the natural α/α diploids are shown to be derived from endoduplication with fewer derived from fusion of two distinct α cells [80]. These lines of evidence suggest that the regulation of bisexual development is different from that of unisexual development in *C. neoformans*.

Our study showed that calcineurin is required for pheromone-independent as well as pheromone-dependent filamentation. Previous studies had shown that both the subunits of calcineurin (Cna1 and Cnb1) are required for hyphal elongation in pheromone-dependent sexual development [219, 220]. However, it was shown that calcineurin mutants can still produce pheromone [216, 219]. Calcineurin is required for an organism to respond to stress and functions in a wide variety of cellular processes including drug tolerance, morphogenesis, and virulence in fungi [221-223]. The requirement of calcineurin for hyphal growth is common in other fungal species as well. Calcineurin is required for hyphal growth in various *Candida* species like *C. dubliniensis* and *C. tropicalis*. In the fungus *Mucor circinelloides*, calcineurin plays a role in yeast to hypha transition [224]. In *Saccharomyces,* calcineurin is required for the cells to recover from pheromone arrest [225, 226]. All these results suggest, most likely nutrient limitation, exposure to pheromone, morphological transition, high copper, and high temperature might represent a stressful situation for fungi for which they require

functional calcineurin. By contrast, Znf2 is not required for various stresses tested, and is a specific master regulator for filamentation [4, 9]. It is yet to be determined how Znf2 and calcineurin coordinate in controlling hyphal morphogenesis. It is possible that some of Znf2's key downstream targets might require de-phosphorylation by calcineurin in order to be functional.

Core features of sexual reproduction are conserved in both pheromone-dependent and pheromone-independent unisex. The pheromone-independent sexual development proceeds through the formation of hyphae, basidia, and spores, similar to what has been previously shown [68, 81]. Similar downstream genetic components are required for both pheromone-dependent and pheromone-independent unisex. Both require the master regulator of filamentation, Znf2. This result further attests Znf2 as the master regulator of filamentation in *C. neoformans* and also suggests that Znf2 can be activated independent of Mat2. Hypha specific protein Cfl1 was shown to be highly induced during pheromone-dependent mating [9]. Induction of *CFL1* was seen here during pheromone-independent unisex in the *mat2*Δ mutant as well. The cell surface protein Dha1, which is localizes at the basidium neck, also shows similar localization at the basidial neck produced by pheromone-independent development (Gyawali et al. unpublished). Other conditions, such as high temperature that was shown to induce unisexual development, also induce this pheromone-independent unisexual development.

What drives *C. neoformans* to a particular mode of reproduction either unisexual or bisexual reproduction is still unknown. Shared features in both include increase in ploidy, and then reduction to haploid gametes through meiosis (Figure 4.1). Increase in

ploidy for bisexual mating in *C. neoformans* occurs through cell-cell fusion between opposite mating partners (**a** and α). For unisexual reproduction, increase in ploidy can occur through cell-cell fusion between two α isolates or through endoduplication [68, 80, 227]. The low frequency of cell fusion during unisexual mating suggests the pheromone sensing pathway has not been optimized for unisexual mating. Moreover, our observations that *mat2*Δ mutant can filament better than WT under some conditions implies that the pheromone pathway is more likely to be inhibitory for unisexual development, which does not take place through cell fusion. This also raises the possibility that unisexual mating is more likely to occur in environmental conditions which is not permissive for pheromone response.

5 CONCLUSIONS AND FUTURE DIRECTIONS

5.1 Summary of the Research

The purpose of this research was to understand some of the key events that take place during sexual reproduction in *C. neoformans*. We specifically focused on understanding the factors controlling of mitochondrial DNA transmission from parent to the progeny. We also examined the changes in cell morphology and gene expression patterns that take place during sexual development. In addition, we identified some of the cues that can activate unisexual development in this fungus.

5.1.1 Understand the role of prezygotic and postzygotic factors in the control of mitochondrial DNA inheritance

We investigated the roles of the postzygotic factors Znf2 and Sxi1α/Sxi2**a**, and the prezygotic factor Mat2 in mtDNA inheritance in *Cryptococcus neoformans*. *C. neoformans* bisexual mating involves the fusion between two isogamous cells, yet the mitochondrial DNA inheritance is uniparental. In the majority of eukaryotes, including plants, animals, and fungi, mitochondrial DNA is inherited uniparentally [131, 228]. The simplest explanation for this phenomenon is that the mating partner with greater cytoplasmic content contributes towards mitochondrial inheritance. This morphological/size difference between mating partners is conceptually simple for the understanding of mitochondrial inheritance in organisms where mating involves anisogamous partners. However, the uniparental mitochondrial DNA inheritance pattern

observed in organisms where mating involves isogamous partners, such as in *C. neoformans*, is hard to explain.

Our findings showed that mtDNA inheritance is established during early stage of mating, in the original zygote, prior to the formation of dikaryotic hyphae that lead to the production of meiotic spores. In addition, we have shown the existence of prezygotic control by Mat2. Although the *MAT2* gene is known to be highly upregulated during mating in both mating partners [146, 148], we conjecture that the timing of Mat2 activation in the parental strains is critical in determining the origin of mitochondria to be inherited. When the *MAT2* gene is placed under the control of the constitutively active promoter from the *GPD1* gene, the cells with $MAT2^{oe}$ act in effect the parent initiating the mating process and their mitochondria are preferentially inherited in the progeny. Our study reinforces the concept that there are intricate connections between factors controlling sexual development and organelle inheritance.

5.1.2 Cell type specific expression pattern is observed within the heterogenous mating colony of *C. neoformans*

One interesting and important finding of this study is the cell-type specificities shown by some of these homologs of Cfl1. Cfl1 was previously shown to be a hyphal specific protein [9]. Consistently, the transcript level of *CFL1* is significantly increased during sexual development with Cfl1 proteins produced by hyphae but not by yeast cells. Dha1, on the other hand, is expressed by multiple cells types, with stronger expression in yeast cells and weaker expression in filaments. Interestingly, Dha1 is enriched on the

neck of basidium and in spores. One of the most surprising findings is the dichotomy between the protein expression pattern of Dha2 and its gene expression pattern. Like *CFL1*, the *DHA2* transcript level is high under mating conditions, and we expected that Dha2 was going to be a hyphal specific protein. Surprisingly, Dha2 protein is only expressed by the yeast cells and not by the hyphal subpopulation of the mating colony. Thus, it is important not to assume a protein's function purely based on the gene expression data collected from a heterogeneous population.

5.1.3 Unisexual development in *C. neoformans* can take place independent of pheromone

The pheromone sensing pathway is crucial for bisexual mating in *C. neoformans* as well as in a wide variety of fungal species across different phyla (e.g. *Saccharomyces*, *Candida*, and *Ustilago*) [147, 229-231]. We showed that *Cryptococcus neoformans* can undergo sexual development without the key transcription factor Mat2 of the pheromone pathway. Unisexual mating has been proposed to have given rise to the sharply skewed population towards the α mating type in *C. neoformans* natural population. However, the inefficiency of unisexual development under laboratory conditions presents a conundrum. We demonstrate that this fungus can undergo sexual development without the need for pheromone or other components of the pheromone sensing pathway. This finding resolves the conflicting observations for and against the crucial role of the pheromone pathway in unisexual development [83, 98, 99, 147]. These lines of evidence suggest that the very process that defines bisexual mating, may not be as crucial for unisexual development in *C. neoformans*. This is not to say that pheromone does not

play a role in unisexual development. In organisms or conditions where sexual development depends on cell-cell fusion (either unisexual mating or bisexual mating), then pheromone is important.

Our study showed that filamentation shown by *mat2*Δ mutant on V8 + Cu^{2+} required the presence of Znf2 and calcineurin. These components also are required for the pheromone dependent filamentation. This finding suggests that downstream components required for filamentation are conserved in both types of filamentation. Another conclusion that we can draw from these results is that in addition to pheromone, there are multiple upstream signals that can trigger sexual development in this fungus. Given that *C. neoformans* is an environmental fungus that has successfully created its niche in a wide range of hosts, it is not surprising that this fungus might have developed various strategies to propagate sexually. Complete dependence on pheromone to complete its sexual development is risky. Some of the conditions might not be favorable for pheromone production itself. Thus, one could imagine that this largely unisexual fungus will be able to undergo sexual reproduction under various conditions in the environment. The ability to be activated by multiple signals also indicates the robustness of sexual reproduction system in this fungus. The presence of a wide variety of environmental cues that can induce sexual development is also observed in other fungi. *Candida albicans*, an opportunistic human fungal pathogen, can undergo reversible switch from the "white" to the mating competent "opaque" state. Environmental cues such as temperature, nutrition starvation, N-acetyl glucosamine, oxidative stress, and genotoxic agents have been shown to induce the switch to the opaque state [232, 233].

Given that *C. neoformans* is a ubiquitous environmental fungus, it might have developed various tactics to propagate sexually through distinct means under different conditions [13, 19].

5.2 Future Directions

5.2.1 Combining Co-IP data and RNA-seq data to identify regulators of pheromone independent filamentation

In this study, we found that *mat2*Δ strain filaments better than WT on V8 + Cu^{2+} medium. This suggests that Mat2 is suppressing the filamentation of WT during unisexual mating under this condition. We will perform CO-IP on *C. neoformans* samples (*MATα*, P_{MAT2}-*MAT2*-FLAG) grown on mating media V8 or V8 + Cu^{2+} for 16 hours using tagged Mat2. Through Co-IP, we hope to obtain candidate proteins interacting with Mat2. For the candidate genes identified through the pull down experiments, we will focus on candidate genes that are being inhibited by Mat2 on V8 + Cu^{2+} as well as in V8. We will select those that show Mat2-dependent transcriptional change with induced expression on V8 + Cu^{2+} in *mat2*Δ mutant.

5.2.2 Dissect the relationship between calcineurin and Znf2 to understand their role in morphogenesis

Our study showed both that Znf2 and calcineurin is required for *Cryptococcus neoformans* to undergo morphological transition from yeast to hyphae. Znf2 is the master regulator of filamentation in *C. neoformans* [9]. Calcineurin is required for the

cells to survive in different environmental stress in *C. neoformans* as well as in other fungi [234, 235]. Both *znf2*Δ and calcineurin deletion mutants have same non-filamentous phenotype. They can undergo cell fusion, but, they are defective in filamentation. Both calcineurin subunits were analyzed. Based on the studies done on other fungi such as *Candida* and *Saccharomyces*, calcineurin regulates the cellular function through dephosphorylation of its substrate. One of the well-known substrate of calcineurin that has been shown to affect filamentation in other fungi is Crz1 [235]. However, this study and a recently published work suggest that though *Crz1* is one of the targets of calcineurin in *C. neoformans*, it does not affect filamentation under the known mating inducing conditions [236]. So, our hypothesis is that calcineurin regulates filamentation through some other unidentified substrate.

The recently published study has also identified other putative substrates of calcineurin. A total of 44 proteins show difference in phosphorylation status in *cna1*Δ compared to WT [236]. We will combine the proteomics data with the data obtained from our insertional mutagenesis screen (list of insertion sites obtained from the strains that showed defect in filamentation). We will find if there are any overlapping genes among the list and pursue with them first to see if they affect filamentation. Through this approach, we hope to identify any upstream regulators of Znf2. The second approach is to examine if calcineurin affects filamentation by directly dephosphorylating some key targets of Znf2 that are important in regulating filamentation. For this, we can combine the proteomics data with the ChIP-DNA seq data of Znf2.

5.2.3 Identify the targets of Mat2 that play a role in determining mitochondrial DNA inheritance

Our study showed that the decision regarding which parent should contribute its mitochondrial DNA to the progeny has to occur during early stages of mating. We found out that the expression level of Mat2 in the parental cell is an important factor in determining the transmission of its mtDNA to the progeny. Before performing ChIP-seq on Mat2, we will determine the ideal expression level of *MAT2* that will be enough to change mitochondrial DNA inheritance pattern.

For manipulating the expression level of Mat2, we will place the *MAT2* gene under the control *CTR4* promoter (*MAT***a**, *mat2*:: NAT, P_{CTR4}-*MAT2*). First we will measure the relative transcript level *MAT2* in different concentrations of the copper chelator BCS through qPCR. We will use two different concentrations of BCS. We will use the concentration of BCS that will give the relative transcript level of *MAT2* in **a** cells lower than that in α cell and vice versa. We will then perform cell fusion assays on this modified strain as described in Chapter II using two (above selected) concentrations of BCS and determine the mitochondrial DNA inheritance pattern.

For ChIP-DNA sequencing, mating samples grown at different conditions will be collected. For bisexual mating samples, *C. neoformans* cells (*MAT***a**, *mat2*Δ, P_{CTR4}-*MAT2*-FLAG x WT (α)) grown on V8+BCS or V8+Cu^{2+} for 16 hours will be used. Two different concentrations of BCS that are selected above will be used to moderate the expression level of Mat2. We will focus on genes that show drastic difference in

enrichment when grown in two different concentrations of BCS. Candidate genes of interest will be grouped into two categories. The first group will consist of genes that have low enrichment in low BCS concentration compared to the high BCS samples. Another group will consist of genes that has high enrichment in low BCS and vice versa. We will then make deletion strains for the selected candidate genes and examine their effect on mitochondrial DNA inheritance.

BIBLIOGRAPHY

1. Toffaletti, D.L., et al., *Cryptococcus neoformans mitochondrial genomes from serotype A and D strains do not influence virulence.* Current Genetics, 2004. **46**(4): p. 193-204.

2. Yan, Z., et al., *The mating type-specific homeodomain genes SXI1α and SXI2**a** coordinately control uniparental mitochondrial inheritance in Cryptococcus neoformans.* Current Genetics, 2007. **51**(3): p. 187-195.

3. Yan, Z., et al., *SXI1α controls uniparental mitochondrial inheritance in Cryptococcus neoformans.* Curr Biol, 2004. **14**(18): p. R743-R744.

4. Lin, X., et al., *Transcription Factors Mat2 and Znf2 Operate Cellular Circuits Orchestrating Opposite- and Same-Sex Mating in Cryptococcus neoformans.* PLoS Genet, 2010. **6**(5): p. e1000953.

5. McClelland, C.M., et al., *Uniqueness of the mating system in Cryptococcus neoformans.* Trends in Microbiology, 2004. **12**(5): p. 208-12.

6. Hull, C.M., M.-J. Boily, and J. Heitman, *Sex-Specific Homeodomain Proteins Sxi1α and Sxi2**a** Coordinately Regulate Sexual Development in Cryptococcus neoformans.* Eukaryotic Cell, 2005. **4**(3): p. 526-535.

7. Hull, C.M., R.C. Davidson, and J. Heitman, *Cell identity and sexual development in Cryptococcus neoformans are controlled by the mating-type-specific homeodomain protein Sxi1α.* Genes & Development, 2002. **16**(23): p. 3046-3060.

8. Chacko, N., et al., *The lncRNA RZE1 Controls Cryptococcal Morphological Transition.* PLoS Genetics, 2015. **11**(11): p. e1005692.

9. Wang, L., B. Zhai, and X. Lin, *The link between morphotype transition and virulence in Cryptococcus neoformans.* PLoS Pathog, 2012. **8**(6): p. e1002765.

10. Kozel, T.R. and B. Wickes, *Fungal Diagnostics.* Cold Spring Harbor Perspectives in Medicine, 2014. **4**(4).

11. Park, B.J., et al., *Estimation of the current global burden of cryptococcal meningitis among persons living with HIV/AIDS.* AIDS, 2009. **23**(4): p. 525-530.

12. Heitman, J., et al., *Cryptococcus*. 2011: American Society of Microbiology.

13. Lin, X., *Cryptococcus neoformans: Morphogenesis, infection, and evolution.* Infection, Genetics and Evolution, 2009. **9**(4): p. 401-416.

14. Griffiths, E.J., M. Kretschmer, and J.W. Kronstad, *Aimless mutants of Cryptococcus neoformans: Failure to disseminate.* Fungal Biology Reviews, 2012. **26**(2–3): p. 61-72.

15. Feldmesser, M., et al., *Cryptococcus neoformans Is a Facultative Intracellular Pathogen in Murine Pulmonary Infection.* Infection and Immunity, 2000. **68**(7): p. 4225-4237.

16. Alvarez, M. and A. Casadevall, *Phagosome Extrusion and Host-Cell Survival after Cryptococcus neoformans Phagocytosis by Macrophages.* Current Biology. **16**(21): p. 2161-2165.

17. Kronstad, J.W., et al., *Expanding fungal pathogenesis: Cryptococcus breaks out of the opportunistic box.* Nat Rev Micro, 2011. **9**(3): p. 193-203.

18. Olszewski, M.A., et al., *Urease Expression by Cryptococcus neoformans Promotes Microvascular Sequestration, Thereby Enhancing Central Nervous System Invasion.* The American Journal of Pathology, 2004. **164**(5): p. 1761-1771.

19. Lin, X. and J. Heitman, *The Biology of the Cryptococcus neoformans Species Complex.* Annual Review of Microbiology, 2006. **60**(1): p. 69-105.

20. Xue, C., et al., *Role of an expanded inositol transporter repertoire in Cryptococcus neoformans sexual reproduction and virulence.* MBio, 2010. **1**(1).

21. Wang, Y., P. Aisen, and A. Casadevall, *Cryptococcus neoformans melanin and virulence: mechanism of action.* Infection and Immunity, 1995. **63**(8): p. 3131-3136.

22. Casadevall, A., J.N. Steenbergen, and J.D. Nosanchuk, *'Ready made' virulence and 'dual use' virulence factors in pathogenic environmental fungi — the Cryptococcus neoformans paradigm.* Current Opinion in Microbiology, 2003. **6**(4): p. 332-337.

23. Casadevall, A. and J.R. Perfect, *Cryptococcus neoformans*. Vol. 595. 1998: Citeseer.

24. Zaragoza, O., et al., *The capsule of the fungal pathogen Cryptococcus neoformans.* Advances in applied microbiology, 2009. **68**: p. 133-216.

25. Kozel, T.R., *Virulence factors of Cryptococcus neoformans.* Trends in Microbiology, 1995. **3**(8): p. 295-299.

26. Belay, T., et al., *Serotyping of Cryptococcus neoformans by dot enzyme assay.* Journal of Clinical Microbiology, 1996. **34**(2): p. 466-470.

27. Dromer, F., et al., *Serotyping of Cryptococcus neoformans by using a monoclonal antibody specific for capsular polysaccharide.* Journal of Clinical Microbiology, 1993. **31**(2): p. 359-363.

28. Boekhout, T., et al., *Hybrid genotypes in the pathogenic yeast Cryptococcus neoformans.* Microbiology, 2001. **147**(4): p. 891-907.

29. Franzot, S.P., I.F. Salkin, and A. Casadevall, *Cryptococcus neoformans var. grubii: Separate Varietal Status for Cryptococcus neoformans Serotype A Isolates.* Journal of Clinical Microbiology, 1999. **37**(3): p. 838-840.

30. Kwon-Chung, K.J., et al., *(1557) Proposal to Conserve the Name Cryptococcus gattii against C. hondurianus and C. bacillisporus (Basidiomycota, Hymenomycetes, Tremellomycetidae).* Taxon, 2002. **51**(4): p. 804-806.

31. Caicedo, L.D., et al., *Cryptococcus neoformans in bird excreta in the city zoo of Cali, Colombia.* Mycopathologia, 1999. **147**(3): p. 121-124.

32. Irokanulo, E.O.A., et al., *Cryptococcus neoformans var neoformans Isolated from Droppings of Captive Birds in Nigeria.* Journal of Wildlife Diseases, 1997. **33**(2): p. 343-345.

33. Staib, F., *The perfect state of Cryptococcus neoformans, Filobasidiella neoformans, on pigeon manure filtrate agar.* Zentralblatt für Bakteriologie, Mikrobiologie und Hygiene., 1981. **248**(4): p. 575-578.

34. Staib, F. and A. Blisse, *Bird Manure Filtrate Agar for the Formation of the Perfect State of Cryptococcus neoformans, Filobasidiella neoformans. A Comparative Study of the Agars Prepared from Pigeon and Canary Manure.* Zentralblatt für Bakteriologie, Mikrobiologie und Hygiene. , 1982. **251**(4): p. 554-562.

35. Lazéra, M.S., et al., *Cryptococcus neoformans var. gattii — evidence for a natural habitat related to decaying wood in a pottery tree hollow.* Medical Mycology, 1998. **36**(2): p. 119-122.

36. Kidd, S.E., et al., *Characterization of Environmental Sources of the Human and Animal Pathogen Cryptococcus gattii in British Columbia, Canada, and the Pacific Northwest of the United States.* Applied and Environmental Microbiology, 2007. **73**(5): p. 1433-1443.

37. Chakrabarti, A., et al., *Isolation of Cryptococcus neoformans var. gattii from Eucalyptus camaldulensis in India.* Journal of Clinical Microbiology, 1997. **35**(12): p. 3340-3342.

38. Fraser, J.A., et al., *Recapitulation of the Sexual Cycle of the Primary Fungal Pathogen Cryptococcus neoformans var. gattii: Implications for an Outbreak on Vancouver Island, Canada.* Eukaryotic Cell, 2003. **2**(5): p. 1036-1045.

39. Kidd, S.E., et al., *A rare genotype of Cryptococcus gattii caused the cryptococcosis outbreak on Vancouver Island (British Columbia, Canada).* Proceedings of the National Academy of Sciences of the United States of America, 2004. **101**(49): p. 17258-17263.

40. Fraser, J.A., et al., *Same-sex mating and the origin of the Vancouver Island Cryptococcus gattii outbreak.* Nature, 2005. **437**(7063): p. 1360-1364.

41. Chaturvedi, S., et al., *Cryptococcus gattii in AIDS Patients, Southern California.* Emerging Infectious Diseases, 2005. **11**(11): p. 1686-1692.

42. Dromer, F., O. Ronin, and B. Dupont, *Isolation of Cryptococcus neoformans var. gattii from an asian patient in France: evidence for dormant infection in healthy subjects.* Journal of Medical and Veterinary Mycology, 1992. **30**(5): p. 395-397.

43. Nishikawa, M.M., et al., *Serotyping of 467 Cryptococcus neoformans Isolates from Clinical and Environmental Sources in Brazil: Analysis of Host and Regional Patterns.* Journal of Clinical Microbiology, 2003. **41**(1): p. 73-77.

44. Spellberg, B., *Vaccines for invasive fungal infections.* F1000 Medicine Reports, 2011. **3**: p. 13.

45. Perfect, J.R., et al., *Clinical Practice Guidelines for the Management of Cryptococcal Disease: 2010 Update by the Infectious Diseases Society of America.* Clinical Infectious Diseases, 2010. **50**(3): p. 291-322.

46. Lewis, R.E., *Current Concepts in Antifungal Pharmacology.* Mayo Clinic Proceedings, 2011. **86**(8): p. 805-817.

47. Orni-Wasserlauf, R., et al., *Fluconazole-Resistant Cryptococcus neoformans Isolated from an Immunocompetent Patient without Prior Exposure to Fluconazole.* Clinical Infectious Diseases, 1999. **29**(6): p. 1592-1593.

48. Maligie, M.A. and C.P. Selitrennikoff, *Cryptococcus neoformans Resistance to Echinocandins: (1,3)β-Glucan Synthase Activity Is Sensitive to Echinocandins.* Antimicrobial Agents and Chemotherapy, 2005. **49**(7): p. 2851-2856.

49. Calo, S., R.B. Billmyre, and J. Heitman, *Generators of Phenotypic Diversity in the Evolution of Pathogenic Microorganisms.* PLoS Pathog, 2013. **9**(3): p. e1003181.

50. Heitman, J., *Evolution of sexual reproduction: A view from the fungal kingdom supports an evolutionary epoch with sex before sexes.* Fungal Biology Reviews, 2015. **29**(3–4): p. 108-117.

51. Lee, S.C., et al., *The Evolution of Sex: a Perspective from the Fungal Kingdom.* Microbiology and Molecular Biology Reviews : MMBR, 2010. **74**(2): p. 298-340.

52. Heitman, J., S. Sun, and T.Y. James, *Evolution of fungal sexual reproduction.* Mycologia, 2013. **105**(1): p. 1-27.

53. Heitman, J., *Sexual Reproduction and the Evolution of Microbial Pathogens.* Current Biology, 2006. **16**(17): p. R711-R725.

54. Sarah P. Otto, *The Evolutionary Enigma of Sex.* The American Naturalist, 2009. **174**(S1): p. S1-S14.

55. Otto, S.P. and T. Lenormand, *Resolving the paradox of sex and recombination.* Nat Rev Genet, 2002. **3**(4): p. 252-261.

56. Lehtonen, J., M.D. Jennions, and H. Kokko, *The many costs of sex.* Trends in Ecology & Evolution, 2012. **27**(3): p. 172-178.

57. Heitman, J., *Evolution of eukaryotic microbial pathogens via covert sexual reproduction.* Cell host & microbe, 2010. **8**(1): p. 86-99.

58. Brown, J.K.M., *The Evolution of Sex and Recombination in Fungi*, in *Structure and Dynamics of Fungal Populations*, J.J. Worrall, Editor. 1999, Springer Netherlands: Dordrecht. p. 73-95.

59. Goddard, M.R., H.C.J. Godfray, and A. Burt, *Sex increases the efficacy of natural selection in experimental yeast populations.* Nature, 2005. **434**(7033): p. 636-640.

60. Cleveland, L.R., *The Origin and Evolution of Meiosis.* Science, 1947. **105**(2724): p. 287-289.

61. Goodenough, U. and J. Heitman, *Origins of Eukaryotic Sexual Reproduction.* Cold Spring Harbor Perspectives in Biology, 2014. **6**(3).

62. Egel, R. and D. Penny, *On the Origin of Meiosis in Eukaryotic Evolution: Coevolution of Meiosis and Mitosis from Feeble Beginnings*, in *Recombination*

and Meiosis: Models, Means, and Evolution, R. Egel and D.H. Lankenau, Editors. 2008, Springer Berlin Heidelberg. p. 249-288.

63. Kondrashov, A.S., *The asexual ploidy cycle and the origin of sex.* Nature, 1994. **370**(6486): p. 213-216.

64. Niklas, K.J., E.D. Cobb, and U. Kutschera, *Did meiosis evolve before sex and the evolution of eukaryotic life cycles?* BioEssays, 2014. **36**(11): p. 1091-1101.

65. Billiard, S., et al., *Sex, outcrossing and mating types: unsolved questions in fungi and beyond.* Journal of Evolutionary Biology, 2012. **25**(6): p. 1020-1038.

66. Heitman, J., et al., *Sex in Fungi*. 2007: American Society of Microbiology.

67. Wilson, A.M., et al., *Homothallism: an umbrella term for describing diverse sexual behaviours.* IMA Fungus, 2015. **6**(1): p. 207-214.

68. Lin, X., C.M. Hull, and J. Heitman, *Sexual reproduction between partners of the same mating type in Cryptococcus neoformans.* Nature, 2005. **434**(7036): p. 1017-1021.

69. Roach, K.C. and J. Heitman, *Unisexual Reproduction Reverses Muller's Ratchet.* Genetics, 2014. **198**(3): p. 1059-1069.

70. Glass, N.L. and M.L. Smith, *Structure and function of a mating-type gene from the homothallic species Neurospora africana.* Molecular and General Genetics MGG, 1994. **244**(4): p. 401-409.

71. Alby, K., D. Schaefer, and R.J. Bennett, *Homothallic and heterothallic mating in the opportunistic pathogen Candida albicans.* Nature, 2009. **460**(7257): p. 890-893.

72. Sun, S., et al., *Unisexual Reproduction Drives Meiotic Recombination and Phenotypic and Karyotypic Plasticity in Cryptococcus neoformans.* PLoS Genet, 2014. **10**(12): p. e1004849.

73. Ni, M., et al., *Unisexual and Heterosexual Meiotic Reproduction Generate Aneuploidy and Phenotypic Diversity De Novo in the Yeast Cryptococcus neoformans.* PLoS Biol, 2013. **11**(9): p. e1001653.

74. Kwon-Chung, K., *A new genus, Filobasidiella, the perfect state of Cryptococcus neoformans* Mycologia, 1975.

75. Kwon-Chung, K., J.E. Bennett, and J. Rhodes, *Taxonomic studies on Filobasidiella species and their anamorphs.* Antonie van Leeuwenhoek, 1982. **48**(1): p. 25-38.

76. Kwon-Chung, K., *Morphogenesis of Filobasidiella neoformans, the sexual state of Cryptococcus neoformans.* Mycologia, 1976: p. 821-833.

77. Ekena, J.L., et al., *Sexual Development in Cryptococcus neoformans Requires CLP1, a Target of the Homeodomain Transcription Factors Sxi1α and Sxi2a.* Eukaryotic Cell, 2008. **7**(1): p. 49-57.

78. Kwon-Chung, K., *Nuclear genotypes of spore chains in Filobasidiella neoformans (Cryptococcus neoformans).* Mycologia, 1980. **72**(2): p. 418-422.

79. Lin, X., et al., *αADα Hybrids of Cryptococcus neoformans: Evidence of Same-Sex Mating in Nature and Hybrid Fitness.* PLoS Genetics, 2007. **3**(10): p. e186.

80. Lin, X., et al., *Diploids in the Cryptococcus neoformans Serotype A Population Homozygous for the α Mating Type Originate via Unisexual Mating.* PLoS Pathog, 2009. **5**(1): p. e1000283.

81. Wickes, B.L., et al., *Dimorphism and haploid fruiting in Cryptococcus neoformans: association with the alpha-mating type.* Proceedings of the National Academy of Sciences of the United States of America, 1996. **93**(14): p. 7327-7331.

82. Idnurm, A. and J. Heitman, *Light Controls Growth and Development via a Conserved Pathway in the Fungal Kingdom.* PLoS Biology, 2005. **3**(4): p. e95.

83. Davidson, R.C., et al., *Characterization of the MFα pheromone of the human fungal pathogen Cryptococcus neoformans.* Molecular Microbiology, 2000. **38**(5): p. 1017-1026.

84. Shen, W.C., et al., *Pheromones Stimulate Mating and Differentiation via Paracrine and Autocrine Signaling in Cryptococcus neoformans.* Eukaryotic Cell, 2002. **1**(3): p. 366-377.

85. Hull, C.M. and J. Heitman, *Genetics of Cryptococcus neoformans.* Annual Review of Genetics, 2002. **36**(1): p. 557-615.

86. Xue, C., et al., *The Human Fungal Pathogen Cryptococcus Can Complete Its Sexual Cycle during a Pathogenic Association with Plants.* Cell Host & Microbe, 2007. **1**(4): p. 263-273.

87. Lin, X., et al., *Virulence Attributes and Hyphal Growth of C. neoformans Are Quantitative Traits and the MATα Allele Enhances Filamentation.* PLoS Genet, 2006. **2**(11): p. e187.

88. Kent, C.R., et al., *Formulation of a Defined V8 Medium for Induction of Sexual Development of Cryptococcus neoformans.* Applied and Environmental Microbiology, 2008. **74**(20): p. 6248-6253.

89. Fraser, J.A., et al., *Convergent Evolution of Chromosomal Sex-Determining Regions in the Animal and Fungal Kingdoms.* PLoS Biol, 2004. **2**(12): p. e384.

90. Lengeler, K.B., et al., *Signal Transduction Cascades Regulating Fungal Development and Virulence.* Microbiology and Molecular Biology Reviews, 2000. **64**(4): p. 746-785.

91. Xue, C., Y.P. Hsueh, and J. Heitman, *Magnificent seven: roles of G protein-coupled receptors in extracellular sensing in fungi.* FEMS microbiology reviews, 2008. **32**(6): p. 1010-1032.

92. Xue, C., et al., *G Protein-coupled Receptor Gpr4 Senses Amino Acids and Activates the cAMP-PKA Pathway in Cryptococcus neoformans.* Molecular Biology of the Cell, 2006. **17**(2): p. 667-679.

93. Hsueh, Y.-P., C. Xue, and J. Heitman, *G protein signaling governing cell fate decisions involves opposing Gα subunits in Cryptococcus neoformans.* Molecular Biology of the Cell, 2007. **18**(9): p. 3237-3249.

94. Alspaugh, J.A., J.R. Perfect, and J. Heitman, *Cryptococcus neoformans mating and virulence are regulated by the G-protein α subunit GPA1 and cAMP.* Genes & Development, 1997. **11**(23): p. 3206-3217.

95. Wang, P., et al., *Mating-Type-Specific and Nonspecific PAK Kinases Play Shared and Divergent Roles in Cryptococcus neoformans.* Eukaryotic Cell, 2002. **1**(2): p. 257-272.

96. Wang, P., J.R. Perfect, and J. Heitman, *The G-Protein β Subunit GPB1 Is Required for Mating and Haploid Fruiting in Cryptococcus neoformans.* Molecular and Cellular Biology, 2000. **20**(1): p. 352-362.

97. Kruzel, E.K., S.S. Giles, and C.M. Hull, *Analysis of Cryptococcus neoformans Sexual Development Reveals Rewiring of the Pheromone-Response Network by a Change in Transcription Factor Identity.* Genetics, 2012. **191**(2): p. 435-449.

98. Chung, S., et al., *Molecular Analysis of CPRα, a MATα-Specific Pheromone Receptor Gene of Cryptococcus neoformans.* Eukaryotic Cell, 2002. **1**(3): p. 432-439.

99. Hsueh, Y.-P. and W.-C. Shen, *A Homolog of Ste6, the a-Factor Transporter in Saccharomyces cerevisiae, Is Required for Mating but Not for Monokaryotic Fruiting in Cryptococcus neoformans.* Eukaryotic Cell, 2005. **4**(1): p. 147-155.

100. Davidson, R.C., et al., *A MAP kinase cascade composed of cell type specific and non-specific elements controls mating and differentiation of the fungal pathogen Cryptococcus neoformans.* Molecular Microbiology, 2003. **49**(2): p. 469-485.

101. Moore, D., *Perception and response to gravity in higher fungi - a critical appraisal.* New Phytologist, 1991. **117**: p. 3-23.

102. Brand, A., et al., *Hyphal orientation of Candida albicans is regulated by a calcium-dependent mechanism.* Curr Biol, 2007. **17**(4): p. 347-52.

103. Aoki, S., et al., *Oxygen as a possible tropic factor in hyphal growth of Candida albicans.* Mycoscience, 1998. **39**(3): p. 231-238.

104. Crombie, T., N.A. Gow, and G.W. Gooday, *Influence of applied electrical fields on yeast and hyphal growth of Candida albicans.* J Gen Microbiol, 1990. **136**(2): p. 311-7.

105. Idnurm, A. and J. Heitman, *Light controls growth and development via a conserved pathway in the fungal kingdom.* PLoS Biol, 2005. **3**(4): p. e95.

106. Moore, D., et al., *Centenary review. Gravimorphogenesis in agarics.* Mycological Research, 1996. **100**: p. 257-273.

107. Hoch, H.C., et al., *Signaling for growth orientation and cell differentiation by surface topography in Uromyces.* Science, 1987. **235**(4796): p. 1659-62.

108. Barrett, K.J., S.E. Gold, and J.W. Kronstad, *Identification and complementation of a mutation to constitutive filamentous growth in Ustilago maydis.* Mol Plant Microbe Interact, 1993. **6**(3): p. 274-83.

109. Vanittanakom, N., et al., *Penicillium marneffei Infection and Recent Advances in the Epidemiology and Molecular Biology Aspects.* Clinical Microbiology Reviews, 2006. **19**(1): p. 95-110.

110. Sil, A. and A. Andrianopoulos, *Thermally Dimorphic Human Fungal Pathogens—Polyphyletic Pathogens with a Convergent Pathogenicity Trait.* Cold Spring Harbor Perspectives in Medicine, 2015. **5**(8).

111. Klein, B.S. and B. Tebbets, *Dimorphism and virulence in fungi.* Current opinion in microbiology, 2007. **10**(4): p. 314-319.

112. Miyaji, M. and K. Nishimura, *Investigation on dimorphism of Blastomyces dermatitidis by agar-implantation method.* Mycopathologia, 1977. **60**(2): p. 73-78.

113. Brandhorst, T.T., et al., *Calcium Binding by the Essential Virulence Factor BAD-1 of Blastomyces dermatitidis.* Journal of Biological Chemistry, 2005. **280**(51): p. 42156-42163.

114. Hogan, L.H. and B.S. Klein, *Altered expression of surface alpha-1,3-glucan in genetically related strains of Blastomyces dermatitidis that differ in virulence.* Infection and Immunity, 1994. **62**(8): p. 3543-3546.

115. San-blas, G., F. San-blas, and D.W.R. Mackenzie, *Molecular Aspects of Fungal dimorphism.* CRC Critical Reviews in Microbiology, 1984. **11**(2): p. 101-127.

116. Lorenz, M.C., J.A. Bender, and G.R. Fink, *Transcriptional response of Candida albicans upon internalization by macrophages.* Eukaryot Cell, 2004. **3**(5): p. 1076-87.

117. Williamson, J.D., et al., *Atypical cytomorphologic appearance of Cryptococcus neoformans.* Acta cytologica, 1996. **40**(2): p. 363-370.

118. Love, G.L., G.D. Boyd, and D.L. Greer, *Large Cryptococcus neoformans isolated from brain abscess.* Journal of Clinical Microbiology, 1985. **22**(6): p. 1068-1070.

119. Zaragoza, O., et al., *Fungal Cell Gigantism during Mammalian Infection.* PLoS Pathog, 2010. **6**(6): p. e1000945.

120. Okagaki, L.H., et al., *Cryptococcal Cell Morphology Affects Host Cell Interactions and Pathogenicity.* PLoS Pathog, 2010. **6**(6): p. e1000953.

121. Shadomy, H.J. and J.P. Utz, *Preliminary studies on a hypha-forming mutant of Cryptococcus neoformans.* Mycologia, 1966. **58**(3): p. 383-390.

122. Neilson, J.B., M.H. Ivey, and G.S. Bulmer, *Cryptococcus neoformans: pseudohyphal forms surviving culture with Acanthamoeba polyphaga.* Infection and Immunity, 1978. **20**(1): p. 262-266.

123. Magditch, D.A., et al., *DNA Mutations Mediate Microevolution between Host-Adapted Forms of the Pathogenic Fungus Cryptococcus neoformans.* PLoS Pathog, 2012. **8**(10): p. e1002936.

124. Shadomy, H.J. and H. Lurie, *Histopathological observations in experimental cryptococcosis caused by a hypha-producing strain of Cryptococcus neoformans*

(Coward strain) in mice. Sabouraudia: Journal of Medical and Veterinary Mycology, 1971. **9**(1): p. 6-9.

125. Zimmer, B.L., H.O. Hempel, and N.L. Goodman, *Pathogenicity of the hyphae of Filobasidiella neoformans.* Mycopathologia, 1983. **81**(2): p. 107-110.

126. Neilson, J., R. Fromtling, and G. Bulmer, *Pseudohyphal forms of Cryptococcus neoformans: decreased survival in vivo.* Mycopathologia, 1981. **73**(1): p. 57-59.

127. Birky, C.W., *Uniparental inheritance of mitochondrial and chloroplast genes: mechanisms and evolution.* Proceedings of the National Academy of Sciences, 1995. **92**(25): p. 11331-11338.

128. Birky, C.W., *The Inheritance of Genes in Mitochondria and Chloroplasts: Laws, Mechanisms, and Models.* Annual Review of Genetics, 2001. **35**(1): p. 125-148.

129. Barr, C.M., M. Neiman, and D.R. Taylor, *Inheritance and recombination of mitochondrial genomes in plants, fungi and animals.* New Phytol, 2005. **168**(1): p. 39-50.

130. Basse, C.W., *Mitochondrial inheritance in fungi.* Curr Opin Microbiol, 2010. **13**(6): p. 712-9.

131. Xu, J., *The inheritance of organelle genes and genomes: patterns and mechanisms.* Genome, 2005. **48**(6): p. 951-8.

132. Bonawitz, N.D. and G.S. Shadel, *Rethinking the Mitochondrial Theory of Aging: The Role of Mitochondrial Gene Expression in Lifespan Determination.* Cell Cycle, 2007. **6**(13): p. 1574-1578.

133. Chase, C.D., *Cytoplasmic male sterility: a window to the world of plant mitochondrial–nuclear interactions.* Trends in Genetics, 2007. **23**(2): p. 81-90.

134. McClelland, C.M., et al., *Uniqueness of the mating system in Cryptococcus neoformans.* Trends Microbiol, 2004. **12**(5): p. 208-12.

135. Yan, Z., et al., *The mating type-specific homeodomain genes SXI1 alpha and SXI2a coordinately control uniparental mitochondrial inheritance in Cryptococcus neoformans.* Curr Genet, 2007. **51**(3): p. 187-95.

136. Sia, R.A., K.B. Lengeler, and J. Heitman, *Diploid Strains of the Pathogenic Basidiomycete Cryptococcus neoformans Are Thermally Dimorphic.* Fungal Genetics and Biology, 2000. **29**(3): p. 153-163.

137. Xu, J., et al., *Uniparental mitochondrial transmission in sexual crosses in Cryptococcus neoformans.* Current Microbiology, 2000. **40**(4): p. 269-73.

138. Yan, Z. and J. Xu, *Mitochondria Are Inherited From the MAT**a** Parent in Crosses of the Basidiomycete Fungus Cryptococcus neoformans.* Genetics, 2003. **163**(4): p. 1315-1325.

139. Yan, Z., et al., *Environment factors can influence mitochondrial inheritance in the fungus Cryptococcus neoformans.* Fungal Genetics and Biology, 2007. **44**(5): p. 315-322.

140. Hull, C.M., R.C. Davidson, and J. Heitman, *Cell identity and sexual development in Cryptococcus neoformans are controlled by the mating-type-specific homeodomain protein Sxi1a.* Genes & Development, 2002. **16**(23): p. 3046-3060.

141. Hull, C.M., M.J. Boily, and J. Heitman, *Sex-specific homeodomain proteins Sxi1alpha and Sxi2a coordinately regulate sexual development in Cryptococcus neoformans.* Eukaryot Cell, 2005. **4**(3): p. 526-35.

142. Zhai, B., et al., *Congenic Strains of the Filamentous Form of Cryptococcus neoformans for Studies of Fungal Morphogenesis and Virulence.* Infection and Immunity, 2013. **81**(7): p. 2626-2637.

143. Kwon-Chung, K.J., et al., *Recent advances in biology and immunology of Cryptococcus neoformans.* J Med Vet Mycol, 1992. **30 Suppl 1**: p. 133-42.

144. Heitman, J., et al., *On the origins of congenic MATa and MAT**a** strains of the pathogenic yeast Cryptococcus neoformans.* Fungal Genet Biol, 1999. **28**(1): p. 1-5.

145. Nielsen, K., et al., *Sexual cycle of Cryptococcus neoformans var. grubii and virulence of congenic **a** and a isolates.* Infect Immun, 2003. **71**(9): p. 4831-41.

146. Lin, X., et al., *Transcription factors Mat2 and Znf2 operate cellular circuits orchestrating opposite and same-sex mating in Cryptococcus neoformans.* PLoS Genet, 2010. **6**(5): p. e1000953.

147. Shen, W.-C., et al., *Pheromones Stimulate Mating and Differentiation via Paracrine and Autocrine Signaling in Cryptococcus neoformans.* Eukaryotic Cell, 2002. **1**(3): p. 366-377.

148. Lin, X., et al., *Impact of mating type, serotype, and ploidy on the virulence of Cryptococcus neoformans.* Infect Immun, 2008. **76**(7): p. 2923-38.

149. Wang, P., et al., *Two cyclophilin A homologs with shared and distinct functions important for growth and virulence of Cryptococcus neoformans.* EMBO Rep, 2001. **2**(6): p. 511-8.

150. Nichols, C.B., J.A. Fraser, and J. Heitman, *PAK kinases Ste20 and Pak1 govern cell polarity at different stages of mating in Cryptococcus neoformans.* Molecular Biology of the Cell, 2004. **15**(10): p. 4476-4489.

151. Bahn, Y.-S., et al., *Adenylyl cyclase-associated protein Aca1 regulates virulence and differentiation of Cryptococcus neoformans via the cyclic AMP-protein kinase A cascade.* Eukaryot Cell, 2004. **3**(6): p. 1476-1491.

152. Hull, C.M., M.J. Boily, and J. Heitman, *Sex-specific homeodomain proteins Sxi1a and Sxi2**a** coordinately regulate sexual development in Cryptococcus neoformans.* Eukaryot Cell, 2005. **4**(3): p. 526-35.

153. Hsueh, Y.-P., J.A. Fraser, and J. Heitman, *Transitions in sexuality: recapitulation of an ancestral tri- and tetrapolar mating system in Cryptococcus neoformans.* Eukaryot Cell, 2008. **7**(10): p. 1847-1855.

154. Semighini, C.P., et al., *Deletion of Cryptococcus neoformans AIF ortholog promotes chromosome aneuploidy and fluconazole-resistance in a metacaspase-independent manner.* PLoS Pathog, 2011. **7**(11): p. e1002364.

155. Varma, A. and K.J. Kwon-Chung, *Formation of a minichromosome in Cryptococcus neoformans as a result of electroporative transformation.* Current Genetics, 1994. **26**(1): p. 54-61.

156. Kwon-Chung, K.J., et al., *Selection of ura5 and ura3 mutants from the two varieties of Cryptococcus neoformans on 5-fluoroorotic acid medium.* Medical Mycology, 1992. **30**(1): p. 61-69.

157. Liu, T.-B., et al., *The F-Box Protein Fbp1 Regulates Sexual Reproduction and Virulence in Cryptococcus neoformans.* Eukaryot Cell, 2011. **10**(6): p. 791-802.

158. Xu, J., et al., *Uniparental mitochondrial transmission in sexual crosses in Cryptococcus neoformans.* Curr Microbiol, 2000. **40**(4): p. 269-73.

159. Yan, Z., et al., *SXI1alpha controls uniparental mitochondrial inheritance in Cryptococcus neoformans.* Curr Biol, 2004. **14**(18): p. R743-4.

160. Yan, Z. and J. Xu, *Mitochondria are inherited from the MATa parent in crosses of the basidiomycete fungus Cryptococcus neoformans.* Genetics, 2003. **163**(4): p. 1315-25.

161. Litter, J., et al., *Differences in Mitochondrial Genome Organization of Cryptococcus Neoformans Strains.* Antonie van Leeuwenhoek, 2005. **88**(3): p. 249-255.

162. Strausberg, R.L. and P.S. Perlman, *The effect of zygotic bud position on the transmission of mitochondrial genes in Saccharomyces cerevisiae.* Mol Gen Genet, 1978. **163**(2): p. 131-44.

163. Berger, K.H. and M.P. Yaffe, *Mitochondrial DNA inheritance in Saccharomyces cerevisiae.* Trends Microbiol, 2000. **8**(11): p. 508-13.

164. Sutovsky, P., et al., *Ubiquitinated Sperm Mitochondria, Selective Proteolysis, and the Regulation of Mitochondrial Inheritance in Mammalian Embryos.* Biology of Reproduction, 2000. **63**(2): p. 582-590.

165. Nishimura, Y., et al., *Active digestion of sperm mitochondrial DNA in single living sperm revealed by optical tweezers.* Proc Natl Acad Sci U S A, 2006. **103**(5): p. 1382-7.

166. Hecht, N.B., et al., *Maternal inheritance of the mouse mitochondrial genome is not mediated by a loss or gross alteration of the paternal mitochondrial DNA or by methylation of the oocyte mitochondrial DNA.* Developmental Biology, 1984. **102**(2): p. 452-461.

167. Smith, L.C. and A.A. Alcivar, *Cytoplasmic inheritance and its effects on development and performance.* J Reprod Fertil Suppl, 1993. **48**: p. 31-43.

168. DeLuca, Steven Z. and Patrick H. O'Farrell, *Barriers to Male Transmission of Mitochondrial DNA in Sperm Development.* Developmental cell, 2012. **22**(3): p. 660-668.

169. Idnurm, A., et al., *Identification of the sex genes in an early diverged fungus.* Nature, 2008. **451**(7175): p. 193-196.

170. Hadjivasiliou, Z., et al., *Selection for mitonuclear co-adaptation could favour the evolution of two sexes.* Proceedings of the Royal Society B: Biological Sciences, 2012. **279**(1734): p. 1865-1872.

171. Ma, H., et al., *The fatal fungal outbreak on Vancouver Island is characterized by enhanced intracellular parasitism driven by mitochondrial regulation.* Proceedings of the National Academy of Sciences, 2009.

172. Ma, H. and R.C. May, *Mitochondria and the regulation of hypervirulence in the fatal fungal outbreak on Vancouver Island.* Virulence, 2010. **1**(3): p. 197-201.

173. Verstrepen, K.J. and G.R. Fink, *Genetic and epigenetic mechanisms underlying cell-surface variability in protozoa and fungi.* Annu Rev Genet, 2009. **43**: p. 1-24.

174. de Groot, P.W.J., et al., *Adhesins in Human Fungal Pathogens: Glue with Plenty of Stick.* Eukaryotic Cell, 2013. **12**(4): p. 470-481.

175. Sundstrom, P., *Adhesion in Candida spp.* Cellular Microbiology, 2002. **4**(8): p. 461-469.

176. Ramage, G., J.P. Martínez, and J.L. López-Ribot, *Candida biofilms on implanted biomaterials: a clinically significant problem.* FEMS Yeast Research, 2006. **6**(7): p. 979-986.

177. Sahni, N., et al., *Genes Selectively Up-Regulated by Pheromone in White Cells Are Involved in Biofilm Formation in Candida albicans.* PLoS Pathog, 2009. **5**(10): p. e1000601.

178. Verstrepen, K.J. and F.M. Klis, *Flocculation, adhesion and biofilm formation in yeasts.* Mol Microbiol, 2006. **60**(1): p. 5-15.

179. Reynolds, T.B. and G.R. Fink, *Bakers' Yeast, a Model for Fungal Biofilm Formation.* Science, 2001. **291**(5505): p. 878-881.

180. Guo, B., et al., *A Saccharomyces gene family involved in invasive growth, cell–cell adhesion, and mating.* Proceedings of the National Academy of Sciences of the United States of America, 2000. **97**(22): p. 12158-12163.

181. Nobile, C.J., et al., *Complementary adhesin function in C. albicans biofilm formation.* Current biology : CB, 2008. **18**(14): p. 1017-1024.

182. Ene, I.V. and R.J. Bennett, *Hwp1 and Related Adhesins Contribute to both Mating and Biofilm Formation in Candida albicans.* Eukaryotic Cell, 2009. **8**(12): p. 1909-1913.

183. Hayek, P., et al., *Characterization of Hwp2, a Candida albicans putative GPI-anchored cell wall protein necessary for invasive growth.* Microbiological Research, 2010. **165**(3): p. 250-258.

184. Granger, B.L., et al., *Yeast wall protein 1 of Candida albicans.* Microbiology, 2005. **151**(5): p. 1631-1644.

185. Granger, B.L., *Insight into the Antiadhesive Effect of Yeast Wall Protein 1 of Candida albicans.* Eukaryotic Cell, 2012. **11**(6): p. 795-805.

186. Moyes, D.L., et al., *Candidalysin is a fungal peptide toxin critical for mucosal infection.* Nature, 2016. **532**(7597): p. 64-68.

187. Brandhorst, T., et al., *A C-terminal EGF-like domain governs BAD1 localization to the yeast surface and fungal adherence to phagocytes, but is dispensable in*

immune modulation and pathogenicity of Blastomyces dermatitidis. Molecular Microbiology, 2003. **48**(1): p. 53-65.

188. Tian, X. and X. Lin, *Matricellular protein Cfl1 regulates cell differentiation.* Communicative & Integrative Biology, 2013. **6**(6): p. e26444.

189. Wang, L., et al., *Fungal adhesion protein guides community behaviors and autoinduction in a paracrine manner.* Proceedings of the National Academy of Sciences of the United States of America, 2013. **110**(28): p. 11571-11576.

190. Hoyer, L.L., *The ALS gene family of Candida albicans.* Trends in Microbiology, 2001. **9**(4): p. 176-180.

191. Lin, X., et al., *Generation of stable mutants and targeted gene deletion strains in Cryptococcus neoformans through electroporation.* Medical mycology, 2015. **53**(3): p. 225-234.

192. Toffaletti, D.L., et al., *Gene transfer in Cryptococcus neoformans by use of biolistic delivery of DNA.* Journal of Bacteriology, 1993. **175**(5): p. 1405-1411.

193. Idnurm, A., *A Tetrad Analysis of the Basidiomycete Fungus Cryptococcus neoformans.* Genetics, 2010. **185**(1): p. 153-163.

194. Lin, X., et al., *Impact of Mating Type, Serotype, and Ploidy on the Virulence of Cryptococcus neoformans.* Infection and Immunity, 2008. **76**(7): p. 2923-2938.

195. Lin, J., A. Idnurm, and X. Lin, *Morphology and its underlying genetic regulation impact the interaction between Cryptococcus neoformans and its hosts.* Medical mycology, 2015. **53**(5): p. 493-504.

196. Qin, Q.-M., et al., *Functional Analysis of Host Factors that Mediate the Intracellular Lifestyle of Cryptococcus neoformans.* PLoS Pathog, 2011. **7**(6): p. e1002078.

197. Mandel, M.A., et al., *The Cryptococcus neoformans Gene DHA1 Encodes an Antigen That Elicits a Delayed-Type Hypersensitivity Reaction in Immune Mice.* Infection and Immunity, 2000. **68**(11): p. 6196-6201.

198. Liu, O.W., et al., *Systematic genetic analysis of virulence in the human fungal pathogen Cryptococcus neoformans.* Cell, 2008. **135**(1): p. 174-188.

199. Cai, J.-P., et al., *Characterization of the antigenicity of Cpl1, a surface protein of Cryptococcus neoformans var. neoformans.* Mycologia, 2015. **107**(1): p. 39-45.

200. Heitman, C.M.H.a.J., *Genetics of Cryptococcus neoformans.* Annual Review of Genetics, 2002. **36**(1): p. 557-615.

201. Waterman, S.R., et al., *Role of a CUF1/CTR4 copper regulatory axis in the virulence of Cryptococcus neoformans.* The Journal of Clinical Investigation, 2007. **117**(3): p. 794-802.

202. Zhai, B., et al., *The Antidepressant Sertraline Provides a Promising Therapeutic Option for Neurotropic Cryptococcal Infections.* Antimicrobial Agents and Chemotherapy, 2012. **56**(7): p. 3758-3766.

203. Kwon-Chung, K.J. and J.E. Bennett, *Distribution of α And α Mating Types Of Cryptococcus neoformans among Natural and Clinical Isolates.* American Journal of Epidemiology, 1978. **108**(4): p. 337-340.

204. Zhu, P., et al., *Congenic Strains for Genetic Analysis of Virulence Traits in Cryptococcus gattii.* Infection and Immunity, 2013. **81**(7): p. 2616-2625.

205. Fu, C., et al., *Unisexual versus bisexual mating in Cryptococcus neoformans: Consequences and biological impacts.* Fungal genetics and biology : FG & B, 2015. **78**: p. 65-75.

206. Gyawali, R. and X. Lin, *Prezygotic and Postzygotic Control of Uniparental Mitochondrial DNA Inheritance in Cryptococcus neoformans.* mBio, 2013. **4**(2).

207. Idnurm, A., et al., *Cryptococcus neoformans Virulence Gene Discovery through Insertional Mutagenesis.* Eukaryotic Cell, 2004. **3**(2): p. 420-429.

208. Ory, J.J., C.L. Griffith, and T.L. Doering, *An efficiently regulated promoter system for Cryptococcus neoformans utilizing the CTR4 promoter.* Yeast, 2004. **21**(11): p. 919-926.

209. Upadhyay, S., et al., *Subcellular Compartmentalization and Trafficking of the Biosynthetic Machinery for Fungal Melanin.* Cell Reports. **14**(11): p. 2511-2518.

210. Trapnell, C., L. Pachter, and S.L. Salzberg, *TopHat: discovering splice junctions with RNA-Seq.* Bioinformatics, 2009. **25**(9): p. 1105-1111.

211. Trapnell, C., et al., *Transcript assembly and abundance estimation from RNA-Seq reveals thousands of new transcripts and switching among isoforms.* Nature biotechnology, 2010. **28**(5): p. 511-515.

212. Pitkin, J.W., D.G. Panaccione, and J.D. Walton, *A putative cyclic peptide efflux pump encoded by the TOXA gene of the plant-pathogenic fungus Cochliobolus carbonum.* Microbiology, 1996. **142**(6): p. 1557-1565.

213. Mondon, P., et al., *Heteroresistance to Fluconazole and Voriconazole in Cryptococcus neoformans.* Antimicrobial Agents and Chemotherapy, 1999. **43**(8): p. 1856-1861.

214. Esher, S.K., J.A. Granek, and J.A. Alspaugh, *Rapid mapping of insertional mutations to probe cell wall regulation in Cryptococcus neoformans.* Fungal Genetics and Biology, 2015. **82**: p. 9-21.

215. Feretzaki, M. and J. Heitman, *Genetic Circuits that Govern Bisexual and Unisexual Reproduction in Cryptococcus neoformans.* PLoS Genet, 2013. **9**(8): p. e1003688.

216. Li, J., et al., *Calcineurin regulatory subunit B is a unique calcium sensor that regulates calcineurin in both calcium-dependent and calcium-independent manner.* Proteins: Structure, Function, and Bioinformatics, 2009. **77**(3): p. 612-623.

217. Stie, J. and D. Fox, *Calcineurin Regulation in Fungi and Beyond.* Eukaryotic Cell, 2008. **7**(2): p. 177-186.

218. Hemenway, C.S. and J. Heitman, *Calcineurin.* Cell Biochemistry and Biophysics, 1999. **30**(1): p. 115-151.

219. Cruz, M., D.S. Fox, and J. Heitman, *Calcineurin is required for hyphal elongation during mating and haploid fruiting in Cryptococcus neoformans.* The EMBO Journal, 2001. **20**(5): p. 1020-1032.

220. Odom, A., et al., *Calcineurin is required for virulence of Cryptococcus neoformans.* The EMBO Journal, 1997. **16**(10): p. 2576-2589.

221. Steinbach, W.J., et al., *Harnessing calcineurin as a novel anti-infective agent against invasive fungal infections.* Nat Rev Micro, 2007. **5**(6): p. 418-430.

222. Yu, S.-J., Y.-L. Chang, and Y.-L. Chen, *Calcineurin signaling: lessons from Candida.* FEMS Yeast Research, 2015. **15**(4).

223. Cyert, M.S., *Calcineurin signaling in Saccharomyces cerevisiae: how yeast go crazy in response to stress.* Biochemical and Biophysical Research Communications, 2003. **311**(4): p. 1143-1150.

224. Lee, S.C., et al., *Calcineurin orchestrates dimorphic transitions, antifungal drug responses and host–pathogen interactions of the pathogenic mucoralean fungus Mucor circinelloides.* Molecular Microbiology, 2015. **97**(5): p. 844-865.

225. Moser, M.J., J.R. Geiser, and T.N. Davis, *Ca2+-calmodulin promotes survival of pheromone-induced growth arrest by activation of calcineurin and Ca2+-calmodulin-dependent protein kinase.* Molecular and Cellular Biology, 1996. **16**(9): p. 4824-31.

226. Withee, J.L., et al., *An essential role of the yeast pheromone-induced Ca2+ signal is to activate calcineurin.* Molecular Biology of the Cell, 1997. **8**(2): p. 263-277.

227. Feretzaki, M. and J. Heitman, *Unisexual Reproduction Drives Evolution of Eukaryotic Microbial Pathogens.* PLoS Pathogens, 2013. **9**(10): p. e1003674.

228. Birky, C.W., Jr., *Uniparental inheritance of mitochondrial and chloroplast genes: mechanisms and evolution.* Proc Natl Acad Sci U S A, 1995. **92**(25): p. 11331-8.

229. Jones, S.K. and R.J. Bennett, *Fungal Mating Pheromones: Choreographing the Dating Game.* Fungal genetics and biology : FG & B, 2011. **48**(7): p. 668-676.

230. Hartmann, H.A., et al., *Environmental Signals Controlling Sexual Development of the Corn Smut Fungus Ustilago maydis through the Transcriptional Regulator Prf1.* The Plant Cell, 1999. **11**(7): p. 1293-1305.

231. Merlini, L., O. Dudin, and S.G. Martin, *Mate and fuse: how yeast cells do it.* Open Biology, 2013. **3**(3).

232. Ene, I.V. and R.J. Bennett, *The Cryptic Sexual Strategies of Human Fungal Pathogens.* Nature reviews. Microbiology, 2014. **12**(4): p. 239-251.

233. Alby, K. and R.J. Bennett, *Stress-Induced Phenotypic Switching in Candida albicans.* Molecular Biology of the Cell, 2009. **20**(14): p. 3178-3191.

234. Lev, S., et al., *The Crz1/Sp1 Transcription Factor of Cryptococcus neoformans Is Activated by Calcineurin and Regulates Cell Wall Integrity.* PLoS ONE, 2012. **7**(12): p. e51403.

235. Chen, Y.-L., et al., *Calcineurin Controls Drug Tolerance, Hyphal Growth, and Virulence in Candida dubliniensis.* Eukaryotic Cell, 2011. **10**(6): p. 803-819.

236. Park, H.-S., et al., *Calcineurin Targets Involved in Stress Survival and Fungal Virulence.* PLoS Pathog, 2016. **12**(9): p. e1005873.